

Faculty of Engineering

Design of Pitch Angle Control Using Improved Strategies for Wind Turbine System

Qin Shengsheng

Doctor of Philosophy
2025

Design of Pitch Angle Control Using Improved Strategies for Wind Turbine System

Qin Shengsheng

A thesis submitted

In fulfillment of the requirements for the degree of Doctor of Philosophy

(Electrical Engineering)

Faculty of Engineering
UNIVERSITI MALAYSIA SARAWAK
2025

DECLARATION

I declare that the work in this thesis was carried out in accordance with the regulations of Universiti Malaysia Sarawak. Except where due acknowledgements have been made, the work is that of the author alone. The thesis has not been accepted for any degree and is not concurrently submitted in candidature of any other degree.

QIN SHENGSHENG

……

Signature

Name: Qin Shengsheng

Matric No.: 21010367

Faculty of Engineering

Universiti Malaysia Sarawak

Date: 17/06/2025

ACKNOWLEDGEMENT

First of all, I would like to dedicate thousands of thank to my supervisor Ir. Dr. Ngu Sze Song and my co-supervisor Ts. Dr. Kho Lee Chin for their supervisions, guidances, advices and encouragements throughout the progress of this research work. They have always been patient in giving motivations during the hard time of research and they are patient in discussing about the problems and the solutions for the research work. Their efforts and contributions are highly appreciated.

Furthermore, I would like to thank all the academicians of the Faculty of Engineering, UNIMAS and all my colleagues in the postgraduate room for their patient in sharing knowledge, giving advices and guidance throughout my research. They are always helpful and their help contributed towards the completion of this thesis.

Then, my sincere gratitude to the Centre for Graduate Studies, for the advice and support given during my period of study in Universiti Malaysia Sarawak. Also, I would like to thank the management of the Universiti Malaysia Sarawak for making it possible for me to complete my study in Sarawak.

Last but not least, I would like to deeply thank my family for their contributions to my doctoral studies. In the past few years, I stayed in the research studio all day, the busy research has deprived me of weekends and holidays, so I have no time to accompany my two children and my husband, making their lives less happy and joyful than before. Especially during the period when I went abroad to Malaysia to do research in Universiti Malaysia Sarawak, my children and I often couldn't see each other for several months, and

we deeply missed each other. But they supported me without any complaints in order to have my doctoral thesis presented to you now, so I am very grateful to them.

ABSTRACT

In the past two decades, energy shortages and environmental pollution have become increasingly serious in the world. Therefore, wind energy, as a renewable and clean energy, has received high attention from many countries such as China, the United States, Brazil and so on. Wind power generation has developed rapidly. However, the difficulty of wind power generation lies in the randomness of wind energy and the strong nonlinearity of wind turbine generator system (WTGS). Traditional control method such as single Proportional Integral Differential (PID) theory is difficult to achieve ideal control effect. In order to improve the dynamic performance of WTGS in the constant power operating region, high-performance hybrid controllers were designed in this research. When the wind speed is above the rated value, the rotor speed and output power of the WTGS can be maintained at the rated value. Firstly, a nonlinear mathematical model of WTGS was established and linearized at multiple operating points by adapting Taylor's formula to obtain multiple linear subsystems. Secondly, the optimal control theory or H-infinity theory was applied to design variable pitch controller for each linear subsystem, then a hybrid variable pitch controller was obtained by combining Takagi-Sugeno (T-S) fuzzy theory or back propagation (BP) neural network theory. Therefore, three hybrid controllers were designed in this research, namely T-S optimal hybrid pitch controller, T-S H-infinity hybrid pitch controller, and BP neural network hybrid pitch controller. Finally, simulations were conducted in MATLAB to verify the performance of the three controllers. The WTGS used in the simulation is a 600kW experimental unit from the National Renewable Energy Laboratory (NREL) of the United States. The simulation was conducted under five different wind conditions: gust wind, gradient wind, step wind, random wind and combined wind. The simulation results show that when the wind speed changes, all the three

controllers can stabilize the rotor speed at the rated value of 4.35 rad/s and the output power at the rated value of 600 kW. The response time and overshoot are both less than that of PID controller, indicating that the control effect is more ideal. When the wind speed jumps from 13 m/s to 15 m/s, comparing the data under the three controllers, from the simulation wave form it can be seen that the response time of the T-S H-infinity hybrid pitch controller is 2 seconds and the overshoot is 25.0%, which are the smallest among the three controllers.

Keywords: Wind turbine, pitch angle, optimal control, H-infinity, T-S fuzzy, BP neural network

Reka bentuk Kawalan Sudut Pitch Menggunakan Strategi yang Ditingkatkan untuk Sistem Turbin Angin

ABSTRAK

Dalam masa dua dekad yang lalu, isu kekurangan sumber tenaga dan pencemaran persekitaran menjadi semakin serius di seluruh dunia. Sebab itu, tenaga angin sebagai tenaga yang boleh diperbaharui dan bersih telah mendapat perhatian yang tinggi oleh banyak negaraseperti negara Cina, Amerika Syarikat, Brazil dan negara lain. Penjanaan tenaga angina telah dimajukan dengan pesat. Walau bagaimanapun, kesukanran penjanaan kuasa angin ditunjukkan dalam ciri-ciri ketidakstabilan sumber tenaga angin danketaklurusan yang ketara oleh Sistem Penjanaan Turbin Angin (WTGS). Cara kawalan tradisional seperti teori Proportional Integral Derivative (PID) sangat susah untuk tujuan mencapai kesan kawalan yang sempurna. Untuk menambahbaikkan prestasi dinamik WTGS dalam kawasan operasi tenaga tetap, sistem kawalan hibridberprestasi tinggi telah direka dalam penyelidikan ini. Apabila kelajuan angin adalah melebihi nilai yang ditetapkan, kelajuan pemutar dan penjanaan kuasa WTGS boleh dikekalkan pada nilai yang ditetapkan. Pertama, satu model matematik ketaklurusan WTGS perlu dibentuk dan diluruskan pada titik-titik operasi dengan menggunakan formula Taylor untuk mendapatkan pelbagai subsistem linear. Kedua, teori kawalan optimal atau teori H-infiniti telah diaplikasikan untuk mereka sistem kawalan bilah pembolehubah setiap subsistem linear, kemudian satu system kawalan bilah pembolehubah hybrid akan dedapati dengan mengintegrasikan teori logic kabur T-S atau teori rangkaian neural back propagation (BP). Dengan itu, tiga system kawalan hybrid telah direka dalam penyelidikan ini, iaitu kawalan bilah hybrid T-S Optimal, kawalan bilah hybrid T-S H-infiniti, dan kawalan bilah rangkaian neural hybrid BP. Akhir sekali, semua simulasi dibuat dengan menggunakan

Matlab/Simulink untuk mengesahkan prestasi ketiga-tiga sistem kawalan tersebut. WTGS yang digunakan dalam simulasi adalah unit eksperimen 600 kW daripada National Renerable Energy Laboratory (NREL) dari Amerika Syarikat, Simulasi tersebut dilakukan di bawah lima keadaan angin yang berlainan: angin kencang terkejut, angin berkecerunan, angin langkah, angin rawak dan kombinasi angin yang berlainan. Hasil simulasi menunjukkan apabila kelajuan angin berubah, ketiga-tiga sistem kawalan dapat menstabilkan kelajuan pemutar pada nilai yang ditetapkan iaitu 4.35 rad/s dan kuasa tenaga pada nilai yang ditetapkan iaitu 600 kW. Kedua-dua masa respons dan overshoot adalah kurang jika dibandingkan dengan sistem yang menggunakan kawalan PID, ini menunjukkan kesan kawalan adalah lebih ideal. Apabila kelajuan angin melonjak daripada 13 m/s ke 15 m/s, perbandingan data di bawah ketiga-tiga sistem kawalan menunjukkan masa respons kawalan bilah hybrid T-S H-infinity adalah 2 saat dan overshoot adalah 25.0%, yang paling kecil di antara tiga pengawal.

Kata kunci: *Turbin angin, sudut bilah, kawalan optimal, H-infiniti, logic kabur T-S, rangkaian neural BP*

TABLE OF CONTENTS

	Page
DECLARATION	i
ACKNOWLEDGEMENT	ii
ABSTRACT	iv
ABSTRAK	vi
TABLE OF CONTENTS	viii
LIST OF TABLES	xiii
LIST OF FIGURES	xiv
LIST OF ABBREVIATIONS	xvii
CHAPTER 1: INTRODUCTION	1
1.1 Introduction	1
1.2 Study Background	3
1.3 Problem Statement	6
1.4 Research Questions	8
1.5 Research Aims and Objectives	8
1.6 Scope of the Research	9
1.7 Hypothesis	11
1.8 Thesis Outlines	11

CHAPTER 2: LITERATURE REVIEW 13

2.1 Introduction 13

2.2 Wind Turbine Generator 15

2.2.1 Classification of Wind Turbine Generator System 16

2.2.2 Horizontal Axis Wind Turbine 18

2.3 Dynamic Model of WTGS 23

2.3.1 Model of Wind Turbine 23

2.3.2 Pitch Angle Actuator 25

2.4 Wind Speed Model 26

2.5 T-S Fuzzy Theory 28

2.5.1 Overview of T-S fuzzy Theory 28

2.5.2 Research Significance and Development Status of T-S Fuzzy Model 32

2.5.3 T-S Fuzzy Modeling of Nonlinear System 34

2.5.4 Dynamic System Based on Parallel Distribution Compensation (PDC) Method 38

2.6 BP neural network theory 40

2.6.1 Neural Network 40

2.6.2 BP Neural Network 42

2.7 Optimal theory 47

2.8 H-infinity theory 49

2.9 Review of WTGS Control Strategies 53

2.9.1 PID Control 53

2.9.2 Fuzzy Control 54

2.9.3 Optimal Control 55

2.9.4 Artificial Neural Network Control 56

2.9.5 Adaptive Control 58

2.9.6 Sliding Mode Control 59

2.9.7 Hybrid Control 59

2.10 Research Gap 61

2.11 Chapter Summary 62

CHAPTER 3: METHODOLOGY 64

3.1 Introduction 64

3.2 Linearization 72

3.2.1 Taylor Formula 72

3.2.2 Linearization of Wind Turbines 73

3.3 Design of Optimal Controller 77

3.4 H-infinity Controller Design 80

3.5 Hybrid Controller Design Based on T-S Fuzzy Theory 82

3.5.1 T-S Fuzzy Theory 82

3.5.2 Design of T-S Optimal Hybrid Controller 84

3.5.3 Design of T-S H-infinity Hybrid Controller 86

3.6 Design of Global Controller Based on BP Neural Network 87

3.6.1 BP Neural Network Controller 87

3.6.2 Design of Hybrid BP Neural Network Optimal Controller 87

3.7 Modeling and Simulation in MATLAB/Simulink 90

3.8 Chapter Summary 93

CHAPTER 4: RESULTS AND DISCUSSION 94

4.1 Introduction 94

4.2 Simulation results of WTGS without Controller 95

4.3 Simulation Results and Analysis with Hybrid T-S Optimal Controller 101

4.3.1 Simulation Results and Analysis of Gust Wind 101

4.3.2 Simulation Results and Analysis of Gradient Wind 103

4.3.3 Simulation Results and Analysis of Step Wind Speeds 106

4.3.4 Simulation Results and Analysis of Random Wind 108

4.3.5 Simulation Results and Analysis of Combined Wind Speed 110

4.3.6 Conclusions 112

4.4 Simulation and Results Analysis with Hybrid T-S H-infinity Controller 113

4.4.1 Simulation Results and Analysis of Gust Wind 113

4.4.2 Simulation Results and Analysis of Gradient Wind 115

4.4.3 Simulation Results and Analysis of Step Wind Speeds 117

4.4.4 Simulation Results and Analysis of Random Wind Speed 120

4.4.5 Simulation Results and Analysis of Combined Wind Speeds 122

4.4.6 Conclusions 124

4.5 Simulation and Results Analysis with BP Neural Network Optimal Controller 125

4.5.1 Simulation Results and Analysis of Gust Wind 125

4.5.2 Simulation Results and Analysis of Gradient Wind 127

4.5.3 Simulation Results and Analysis of Step Wind Speed 129

4.5.4 WTGS Response Curves to Random Wind Speed 131

4.5.5 Response Curves to Combined Wind 133

4.5.6 Conclusions 135

4.6 Conclusions 136

CHAPTER 5: CONCLUSIONS AND RECOMMENDATIONS 140

5.1 Conclusions 140

5.2 Recommendations 141

REFERENCES 143

APPENDICES 154

LIST OF TABLES

		Page
Table 2.1	Some literature	14
Table 3.1	Values of Elements A_{21} and A_{22}	76
Table 4.1	Rotor speed parameters at the 40th second under different controllers	138
Table 4.2	Output power parameters at the 40th second under different controllers	138

LIST OF FIGURES

		Page
Figure 1.1	Global New Wind Power Installations and Cumulative Wind Power Installations 2015-2023	3
Figure 1.2	Distribution of Global Cumulative Wind Power Installations in 2023	4
Figure 1.3	Proportions of Global New Wind Power Installations 2023	5
Figure 1.4	Global New Wind Power Installations Outlook 2024-2028	5
Figure 2.1	Block Diagram of Wind Turbine Structure Generator System	16
Figure 2.2	Horizontal Axis Wind Turbine (a) Few-blades (b) Multi-blades	17
Figure 2.3	Vertical Axis Wind Turbine Generator Systems	18
Figure 2.4	Diagram of Power Generation Principle of Wind Turbine	19
Figure 2.5	Pitch Angle (a) High Wind Speed (b) Low Wind Speed	20
Figure 2.6	Operation Regions of Variable-Speed Wind Turbine	22
Figure 2.7	Rotor Power Coefficient Curve	25
Figure 2.8	Block Diagram of Pitch System	26
Figure 2.9	Membership Function (a) Triangle Membership Function (b) Z-shaped Membership Function	37
Figure 2.10	Anatomical Map of Individual Neurons	41
Figure 2.11	BP Neural Network	44
Figure 2.12	BP Network Approximation Structure Diagram	44
Figure 2.13	Standard H-infinity Control	51
Figure 3.1	Methodology Flow Chart of the Hybrid Controller Designing	66
Figure 3.2	Sub Flow Chart for Linearizing the WTS in Objective1	67
Figure 3.3	Design Flow Chart of T-S Optimal Controller in Objective 2	68
Figure 3.4	Design Flow Chart of T-S H-infinity Controller in Objective 2	69

Figure 3.5 Design Flow Chart of BP Neural Network Optimal Controller in Objective 2 70

Figure 3.6 Curve of Membership Function 86

Figure 3.7 BP Neural Network Structure Diagram 88

Figure 3.8 Data-set Prediction Chart 90

Figure 3.9 Overall model 91

Figure 3.10 Wind speed module 91

Figure 3.11 Wind turbine module 92

Figure 3.12 Overall controller module 92

Figure 3.13 T-S Optimal controller module 92

Figure 3.14 T-S H-infinity controller module 93

Figure 3.15 BP neural network controller module 93

Figure 4.1 Wind Speed Profile 97

Figure 4.2 Response Curves of WTGS without Controller 100

Figure 4.3 Responses of the WTGS to Gust Wind 102

Figure 4.4 Responses of the WTGS to Gradient Wind Speed 105

Figure 4.5 Responses of WTGS to Step Wind 107

Figure 4.6 Responses of the WTGS to Random Wind 110

Figure 4.7 Responses to Superposition of Multiple Wind Components 112

Figure 4.8 Responses to Gust Wind 115

Figure 4.9 Responses to Gradient Wind 117

Figure 4.10 Response Curves to Step Wind 119

Figure 4.11 Responses to Random Wind Speed 121

Figure 4.12 Responses to Combined Wind Speed 123

Figure 4.13 Responses to Gust Wind of the Two Controllers 126

Figure 4.14 Responses to Gradient Wind of the Two Controllers 128

Figure 4.15 Response Curves to Step Wind 130

Figure 4.16 Responses to Random Wind 132

Figure 4.17 Response Curves at Combined Wind Speed 134

Figure 4.18 Response Curves at Step Wind Speed Under All Controllers 137

LIST OF ABBREVIATIONS

ABC	Artificial Bee Colony
AC	Alternating-Current
ADRC	Active Disturbance Rejection Control
AIGA	Advanced Intelligent Genetic Algorithm
ANN	Artificial Neural Network
ART	Adaptive Resonance Theory
BAM	Bidirectional Associative Memory
BP	Back Propagation
CMAC	Cerebellar Model Articulation Controller
DC	Direct-Current
DPDC	Dynamic Parallel Distributed Compensation
GWEC	Global Wind Energy Council
PDC	Parallel Distributed Compensation
PI	Proportional Integral
PID	Proportional Integral Differential
RBF	Radial Basis Function
SOM	Self-Organizing Map
T-S	Takagi-Sugeno
WTG	Wind Turbine Generator
WTGS	Wind Turbine Generator System

CHAPTER 1

INTRODUCTION

1.1 Introduction

With the increase of human population and improvement of social lifestyle, energy shortages and environmental pollution are becoming more and more serious in China. In the past 20 years, the acceleration of China's industrialization process and the growth of its population have consumed a large amount of energy, especially during high temperature and drought weather. The hydro-power generation capacity has significantly decreased, while the electricity load for air conditioning and refrigeration has increased significantly, leading to multiple instances of energy supply shortages (Zhang et al., 2023). Over the past century, industries have developed rapidly, population has soared, and fossil fuels such as coal, oil and natural gas have been consumed in large quantities. At the same time, the use of fossil fuels has caused serious environmental pollution and climate change. This has become a major issue worldwide where we need to look for alternatives to solve the environmental ecological problems and to ensure the sustainability of energy supply for the betterment of everyone in the world.

To solve the problems, most of the countries in the world have turned their attention to the development and utilization of renewable energy.

In 2016, 178 contracting parties agreed to sign the Paris Agreement, a legally binding global climate agreement. In 2021, the contracting parties finally completed the implementation details of the Paris Agreement at the United Nations Climate Change Conference. According to the requirements of the agreement, all countries need to

gradually reduce the global total carbon dioxide emissions and increase the proportion of non-fossil energy in the energy structure (Olfa et al., 2024).

Non-fossil energy mainly includes water energy, wind energy, solar energy, biomass energy and so on. Among these energy sources, wind energy has the advantages of clean, pollution-free, sustainable, large reserves and wide distribution. Moreover, compared to other clean energy sources, wind energy has the following advantages.

i. Compared with hydro-power, the storage capacity of wind energy resources is larger, and there is no need to build dams, which could further reduce the environmental damage and investment costs.

ii. Compared with solar energy, the conversion technology of wind energy is relatively mature, and it has the advantages of low unit power generation cost and large-scale grid-connected power generation. The cost of solar power generation equipment is relatively high, and the amount of investment is huge. The cost of solar power generation equipment of the same scale is several times that of wind energy equipment (Chen et al., 2024).

iii. Compared with biomass power generation, the distribution of wind energy is extremely wide. Although biomass energy can be generated using local materials, the distribution of biomass energy resources is very uneven, the fuel used for power generation needs to go through the collection, transportation and storage and other links, and the general biomass combustion calorific value is very low. All these factors increase the cost of biomass power generation.

Due to these outstanding advantages, wind energy has become the most important renewable energy in the world.

1.2 Study Background

GWEC (2024a) has released the "2024 Global Wind Energy Report", which shows that the newly installed capacity of global wind power in 2023 is 117.2 GW, and by the end of 2023, the cumulative installed capacity of the world is 1021 GW, with a year-on-year growth of 12.7%. Since 2015, global installed wind power capacity has increased year after year. The global newly added and accumulated installed capacity from 2015 to 2023 is shown in Figure 1.1 (2024 Global Wind Energy Report).

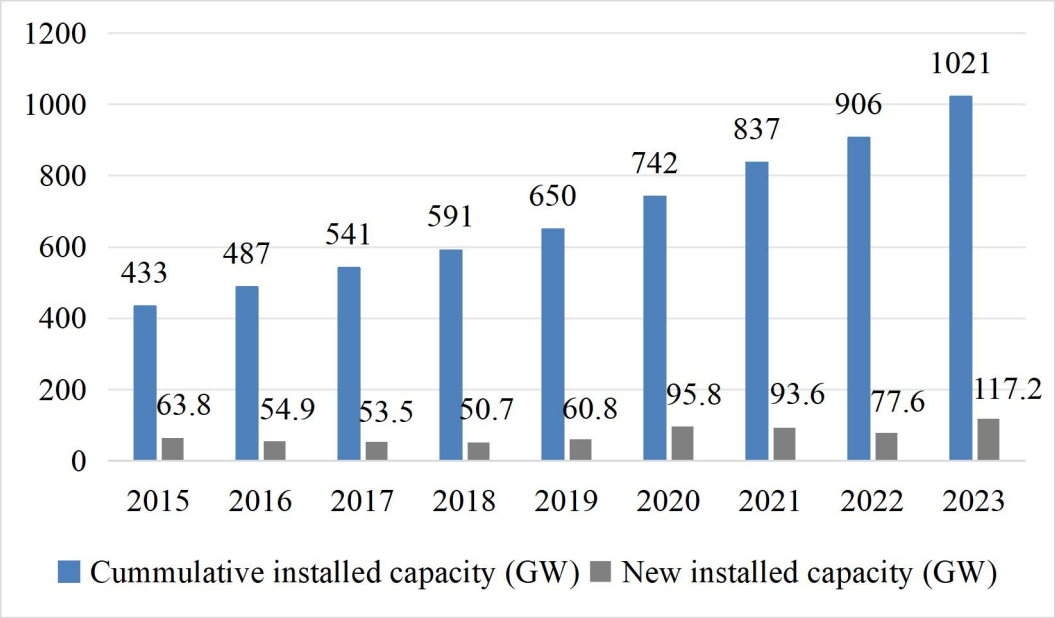


Figure 1.1: Global New Wind Power Installations and Cumulative Wind Power Installations 2015-2023

In 2023, China's cumulative installed capacity is 410 GW, accounting for 40.16%, ranking the first in the world. The detailed distribution of global cumulative wind power installations is shown in Figure 1.2. The total installed wind power capacity of the United States is 140 GW, accounting for 13.71%. Although the newly installed capacity of

Germany is low in 2023, the accumulated installed capacity of Germany still occupies the third place, the total installed capacity of wind power is 70 GW, accounting for 6.86%. India and the UK had a total installed capacity of 42 GW and 29 GW, accounting for 4.11% and 2.84% respectively. All these data are shown in Figure 1.2 (2024 Global Wind Energy Report).

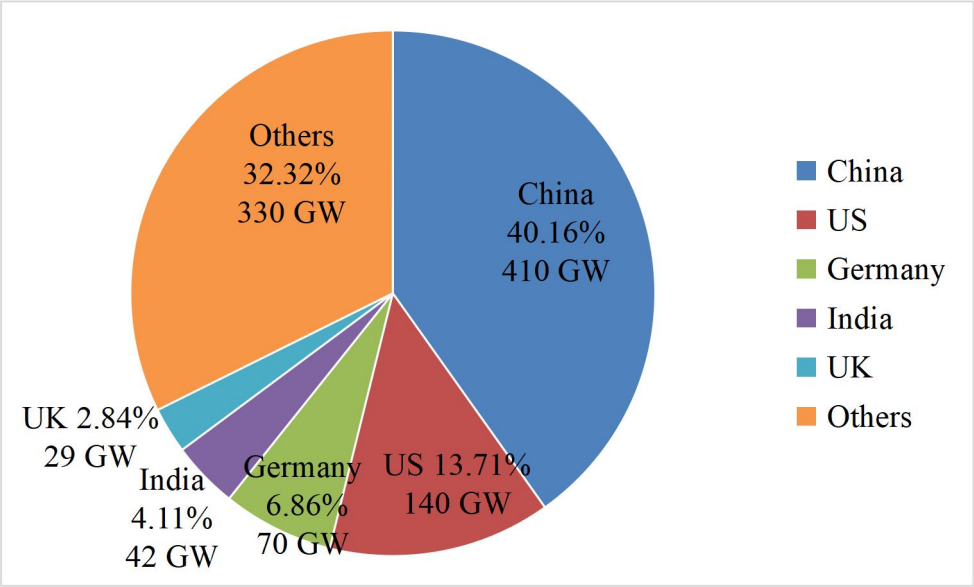


Figure 1.2: Distribution of Global Cumulative Wind Power Installations in 2023

From the "2024 Global Wind Energy Report", we also know the ranking of newly installed wind power capacity worldwide in 2023. The top ranked country is China, accounting for 26.92%, followed by the US with 14.42%, and the UK ranked third with 3.37%, as shown in Figure 1.3 (2024 Global Wind Energy Report).

GWEC (2024b) has also released the "Global Offshore Wind Report 2024", according to the Report, the cumulative installed capacity of offshore wind power in the world reached 200 GW, accounting for 19.6% of the global total. In 2023, the newly added offshore installed capacity is 30 GW, a year-on-year increase of 150%. It can be seen that the proportion of offshore wind power is not high, but with a very rapid growth.

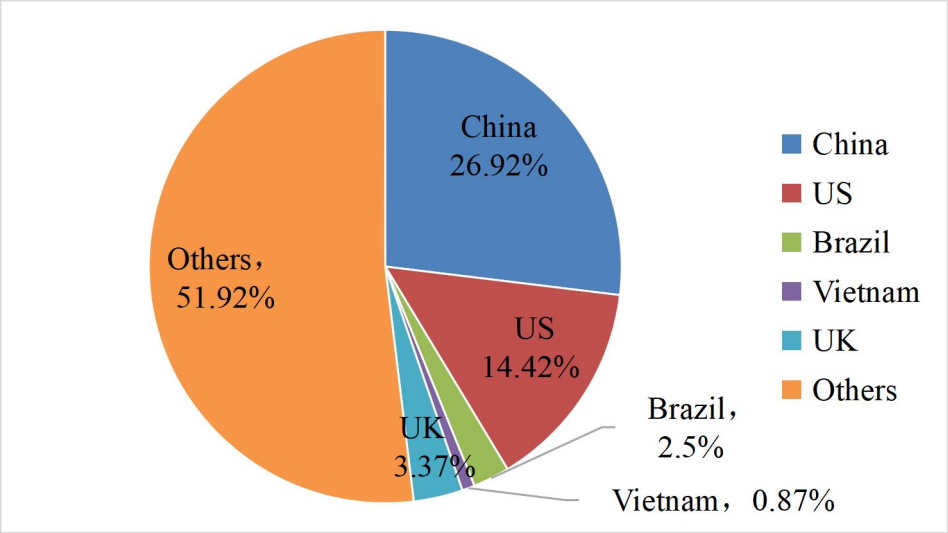


Figure 1.3: Proportions of Global New Wind Power Installations 2023

Wind power and other new energy generation industry has a very broad prospect and is expected to maintain rapid development for a long time in the future. In the next five years (2024-2028), the Global Wind Energy Council predicts that 822 GW of wind power will be added globally, with an average annual growth rate of 5.1%. Global wind power capacity will increase by 183 GW in 2028. Among them, the newly installed capacity of onshore wind power is 145 GW, while that of offshore wind power is 38 GW, as shown in Figure 1.4 (Global Offshore Wind Report 2024).

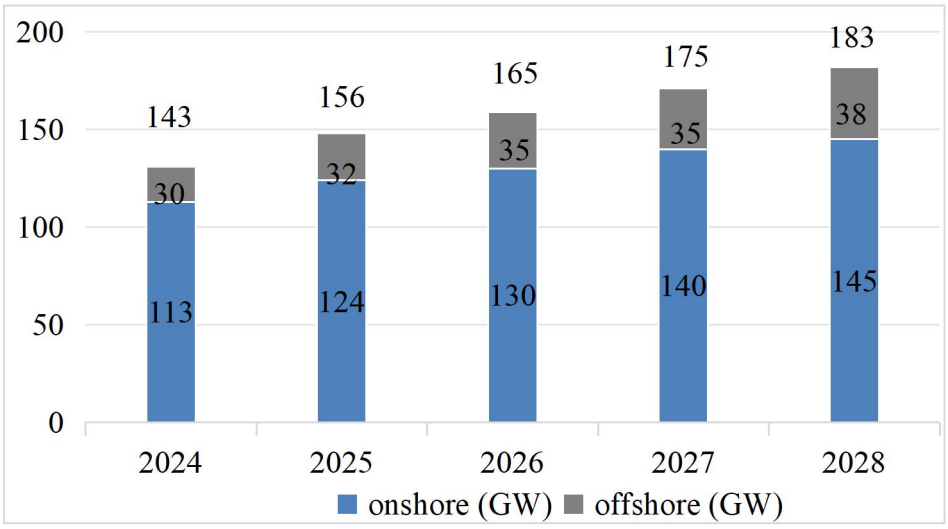


Figure 1.4: Global New Wind Power Installations Outlook 2024-2028

1.3 Problem Statement

As the core device of wind energy conversion, the operation of wind turbines is affected by various external factors and requires effective control strategies to ensure their operation (Tan et al., 2023). Pitch control, as an important control type for wind turbines, in-depth research on it can provide powerful assistance for the operation of wind turbines.

The traditional pitch control method is PID control, which has a simple algorithm and is easy to apply in engineering. However, it is difficult to achieve ideal results in solving the strong non-linearity of wind turbines and the randomness of wind energy. It can cause problems such as long response time and big overshoot. Li and Chen (2013) proposed a PID pitch control based on variable gain, which changes the gain of the PID pitch controller according to the size of the output pitch angle, making the response curve of the system smoother. Zhao et al. (2014) proposed a method based on additive decomposition principle to optimize PID controller parameters, decomposing complex system problems into two simple sub problems: linear time invariant main system and auxiliary system, enabling the WTG to further output power smoothly. Compared with traditional PID, the above methods have achieved certain improvements in control performance. However, wind turbines are susceptible to external disturbances, and the randomness of wind speed makes it difficult to meet the current control requirements in terms of pitch control.

At present, the variable pitch control method is developing from PID control to intelligent control such as optimal control, fuzzy control, sliding mode control, active disturbance rejection control, and artificial neural network control. However, a single control strategy is still difficult to achieve particularly ideal control effects. Zhang et al.

(2023) proposed a variable pitch control method, which used a wind turbine model as the training environment, built a deep neural network model based on typical wind conditions, and used power as the variable pitch control objective. The optimal power solution for variable pitch control under typical operating conditions can achieve relatively stable variable pitch control. However, due to only considering typical operating conditions, the accuracy of pitch control for wind turbines is not high when wind speed undergoes random changes. Xu et al. (2022) used the Wiener model to design a pitch control method for wind power generation systems, separating linear and nonlinear control elements in the model, simplifying the nonlinear pitch control problem into linear control, and identifying control parameters according to different signals to achieve more accurate pitch control. However, there are still error problems in complex wind conditions. Aghaeinezhhad et al. (2021) proposed an adaptive fractional order non-singular fast terminal sliding mode controller based on a simplified mathematical model of wind turbines and a single pitch control strategy to control the pitch angle. However, it is often difficult to find the optimal parameters for sliding mode control. Mendi et al. (2023) proposed a new adaptive step size and drift free adaptive step size maximum power point tracking method for controlling small variable speed wind power generation systems to improve wind energy capture efficiency. When the wind speed changes rapidly, it may not be possible to adjust the step size in a timely manner to achieve maximum power tracking, which affects system stability.

To address these issues, some hybrid control methods can be proposed as the new methods to overcome the limitations of the above methods. Linear controller design methods, such as optimal theory or H-infinity theory, can be combined with T-S fuzzy theory or BP neural network theory to design high-performance controllers that can achieve precise control at any wind speed higher than the rated value, with fast response

speed and small overshoot.

1.4 Research Questions

In order to design high-performance controllers, make the rotor speed and output power to be adjusted to rated values with fast response time and low overshoot, the following research questions are faced:

i. How to linearize the nonlinear WTG mathematical model?

ii. How to design and analyze the controllers to maintain the rotor speed and output power constant when the wind speed is changing above the rated value?

iii. Which pitch angle controller show the fastest response time and lowest overshoot?

1.5 Research Aims and Objectives

The aim of this research is to design novel high-performance hybrid variable pitch controllers for the wind turbine, to quickly stabilize the rotor speed and output power at rated values while the wind speed is changing above the rated value. Then the performance of different controllers will be compared to determine which one performs the best, so the objectives of this research are as follows:

i. To linearize the nonlinear wind turbine system into linear subsystems at six different wind speeds with Taylor expansion. The dynamic characteristics of nonlinear systems are complex, and direct controller design faces problems such as insufficient mathematical tools and difficult stability analysis. Linearization enables designers to utilize mature linear control theories such as

PID and state space methods to simplify stability analysis, parameter tuning, and performance optimization. The commonly used linearization methods include precise feedback linearization, local linearization, etc. Accurate feedback linearization has a high dependence on model accuracy and is difficult to implement, so local linearization is commonly used. Taylor expansion is a universal tool for local linearization, which converts nonlinear models into linear form near the operating point through first-order approximation. It can be achieved by calculating partial derivatives, and the algorithm is simple with high accuracy.

ii. To design three novel high-performance hybrid pitch angle controllers by T-S theory, optimal theory, H-infinity theory and BP neural network theory, so the three controllers are T-S optimal hybrid controller, T-S H-infinity hybrid controller and BP neural network optimal hybrid controller.

iii. To obtain appropriate parameters through continuous simulation attempts. To analyze the performance of the proposed controllers using the critical parameters such as the response time and overshoot of rotor speed and output power, to identify the controller with the fastest response time and the lowest overshoot.

1.6 Scope of the Research

According to different wind speeds, the operation of WTGS can be divided into three regions. The first region is the start-up phase, during which the wind speed rises from zero to the cut-in wind speed. The second region is the low-power stage, where the wind speed reaches the cut-in wind speed of the WTGS, and the wind turbine begins to rotate.

The output power of the WTGS is below the rated value, which is the low-power operating state. In this region, the WTGS is operating at a fixed pitch angle with the goal of maximum wind energy capture. The third region is for constant power operation. When the wind speed exceeds the rated wind speed, the WTGS enters the constant power operation zone, where the generator and frequency converter will reach their power limits. In order to protect the safety of the WTGS, it is necessary to control the input power of the WTGS to be less than its power limit. The most effective method is to limit the energy captured by changing the pitch angle of the blades through the variable pitch control system of the WTGS, so that the output power of the WTGS is maintained near the rated value.

Many scholars have conducted research on the first and second regions and have mature control strategies, which are detailed in Chapter 2. The third region is the most important region in WTGS control, and although many scholars have conducted research, there are still some research gaps. This region has been studied for more than ten years by me, and although twelve articles on it have been published in English and Chinese journals, it is believed that this region is still worth further research. Therefore, the scope of this research is still region three.

The scope of this research is to design new high-performance pitch controllers for wind turbines. The detailed scopes of this study are listed as follows:

i. Design a T-S optimal hybrid variable pitch controller for wind turbine.

ii. Design a T-S H-infinity hybrid variable pitch controller for wind turbine.

iii. Design a BP neural network optimal hybrid variable pitch controller for wind turbine.

1.7 Hypothesis

At the end of this research, the following outcomes are expected:

i. If the appropriate theory is proposed to linearize the nonlinear WTG mathematical model, then the nonlinear model will be linearized successfully, making it easier to design controllers.

ii. If the appropriate control theories are used to design the hybrid controllers, the rotor speed and output power can return to the rated value when the wind speed changes.

iii. If the response time and overshoot of rotor speed and output power are smallest, the relevant controller is the best.

1.8 Thesis Outlines

This thesis is divided into five chapters. This chapter is the introductory chapter that provides the background of wind power generation, current situation of global wind power generation, research scope, main research problems and research objectives. A complete overview of the research is given in this chapter. The remainder of this thesis is organized as follows:

Chapter 2 presents various categories of wind turbines, determines the categories of wind turbines required for this study, and determines the mathematical model of the wind turbine. T-S fuzzy theory, optimal control theory, H-infinity control theory and artificial neural network control theory are all presented. The reviews of the current work done on variable-pitch control, problems and limitations of the available methods, the research gap, and proposes solutions in this study are completed.

In Chapter 3, the nonlinear wind turbine system is linearized at multiple points by adapting Taylor expansion, then controllers are designed for each subsystem by optimal control theory or H-infinity control theory, and finally several sub controllers are integrated into a whole controller by T-S fuzzy theory or BP neural network theory. The content of the chapter 3 can be divided into the following four parts:

i. Taylor expansion is used to linearize the nonlinear wind turbine at multiple different wind speed points, then multiple linear subsystems are obtained.

ii. Apply optimal control theory to design several subsystem pitch controllers for wind turbine, then combine these subsystem controllers into one whole controller through T-S fuzzy theory.

iii. Apply H-infinity control theory to design several subsystem pitch controllers for wind turbine, then combine these subsystem controllers into one whole controller through T-S fuzzy theory.

iv. Apply optimal control theory to design several subsystem pitch controllers for wind turbine, then combine these subsystem controllers into one whole controller through BP neural network theory.

Chapter 4 shows the simulation using MATLAB to observe the performance of the controller. Three different controllers are simulated using MATLAB. The pitch-angle curves, wind energy utilization coefficient curves, rotor speed curves and output power curves under different controllers are obtained for comparison and analysis.

Chapter 5 summarizes the full thesis and provides the outlook for future work.

CHAPTER 2

LITERATURE REVIEW

2.1 Introduction

Wind energy is a kind of energy with low energy density and poor stability. Due to the random change of wind speed and direction, the angle of attack of wind turbine blade always changes, and the aerodynamic efficiency of wind turbine and the power input to the transmission chain fluctuate, which affects the grid-connection in serious cases (Goyal, 2024). As the wind energy is a function of the cube of wind speed, when the wind speed changes rapidly, the control system must adjust the wind turbine quickly and effectively to ensure the stable and optimal operation of the wind turbine (M. Yoshitake et al., 2022). In order to cope with the change of wind speed and direction, the wind turbine should adjust the pitch angle to ensure the stability of the rotor speed and output power at high wind speed. With the increase of the capacity of grid-connected wind turbines, the blades of large wind turbines have already weighed several tons. It is very difficult to control such a huge inertial body and ensure a fast response speed. Therefore, variable pitch control technology has always been the focus of research on large wind turbines.

The core of variable pitch control system is variable pitch controller, and the control performance mainly depends on whether the control algorithm is in line with the characteristics of the controlled object. At present, wind turbine pitch controllers mainly use traditional control algorithms based on mathematical models and modern control algorithms. Traditional control methods are generally PID and PI controllers, based on a linearized model, using wind speed and speed measurement values for feedback control. Modern control methods include robust control, variable structure control, fuzzy control,

adaptive control, optimal control, neural network control, and so on, but they are not yet applied on a large scale and are still in the process of simulation research and test prototypes. However, each optimization control method has its own advantages and disadvantages and limitations in the specific unit environment, some representative literature are shown in Table 2.1.

Table 2.1: Some literature

Authors & Year	**Methods**	**Main findings**	**Drawbacks**
Khezami (2012)	Optimal control	The optimal control is adopted to regulate the variable pitch control system of the wind turbine, ensuring a constant output power.	This algorithm excessively pursues superior performance and is not easy to implement in practical engineering applications.
Liu & Gao (2016)	PID control	The control effect of the linear operating is excellent.	The reliability is poor at other work points and cannot effectively resist random interference.
Lasheen et al. (2020)	A discrete time L_1 adaptive collective pitch-controller	Eliminating errors related to tracking reference signals and improving the steady-state performance of the system.	May result in slower response times or inability to meet rapidly changing wind speed requirements.
Yarmohammadi et al. (2020)	Gain Scheduling (GS) control algorithm	Track the maximum power to adjust the pitch angle of the blades.	Over-reliance on L_2 regular terms can lead to over-fitting problems, making the model less able to generalize on new data.

Table 2.1 continued

Bustan & Moodi (2022)	An adaptive interval 2 fuzzy control	The estimation of wind speed can be disregarded, thereby reducing the computational complexity.	The selection of membership functions and control rule tables largely relies on people's experience, leading to subjectivity and arbitrariness in the results.
Zhu et al. (2023)	Neural network control	Utilize the self-learning and adaptive capabilities of neural networks to optimize real-time output power.	The training process is complex. Numerous parameters are required. The issue of over-fitting may arise.

2.2 Wind Turbine Generator

From the perspective of energy conversion, the principle of wind power generation is the wind acts on the blades of the wind turbine at a certain speed and angle of attack, causing the rotational torque of the blades to rotate. Then, the wind energy is transformed into rotational mechanical energy of the wind turbine shaft, which is connected to the generator shaft through the transmission mechanism, and the generator rotor obtains rotational mechanical energy. The mechanical energy is converted into electrical energy finally. The structure of a wind turbine is shown in Figure 2.1, V is wind speed, T_a is the torque transmitted from the fan rotor to the transmission system, T_g is the torque transmitted from the transmission system to the generator, and P_g is the output power of the generator, ω_r is the speed of the wind turbine, ω_g is the speed of the generator.

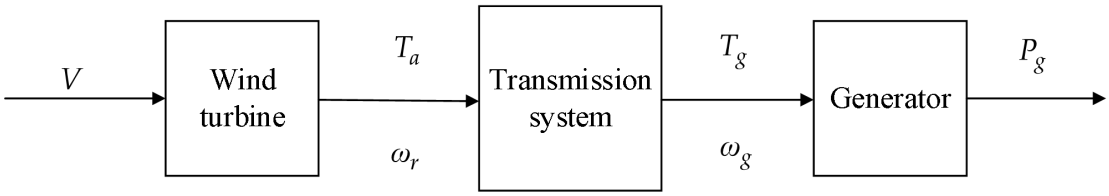


Figure 2.1: Block Diagram of Wind Turbine Structure Generator System

2.2.1 Classification of Wind Turbine Generator System

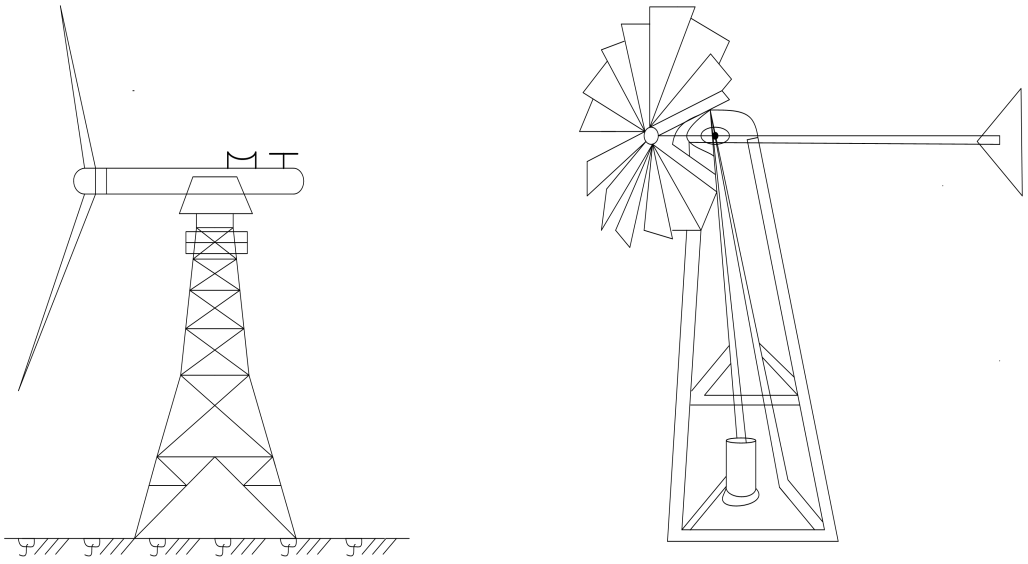
Wind turbines can be classified according to different classification standards such as the connection between the turbine and the generator, fixed or variable pitch wind turbines, load forms of the wind turbines and also horizontal or vertical axis wind turbines (Ulazia, A. et al. 2024).

According to the connection method between the wind turbine and the generator, wind turbines can be divided into direct drive wind turbines and variable speed wind turbines. A wind turbine with a speed increasing gearbox is called a variable speed wind turbine. Due to frequent starting and stopping of large wind turbines, the inertia of the wind turbine is high and the speed is low, which cannot reach the high speed required by the generator. Therefore, a speed reducer needs to be installed between the wind turbine and the high-speed generator. In order to reduce the probability of failure, micro and small wind turbines are directly driven without gearboxes.

For turbine blades that rotate around their longitudinal axis, they can be divided into fixed pitch wind turbines and variable pitch wind turbines. The wind turbine blades of a fixed pitch wind turbine are rigidly connected to the hub. When the wind speed changes, the windward angle of the blades cannot change accordingly. The wind turbine blades of a variable pitch wind turbine are connected to the hub through bearings, and when the wind speed changes, the windward angle of the blades can also change accordingly.

According to the load form of wind turbines, they can be divided into grid connected wind turbines and off grid wind turbines. Grid connected wind turbines must be integrated with the existing power grid in order to work effectively. Their basic purpose is to transmit electricity to the power grid, which in turn delivers the electricity to users. Off grid wind turbines are completely independent of the existing power grid, providing electricity services to users without conventional power supply, and require battery packs for energy storage.

According to the spatial position of the wind turbine shaft, wind turbines can be divided into horizontal axis wind turbines and vertical axis wind turbines. A wind turbine with a wind axis parallel to the horizontal plane is called a horizontal axis wind turbine. A few-blade horizontal axis wind turbine is shown in Figure 2.2 (a), and a multi-blade horizontal axis wind turbine is shown in Figure 2.2 (b).



(a) (b)

Figure 2.2: Horizontal Axis Wind Turbine (a) Few-blades (b) Multi-blades

A wind turbine with a wind axis perpendicular to the horizontal plane is called a vertical axis wind turbine, also known as a vertical axis wind turbine or a vertical wind turbine, as shown in Figure 2.3.



Figure 2.3: Vertical Axis Wind Turbine Generator Systems

The rotor structure and blade form of horizontal axis wind turbines and vertical axis wind turbines are very different. Compared to vertical axis wind turbines, horizontal axis wind turbines are more widely used.

2.2.2 Horizontal Axis Wind Turbine

Horizontal axis wind turbines are currently the most widely used and technologically mature form in various countries around the world. There are three main types of horizontal axis wind turbines: fixed pitch stall type, full blade variable pitch type, and variable speed type based on variable speed constant frequency technology. The impellers of various models are arranged in the upwind direction with horizontal shafts and three blades.

The main structural feature of a fixed pitch wind turbine is that the connection between the blades and the hub is a fixed rigid connection. That is, when the wind speed

changes, the windward angle of the blade does not change accordingly.

In large wind turbines, variable pitch wind turbines have been adopted, and the blades and hub are no longer rigidly connected, but are connected through specially designed variable pitch bearings for the variable pitch mechanism. This type of wind turbine can adjust the angle of attack of the airflow on the blades according to changes in wind speed. When the wind speed exceeds the rated wind speed, by adjusting the blade pitch angle and changing the wind energy utilization coefficient, the output power can be basically maintained at the rated power; especially in the case of strong wind shutdown, the wind turbine generator is in a feathering state, which greatly improves the stress situation of the blades and the whole machine. When the power is below the rated power, the controller places the blade pitch angle around 0° without any change, which can be equivalent to a fixed pitch unit. The power of the generator varies according to the aerodynamic performance of the blades and the wind speed. The power generation principle of a variable pitch wind turbine is shown in Figure 2.4.

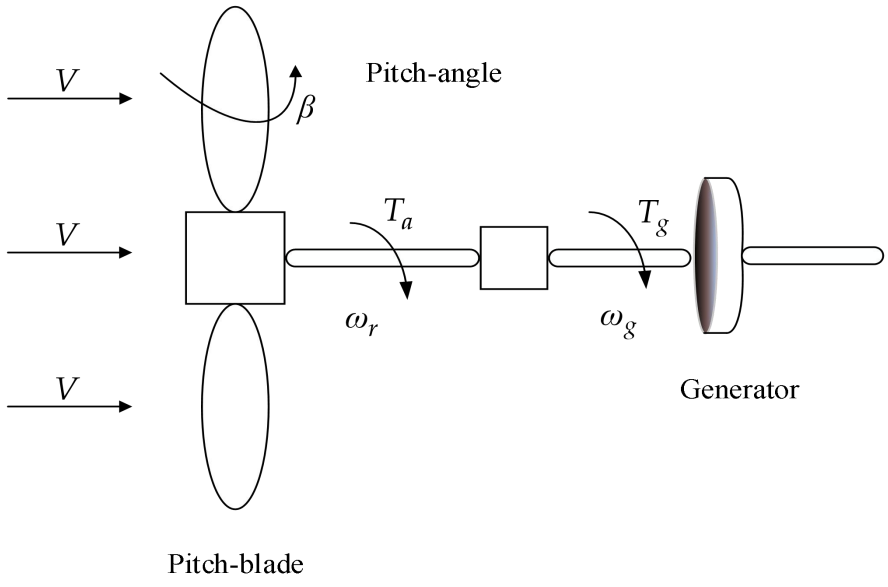
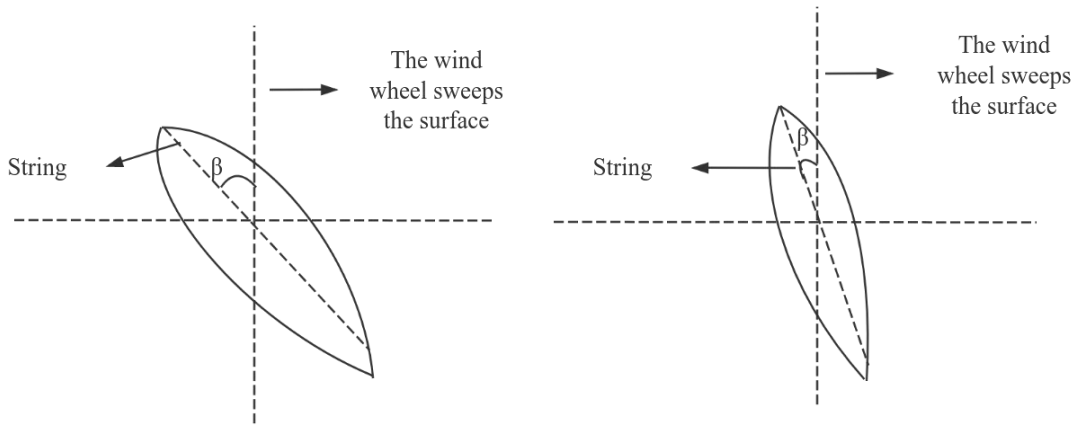


Figure 2.4: Diagram of Power Generation Principle of Wind Turbine

Figure 2.5 shows the variation of pitch angle under different wind speed. It can be seen that when the wind speed is high the pitch angle is large, while the wind speed is low the pitch angle is small.



(a) (b)

Figure 2.5： Pitch Angle (a) High Wind Speed (b) Low Wind Speed

In recent years, with the development of power electronics technology, variable-speed constant frequency wind turbines have become the mainstream model of large-scale grid connected wind turbines. The main feature of variable-speed constant frequency wind turbines is the use of doubly fed asynchronous generators or permanent magnet synchronous generators with a wide range of speed changes, as well as corresponding power electronics technology, based on variable pitch wind turbines. By tracking the optimal tip speed ratio, the wind turbine can achieve the best power output at all wind speeds. Compared with constant speed wind turbines, the superiority of variable speed wind turbines lies in their ability to maintain the optimal tip speed ratio during operation according to changes in wind speed at low wind speeds, in order to obtain maximum wind energy. At high wind speeds, it can utilize changes in wind turbine speed to store or release some energy, improve the flexibility of the transmission system, and achieve smoother

power output.

According to the magnitude of wind speed, the operation of variable-speed constant frequency wind turbines can be divided into three regions, as shown in Figure 2.6. The operational objectives vary in different regions, and there are also different focuses on the control of wind turbine systems and generator systems.

The first operating area is the start-up phase, during which the wind speed rises from zero to the cut-in wind speed. At this stage, the generator is separated from the power grid, and the main task of the generator is to achieve grid connected control. In grid connected control, the task of the wind turbine control system is to adjust the speed of the unit by changing the pitch of the blades through a variable pitch system, so that it remains constant or varies within an allowable range. The task of the generator control system is to regulate the stater voltage of the generator to meet the grid connection conditions and perform grid connection operations at appropriate times.

The first half of Zone 2 is the C_p constant zone, where the unit operates at varying speeds with wind speed to track maximum wind energy. The latter half is the constant speed zone, when the wind speed increases, the power increases but the speed remains constant. The speed control task in the constant speed zone can be completed by the generator control subsystem or by the wind turbine pitch control system.

The third operating area is the constant power zone. When the actual wind speed exceeds the rated wind speed, the wind turbine enters the constant speed operation zone. In this operation zone, the generator and frequency converter will reach their power limits. In order to protect the safety of the wind turbine, it is necessary to control the input power of

the unit to be less than its power limit. The most effective method is to limit the energy captured by the wind turbine by changing the pitch angle of the blades through the pitch control system of the wind turbine, so that the output power of the wind turbine is maintained near the rated power and the unit enters the rated power state. For this research, the control system will be designed and analyzed when the wind turbine works under region 3.

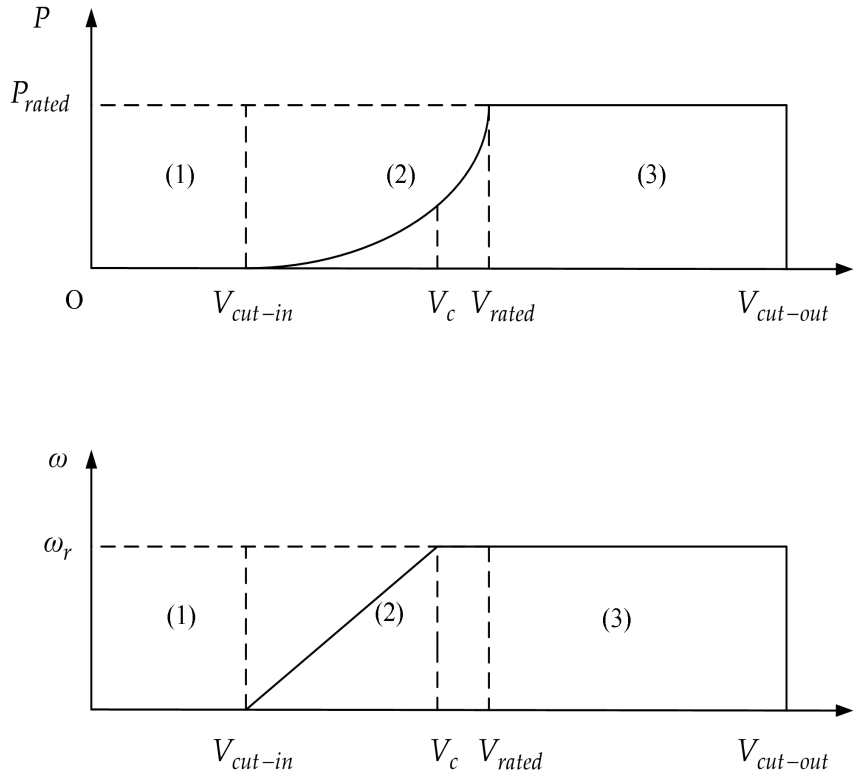


Figure 2.6: Operation Regions of Variable-Speed Wind Turbine

In summary, to ensure the stable operation of region 3, effective control of the pitch angle is necessary. Before applying control strategies to wind turbines, their dynamic characteristics need to be modeled. The dynamic characteristics of wind turbines are the sum of the dynamic characteristics of the various components that make up the unit, including the aerodynamic characteristics of the wind turbine blades, the dynamic

characteristics of the transmission system, the dynamic characteristics of the generator, and the dynamic characteristics of the control system. Therefore, it is necessary to model the wind turbine, transmission system, generator, etc. one by one, and also model the input (wind speed) of the system.

2.3 Dynamic Model of WTGS

Wind turbine is the prime mover of the whole wind power generation system. Wind turbine not only determines the output power of the whole wind power generation system, but also directly affects the stable and optimal operation of the unit. The function of wind turbines is to convert wind energy into electricity. To accurately model the energy conversion of wind turbines, basic theories based on aerodynamics must be used. However, if the basic theory of aerodynamics is used for modeling, it will inevitably solve the geometry of wind turbine, complex and lengthy analysis and calculation problems and other difficulties. In order to avoid these problems, a simple model is often designed to describe the energy conversion process of wind turbine generator system, which reflects the relationship between wind speed and conversion from wind energy.

2.3.1 Model of Wind Turbine

According to the aerodynamics, the input power of wind turbine is as follows (Ceng, 2016):

$$P_0 = \frac{\pi}{2} \rho R^2 V^3 \qquad \text{Equation 2.1}$$

Where, ρ is the air density (kg/m), generally 1.25-1.29, R is the radius of a wind wheel (m), V is wind speed (m/s), and P_0 is the input power of wind turbine (kW).

However, the input power of wind turbine cannot be all absorbed and utilized by wind turbine. According to Betz theory, the maximum utilization rate (called rotor power coefficient or wind energy utilization coefficient) of wind turbine is 0.593 in theory, but in practical, the maximum rotor power coefficient of wind turbine is usually around 0.4. Therefore, the power and aerodynamic torque captured by the wind turbine from the wind energy is:

$$T_m = \frac{1}{2} C_T(\beta, \lambda) \rho \pi R^3 V^2 \qquad \text{Equation 2.2}$$

$$P_m = \frac{1}{2} C_p(\beta, \lambda) \rho \pi R^2 V^3 \qquad \text{Equation 2.3}$$

$$C_p(\beta, \lambda) = \lambda C_T(\beta, \ \lambda) \qquad \text{Equation 2.4}$$

$$\lambda = \frac{\omega_r R}{V} \qquad \text{Equation 2.5}$$

Where, P_m is the power absorbed by wind wheel, T_m is the pneumatic torque of wind turbine, ρ is the density of air (kg/m), R is radius of wind wheel (m), C_P is rotor power coefficient, C_T is aerodynamic torque coefficient, β is angle of pitch, λ is blade tip ratio, ω_r is rotor speed of the wind turbine (rad/s).

C_P is the rotor power coefficient, it represents the ability of wind rotor to absorb power from wind energy, and is a high-order nonlinear function of blade tip speed ratio λ and pitch angle β. The following nonlinear function can be used for simulation (Chen, 2017):

$$C_p(\beta, \lambda) = 0.22\left(\frac{116}{\lambda_i} - 0.4\beta - 5\right) e^{-\frac{12.5}{\lambda_i}} \qquad \text{Equation 2.6}$$

$$\frac{1}{\lambda_i} = \frac{1}{\lambda + 0.08\beta} - \frac{0.035}{\beta^3 + 1} \qquad \text{Equation 2.7}$$

From Figure 2.7, it can be seen that the wind energy utilization coefficient curve varies with the pitch angle. As the pitch angle increases, the wind energy utilization coefficient significantly decreases. If the pitch angle is kept constant, a curve can be used to describe its function and represent the maximum power obtained from wind energy.

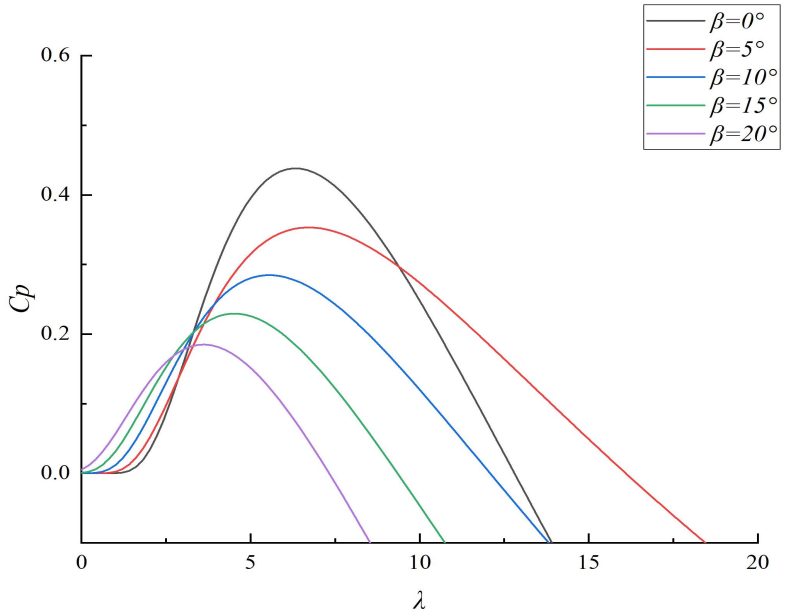


Figure 2.7: Rotor Power Coefficient Curve

2.3.2 Pitch Angle Actuator

The variable pitch system is a nonlinear servo mechanism whose closed-loop characteristics can be regarded as a first-order inertial system with finite amplitude and rate-limiting links, as shown in Figure 2.8 (Yang & Zhang, 2013). In its nearly linear operation interval, the dynamic model of variable pitch system can be expressed as:

$$\dot{\beta} = \frac{1}{T_\beta}(\beta^* - \beta)$$ Equation 2.8

where,

β —— actual pitch angle, °.

β^* —— pitch angle reference value, °.

$\dot{\beta}$ —— derivative of β over time, i.e. the rate of change of β, °/s.

T_β—— node inertia link time constant, *s*.

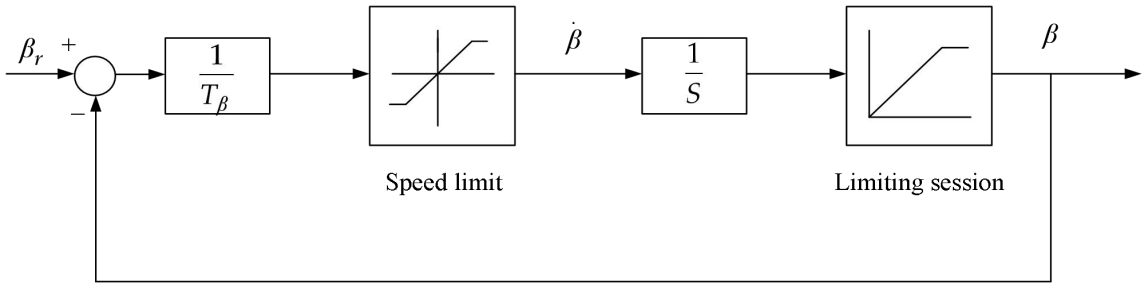


Figure 2.8: Block Diagram of Pitch System

2.4 Wind Speed Model

Wind energy is the energy input of wind power systems. Wind speed data is the most basic data for wind turbine design. For a long time, people have done a lot of research on it, hoping to be able to describe it accurately with a theoretical model, but it has not been achieved. At present, only the wind characteristics of the surface within 100 m height are relatively well understood, and the actual wind speed is the quantity that changes constantly with time. The four-component wind speed model is widely used at home and abroad, namely, basic wind $\overline{V}$, gust wind V_{WG} , gradual wind V_{WR} and random wind V_{WN} (Dai, 2018), and the actual wind speed can be regarded as the superposition of this four components.

i. Basic wind speed $\overline{V}$

The basic wind speed model is:

$$\overline{V} = A \cdot \Gamma(1+\frac{1}{K}) \qquad \text{Equation 2.9}$$

Where, $\overline{V}$ is the basic wind (m/s), A is the scale parameter of the Wei-bull distribution, K is the shape parameter of the Wei-bull distribution, and $\Gamma(1+\frac{1}{K})$ is the gamma function, as the extension of factorial function, it is a meromorphic function defined in the complex range.

ii. Gust wind speed V_{WG}

Gusts are used to describe the characteristics of sudden changes in wind speed. Generally, the gust wind speed can be:

$$V_{WG} = \begin{cases} 0 & t < T_{1G} \\ V_{\cos} & T_{1G} \le t < T_{1G} + T_G \\ 0 & t \ge T_{1G} + T_G \end{cases} \qquad \text{Equation 2.10}$$

Where, $V_{\cos} = (V_{WGmax}/2)\left\{1-\cos 2\pi\left[\left(t/T_G\right)-\left(T_{1G}/T_G\right)\right]\right\}$, V_{WG} is gust wind speed, T_G is the gust period, T_{1G} is the gust start time, and V_{WGmax} is the maximum gust speed.

iii. Gradient wind speed V_{WR}

The mathematical model of the gradient wind speed is:

$$V_{WR}=\begin{cases}0 & t<T_{1R}\\ V_{ramp} & T_{1R}\le t<T_{2R}\\ V_{WR\max} & T_{2R}\le t<T_{2R}+T_R\\ 0 & t\ge T_{2R}+T_R\end{cases} \qquad \text{Equation 2.11}$$

Where, $V_{\text{ranp}}=V_{WR\max}\left[1-\left(t-T_{2R}\right)/\left(T_{1R}-T_{2R}\right)\right]$, V_{WR} is the gradient wind speed, V_{WRmax} is the maximum gradient wind speed, T_{1R} is the start time of the gradient wind, T_{2R} is the end time of the gradient wind, T_R is the hold time of the gradient wind.

iv. Random wind speed V_{WN}

The random wind speed model is:

$$V_{WN}=2\sum_{i=1}^{N}\left[S_v\left(w_i\right)\Delta w\right]^{1/2}\cos\left(w_i t+\varphi_i\right) \qquad \text{Equation 2.12}$$

where, $v_i=\left(i-\frac{1}{2}\right)\Delta w$, $S_v\left(w_i\right)=\frac{2K_N F^2\left|w_i\right|}{\pi^2\left[1+\left(Fw_i/\mu\pi\right)^2\right]^{4/3}}$, N is the total number of statistical wind speeds, Δw is the wind speed frequency interval, φ_i is a random variable uniformly distributed between 0~2π, K_N is the surface roughness coefficient, F is the disturbance range, and μ is the mean wind speed of the relative altitude.

2.5 T-S Fuzzy Theory

2.5.1 Overview of T-S fuzzy Theory

With the development of science and technology, the study of nonlinear system dynamics has become increasingly important. Its research purpose is to use nonlinear dynamics theory to elucidate the mechanisms of complex mechanical phenomena, and to

study the qualitative and quantitative changes in the system under different initial conditions and changes in system parameters. Stability and control have always been important topics in system theory research and practical applications. Famous Chinese scientists Qian Xuesen and Song Jian once said in their monograph "Engineering Cybernetics": The first requirement for a control system is stability. Lyapunov, a famous Russian numerical mechanic, put forward the central idea of "stability and asymptotic stability of a system in motion" in his paper "General Problems of Motion Stability" completed in 1892. So far, scholars around the world have conducted a lot of research under the basic research framework of this stability theory and obtained a lot of research results on motion stability (Bachmann et al., 2024).

However, modern control theory has encountered many difficulties or problems in practical engineering applications: most of the controlled systems in practice have characteristics such as non-linearity, time-varying, dynamics, system uncertainty, controller gain disturbance, large random disturbances, and multi parameter coupling, which are often difficult to describe with an accurate mathematical model; At the same time, many practical processes (such as vehicle driving) have significantly strict requirements for the response speed, response time, control accuracy, system stability, and adaptability of the control system. The control performance requirements are becoming increasingly high, making it more difficult to control and meet various performance requirements of the control system. Therefore, introducing the function of fuzzy systems is mainly aimed at addressing the problem of uncertain system parameters in actual system dynamics analysis and control. It provides an alternative fuzzy model control method for actual physical system models, supplements the model with expert knowledge and experience, and conducts fuzzy control research under various practical working

conditions and performance characteristics. This makes it possible to improve the control performance of complex systems.

Fuzzy Control is an advanced control strategy based on fuzzy mathematics theory in modern control theory, which uses language rules and fuzzy reasoning systems to implement. It is an important branch of artificial intelligence control and a current research hot-spot. In recent years, fuzzy control has developed rapidly and has been widely applied, attracting great attention. Fuzzy control is not only applicable to conventional nonlinear univariate systems, but also gradually expanding to large-scale and complex nonlinear systems. It has obvious advantages: easy familiarity, high reliability, strong practicality, and good automation effects that can obtain expert knowledge and proficient operating experience.

In 1965, Dr. L.A.Zadehl from the University of California published a paper called “fuzzy sets” on “Information and Control”, and then conducted research on fuzzy mapping and fuzzy reasoning. He proposed and improved concepts such as fuzzy knowledge representation, semantic variables, fuzzy rules and fuzzy graphs, and opened a new process of fuzzy control (Zhang, 2021). In the past few decades, scholars at home and abroad have developed a variety of design schemes based on fuzzy logic model, the theoretical research mainly includes: adaptive self-learning fuzzy control theory research. fuzzy reasoning strategy research, fuzzy identification model research, fuzzy control system stability research, and fuzzy controller hardware realization.

Among various fuzzy control methods, fuzzy control based on Takagi-Sugeno (T-S) model is the only method that can obtain systematic analysis and synthesis theory (Mlayeh & Khedher, 2024). T-S fuzzy model proposed by Takagi and Sugeno in 1985 is a typical

and practical dynamic model for fuzzy modeling of complex nonlinear systems (Takagi & Sugeno, 1985). The model includes two parts: One part is quantitative description, that is, the premise parts are divided according to whether there is a local linear relationship between the input and output of the system, while the conclusion parts are expressed by linear equations. The other part is qualitative description. Finally, the superposition processing of fuzzy membership function is applied to form a unified mathematical model, which makes the global output of nonlinear system have good linear description characteristics (Hamadou & Belarbi, 2023). The universal approximation theorem of fuzzy model system is described as follows:

Theorem 1.1: (Universal approximation theorem) For any continuous function *g(x)* defined on the denser $U \in R^n$, and any positive number ε, there must be a fuzzy logic system *f(x)*, so that the following inequalities are true.

$$\sup_{x \in U} |f(x) - g(x)| < \varepsilon \qquad \text{Equation 2.13}$$

Since then, many scholars have studied fuzzy controller and filter design methods, mainly including Parallel Distributed Compensation (PDC) (Rajesh & Kaimal, 2007), Dynamic Parallel Distributed Compensation (DPDC) (Razavi & Majd, 2008), etc. Aiming at the control of T-S fuzzy system, Wang, etc. First proposed a so-called PDC method, which can be used as a framework for the control design of nonlinear system based on T-S fuzzy model. A control algorithm is developed and the Tanaka stability theorem is modified. The PDC method is to design the filter for each linear subsystem respectively, and then keep the weight of the sub-filter and the weight of the subsystem are combined together to form a global filter method. The advantage of this method is that it can use the

existing theory and tools of linear system analysis to facilitate the analysis and design of the controller and filter. The controller designed by fuzzy parallel distribution compensation principle is actually the global approximation of a nonlinear controller. Therefore, by using the T-S fuzzy model, the analysis and synthesis of a nonlinear system are successfully decomposed into a cluster of local linear models and their analysis and synthesis. Thus, it is possible to apply the existing rich analysis and controller synthesis methods to complex nonlinear systems.

2.5.2 Research Significance and Development Status of T-S Fuzzy Model

In practice, most physical systems are nonlinear. Compared with the simplicity of linear systems and the corresponding research results, a mature system has been formed. The modeling and control of nonlinear characteristics are much more difficult. This makes many scholars study and find a variety of convenient and easy to control approximation models to describe nonlinear systems. Due to the universal approximation ability of T-S fuzzy model, since it was proposed in the 1980s, it has immediately attracted sufficient attention from scholars at home and abroad. Various stability analysis of T-S fuzzy model, controller and filter design and synthesis methods under various performance indexes emerge endlessly, and a hundred flowers are blooming.

In recent years, in the process of controller design for complex nonlinear systems, T-S fuzzy control method is combined with various control strategies (random control, sliding mode variable structure control, H-infinity control, etc.), which has become a research hot spot for nonlinear system control at present (Hamadou & Belarbi, 2023). However, there are still many defects and deficiencies in the literature results of T-S fuzzy control method used to deal with uncertain nonlinear time-delay systems. Among various

control strategies of nonlinear time-delay systems, the controller of nonlinear time-delay systems will have faster convergence speed, less conservative and stronger computing power by using the universal approximation ability of T-S fuzzy control method. And to ensure that the closed-loop system has good dynamic performance and (non-fragile) robust H-infinity performance is the original motivation of this paper.

T-S fuzzy control method is a very effective nonlinear control method. Its biggest advantage is that it represents a complex nonlinear system as a weighted sum of a group of simple linear subsystems. When the uncertainty of the system, unknown system parameters or human factors change, the control system can still achieve the expected characteristics. The basic idea is that the T-S fuzzy model is a nonlinear model which uses the fuzzy membership function to superimpose a series of linear models representing the local input-output relationship through interpolation. Based on the universal approximation theorem of fuzzy logic system, a way to identify the nonlinear system as T-S fuzzy model is given according to the input and output data, which provides a theoretical basis for T-S model to approximate the complex nonlinear system. In terms of form, this approach is similar to the typical piece wise linear model approach to nonlinear systems, and also similar to the approach of some locally linear smooth models compound through membership functions describing global properties. It should be pointed out that although T-S fuzzy system has much in common with linear time-varying system, polyhedral uncertain system and switching system from the surface of form, it is nonlinear dynamic system in essence, which is very different from these systems. In general, T-S fuzzy model is different from other systems and has its own significant advantages and characteristics. T-S model provides a kind of stability and performance analysis based on the global nonlinear model, but it is based on the local linear model for controller design. On the one hand, the T-S

model has adaptability to parameter changes, and there is no fast vibration in the output of the controller. On the other hand, there are many systematic analysis and synthesis methods that can be applied to the T-S model. After nearly half a century of continuous development and improvement, it has become an effective tool to solve nonlinear problems by using mature linear system theory. Therefore, the study of T-S fuzzy control theory and its control method, and the application of its results in the design of various controllers or filters in industrial engineering systems, has important theoretical significance and urgent practical application value.

2.5.3 T-S Fuzzy Modeling of Nonlinear System

Fuzzy control is a kind of computer mathematical control based on fuzzy set theory, fuzzy language variables and fuzzy logic reasoning. It is a nonlinear control method, belongs to the category of intelligent control and has become an important and effective form to realize intelligent control at present, with great application potential. The core of fuzzy control is the control rules described by language. Language control rules usually start with "If..., Then... " to express expert knowledge and experience in practical control. The If part, also known as the conditional part, belongs to the antecedent of fuzzy reasoning and is a proposition composed of controlled quantities, etc. The Then part, also called the conclusion part, is the proposition that describes the quantity of control. The biggest characteristic of fuzzy control is to express the expert control experience and knowledge into language control rules, and then use these rules to control the system. Therefore, fuzzy control is especially suitable for simulation experts to control complex nonlinear systems with unknown mathematical models.

2.5.3.1 Constitution of T-S fuzzy Model

T-S fuzzy modelling can use some fuzzy words to describe the performance of the system. The operator can make a series of successful control rules according to the language description of the process and expert information.

The equation of state for a nonlinear system is written as follows：

$$\dot{\boldsymbol{x}} = \boldsymbol{F}(\boldsymbol{x},\boldsymbol{u}) = \boldsymbol{f}(\boldsymbol{x}) + \boldsymbol{g}(\boldsymbol{x})\boldsymbol{u} \qquad \text{Equation 2.14}$$

Then its fuzzy equation of state model can be expressed as

R_p^i： If $x_1(t)$ is M_1^i and…and if $x_n(t)$ is M_n^i， then $\dot{\boldsymbol{x}}(t) = \boldsymbol{A}_i\boldsymbol{x}(t) + \boldsymbol{B}_i\boldsymbol{u}(t)$， i=1，2，…，l

Then the equation of state of the whole system can be written as

$$\dot{\boldsymbol{x}}(t) = \sum_{i=1}^{l} h_i(\boldsymbol{x})[\boldsymbol{A}_i\boldsymbol{x}(t) + \boldsymbol{B}_i\boldsymbol{u}(t)] \qquad \text{Equation 2.15}$$

where, $h_i(\boldsymbol{x}) = \mu^i(\boldsymbol{x}) / \sum_{j=1}^{l} \mu^j(\boldsymbol{x})$， $\mu^j(\boldsymbol{x}) = \prod_{j=1}^{n} \mu_j^i(\boldsymbol{x})$， $\mu^i(\boldsymbol{x})$ Represents the membership function of M^i， it also represents the application of Rule i. It can be seen that the output of T-S fuzzy inference is linear or constant. It is convenient for mathematical analysis by eliminating fuzzification and anti-fuzzification.

2.5.3.2 Calculation of T-S Model

Find near the equilibrium point $(\boldsymbol{x}_0, \boldsymbol{u}_0)$, that is satisfied

$$\boldsymbol{F}(\boldsymbol{x}_0, \boldsymbol{u}_0) = 0 \qquad \text{Equation 2.16}$$

The linear model can be obtained by Taylor series expansion, and the higher order terms are ignored

$$\Delta \dot{\boldsymbol{x}} = \boldsymbol{A}\Delta \boldsymbol{x} + \boldsymbol{B}\Delta \boldsymbol{u} \qquad \text{Equation 2.17}$$

There into $\Delta \boldsymbol{x} = \boldsymbol{x} - \boldsymbol{x}_0$, $\Delta \boldsymbol{u} = \boldsymbol{u} - \boldsymbol{u}_0$, $\boldsymbol{A} = \left.\frac{\partial \boldsymbol{F}}{\partial \boldsymbol{x}}\right|_{\substack{\boldsymbol{x}=\boldsymbol{x}_0 \\ \boldsymbol{u}=\boldsymbol{u}_0}}$, $\boldsymbol{B} = \left.\frac{\partial \boldsymbol{F}}{\partial \boldsymbol{u}}\right|_{\substack{\boldsymbol{x}=\boldsymbol{x}_0 \\ \boldsymbol{u}=\boldsymbol{u}_0}}$.

2.5.3.3 Determine the Membership Function

The fuzzy theory has been increasingly mature, the use of fuzzy control theory in the design of control system does not need to establish an accurate mathematical model of the controlled object, so it can effectively improve the accuracy of modelling, so it has been widely used. The quantitative description of fuzzy language variable is determined by its membership function, which is the basis of applying fuzzy set theory to solve practical problems.

At present, there is not a set of mature and effective methods for the establishment of membership function, and most of them remain on the basis of experience and experiment. For the same fuzzy concept, different people will establish different membership functions. Although the forms are not exactly the same, as long as the same fuzzy concept can be reflected, it can still lead to the same destination in solving and processing the actual fuzzy information (Shi & Hao, 2018). Common membership functions are three types below (Shi & Hao, 2018):

i. Normal membership function

The normal distribution is the most dominant and the most common distribution

$$\mu(x) = e^{-(\frac{x-a}{b})^2}$$ Equation 2.18

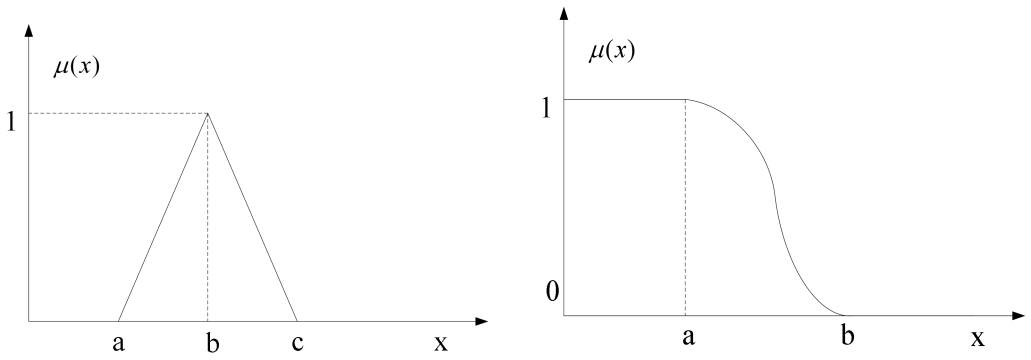
ii. Triangular membership function

Trigonometric membership function is one of the most widely used membership degrees. As shown in Figure 2.8(a), it can be expressed as

$$\mu(x) = \begin{cases} \dfrac{x-a}{b-a}, & a < x < b \\ \dfrac{x-c}{b-c}, & b < x < c \\ 0 \quad , \quad \text{else} \end{cases}$$ Equation 2.19

iii. Z-shaped membership function

The Z-shaped membership function has two parameters, a and b, which are the positions of the poles in the membership function curve, refer to Figure 2.9.



(a) **(b)**

Figure 2.9: Membership Function **(a)** Triangle Membership Function **(b)** Z-shaped Membership Function

2.5.4 Dynamic System Based on Parallel Distribution Compensation (PDC) Method

2.5.4.1 Parallel Allocation Compensation Design Idea

The conclusion of the T-S model is that the fuzzy after parts are described by linear equations, which is convenient for the design of related controllers by using the traditional linear control strategy. Tanaka et al. adopted the PDC method to design the controller, that is, to design a local linear state feedback controller for each linear subsystem. Pole assignment design method or linear quadratic optimal controller design method can be adopted. PDC controller design is as follows

R_p^i： if $x_1(t)$ is M_1^i and…and if $x_n(t)$ is M_n^i, then $\boldsymbol{u}(t) = -\boldsymbol{K}_i\boldsymbol{x}(t)$.

According to PDC idea, the control law of the whole system is the weighted sum of local feedback control of each subsystem, namely

$$\boldsymbol{u}(t) = -\sum_i^l h_i(x)\boldsymbol{K}_i\boldsymbol{x}(t) \qquad \text{Equation 2.20}$$

There into， $h_i(\boldsymbol{x}) = \mu^i(\boldsymbol{x}) / \sum_{j=1}^{l} \mu^j(\boldsymbol{x})$.

It can be seen that the control essence of the whole system is nonlinear time-varying state feedback. The above controller is designed according to the local linear subsystem, and the stability of the whole system needs to be reverified.

Lemma 1 (Wu, 2005 & Tong et al., 2004): For nonlinear systems $\dot{\boldsymbol{x}} = \boldsymbol{f}(\boldsymbol{x}(t))$， of which， $\boldsymbol{x}(t) \in \boldsymbol{R}^n$， $\boldsymbol{f}(\boldsymbol{0}) = \boldsymbol{0}$. Suppose there is a scalar function $V(\boldsymbol{x}(t))$ that satisfies the following conditions：

i. $\boldsymbol{V}(\boldsymbol{0}) = \boldsymbol{0}$,

ii. $\forall \boldsymbol{x}(t) \neq \mathbf{0}, \boldsymbol{V}(\boldsymbol{x}(t)) > 0$,

iii. 当 $\|\boldsymbol{x}(t)\| \to \infty, \boldsymbol{V}(\boldsymbol{x}(t)) \to \infty$,

iv. $\forall \boldsymbol{x}(t) \neq \mathbf{0}, \dfrac{d\boldsymbol{V}(\boldsymbol{x}(t))}{dt} < 0$.

Then the nonlinear system is globally asymptotically stable with respect to the equilibrium point $\boldsymbol{x}(t) = \mathbf{0}$

Theorem 1 (Wu, 2005 & Tong et al., 2004): If there is a positive definite symmetric matrix P, such that the linear matrix inequality ($\boldsymbol{G}_{ij} = \boldsymbol{A}_i - \boldsymbol{B}_i \boldsymbol{K}_j$)

$$\begin{aligned} &\boldsymbol{G}_{ii}^T \boldsymbol{P} + \boldsymbol{P}\boldsymbol{G}_{ii} < 0, \quad i = 1, 2, \cdots N \\ &\left(\frac{\boldsymbol{G}_{ij} + \boldsymbol{G}_{ji}}{2}\right)^T \boldsymbol{P} + \boldsymbol{P}\left(\frac{\boldsymbol{G}_{ij} + \boldsymbol{G}_{ji}}{2}\right) < 0, \quad i < j \le N \end{aligned} \qquad \text{Equation 2.21}$$

If so, the closed-loop system is asymptotically stable.

Refer the literature for the detailed proof of theorem 1 (Wu, 2005 & Tong et al., 2004), taking

$V(\boldsymbol{x}(t)) = \boldsymbol{x}^T(t)\boldsymbol{P}\boldsymbol{x}(t)$ Take the derivative of $V(\boldsymbol{x}(t))$ with respect to time

$$\dot{V}(\boldsymbol{x}(t)) = \sum_{i=1}^{N}\sum_{j=1}^{N} \mu_i(\boldsymbol{z}(t))\mu_j(\boldsymbol{z}(t))\boldsymbol{x}^T(t) \times \left[(\boldsymbol{A}_i - \boldsymbol{B}_i\boldsymbol{K}_j)^T \boldsymbol{P} + \boldsymbol{P}(\boldsymbol{A}_i - \boldsymbol{B}_i\boldsymbol{K}_j)\right]\boldsymbol{x}(t)$$

$$= \sum_{i=1}^{N} \mu_i^2(\boldsymbol{z}(t))\boldsymbol{x}^T(t) \times \left[\boldsymbol{G}_{ii}{}^T \boldsymbol{P} + \boldsymbol{P}\boldsymbol{G}_{ii}\right]\boldsymbol{x}(t)$$

$$+ \sum_{i<j}^{N} 2\mu_i(\boldsymbol{z}(t))\mu_j(\boldsymbol{z}(t))\boldsymbol{x}^T(t) \times \left[(\frac{\boldsymbol{G}_{ij} + \boldsymbol{G}_{ji}}{2})^T \boldsymbol{P} + \boldsymbol{P}(\frac{\boldsymbol{G}_{ij} + \boldsymbol{G}_{ji}}{2})\right]\boldsymbol{x}(t)$$

If equation 2.21 is true, then $\boldsymbol{x}(t) \neq 0$, can get $\dot{V}(\boldsymbol{x}(t)) < 0$, it can be known from lemma 1 that the fuzzy system is asymptotically stable.

2.6 BP neural network theory

2.6.1 Neural Network

Fuzzy control starts from human experience and solves the problem of describing and reasoning human language in intelligent control, especially for some uncertain descriptions and reasoning. However, fuzzy control is far from reaching the level of the human brain in terms of processing numerical data and self-learning ability. Artificial neural networks (referred to as neural networks) start from the physiology and psychology of the human brain, and achieve partial intelligent behavior of machines by artificially simulating the working mechanism of the human brain.

Research in neurophysiology and neuroanatomy has shown that the human brain is extremely complex, consisting of a network of over 100 billion neurons (nerve cells) intertwined together, with approximately 14 billion neurons in the cerebral cortex and 100 billion neurons in the cerebellar cortex. Therefore, the human brain can complete advanced activities such as intelligence and thinking. In order to utilize mathematical models to simulate the activity of the human brain, research on neural networks has been led.

Neurons are the basic units that process information transmission between various parts of the human body, and each neuron is composed of four parts: cell body, dendrites, axons, and synapses. Its structure is shown in Figure 2.10.

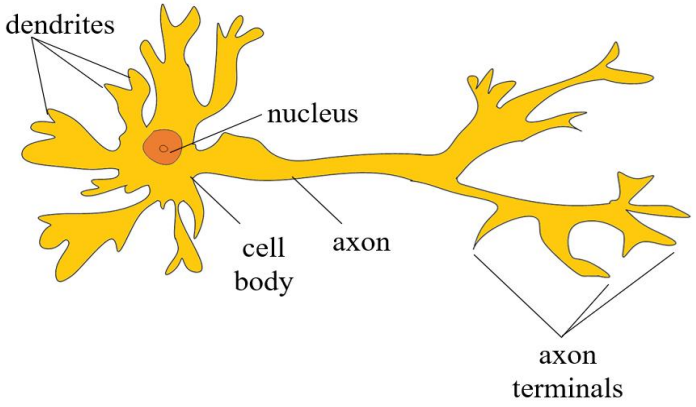


Figure 2.10: Anatomical Map of Individual Neurons

i. Cell body: including cytoplasm, cell membrane, and nucleus.

ii. Dendritic: Used to transmit information to the cell body.

iii. Axon: Sends information from the cell body, with nerve endings at the end containing chemicals that transmit information.

iv. Synapse: The interface between neurons. A neuron is connected to another neuron's dendrite through its axon's nerve endings, through synapses, to achieve information transmission.

Neurons have the following functions:

i. Excitation and inhibition: If the impulses transmitted to neurons are integrated to increase the potential of the cell membrane, exceeding the threshold of the action potential, it becomes an excited state and generates nerve stimulation, which is transmitted from axons through nerve endings. If the integration of impulses into neurons reduces the potential of the cell membrane and falls below the threshold of action potential, it becomes an inhibitory state and does not generate neural stimulation.

ii. Learning and forgetting: Due to the plasticity of neuronal structures, the transmission of synapses can be enhanced and weakened, thus neurons have the function of learning and forgetting.

Since the 1980s, neural network control has developed an intelligent control method that combines neural networks with control theory, and has become a new branch of intelligent control. It has opened up a new path for solving control problems in complex nonlinear, uncertain, and uncertain systems.

A neural network model is a system that uses mathematical means to simulate the structure and characteristics of human brain neural networks. By utilizing neurons, various neural network models with different topological structures can be constructed to simulate and approximate human brain neural networks.

2.6.2 BP Neural Network

In 1986, in the book "Parallel Distributed Processing" published by Rumelhart and MeCelland et al., a famous error back-propagation neural network, known as the BP (Back Propagation) neural network, was proposed. This network is a one-way propagation multi-layer forward neural network, which is the most widely used neural network to date and has been used to solve a large number of practical problems. The learning algorithm for error back propagation, abbreviated as BP algorithm, is based on the gradient descent method. It uses gradient search technology to minimize the mean square error between the actual output value of the network and the expected output value. The BP neural network has the following characteristics:

i. BP network is a multi-layer network that includes input layer, hidden layer, and output layer;

ii. The layers are fully interconnected, and there is no connection between neurons (nodes) in the same layer;

iii. Weight passing δ Learning rules for regulation;

iv. The neuron excitation function is the S function;

v. The learning algorithm consists of forward propagation and backward propagation;

vi. The connection between layers is unidirectional, and the dissemination of information is bidirectional.

The structure of the BP neural network is shown in Figure 2.11. The figure shows a BP neural network with one hidden layer, where *i* is the input layer neuron, *j* is the hidden layer neuron, and *k* is the output layer neuron. There is no coupling among nodes in the same layer, and the output of each layer node only affects the output of the next layer node. The learning process of a network consists of two parts: forward and backward propagation. The node element characteristics of back-propagation are usually *sigmoid* type $\{ f(x) = 1/[1+\exp(-Bx)], B > 0 \}$. During the network training stage, prepared sample data is sequentially passed through the input layer, hidden layer, and output layer to compare the output results and expected values. If the required error level or training frequency is not reached, the weight values are adjusted through the output layer, hidden layer, and input layer to make the network a model with certain adaptability.

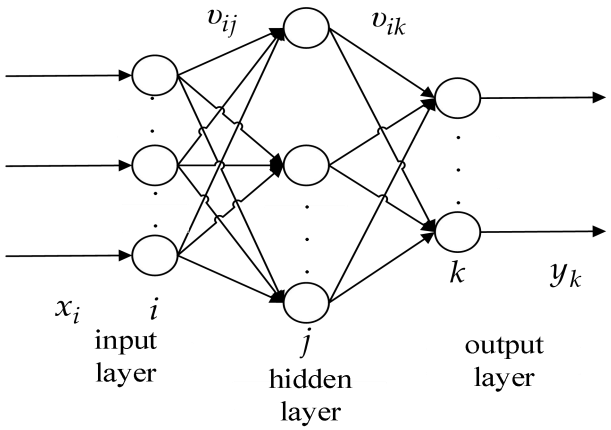


Figure 2.11: BP Neural Network

The structure of BP network approximation is shown in Figure 2.12, where *k* represents the iterative steps of the network, BP is the network approximation, *y(k)* is the actual output of the controlled object, and $y_n(k)$ is the output of the approximation. The values of the system output *y(k)* and input *u(k)* are used as inputs to the approximation, and the error between the system output and the network output is used as the adjustment signal of the approximation.

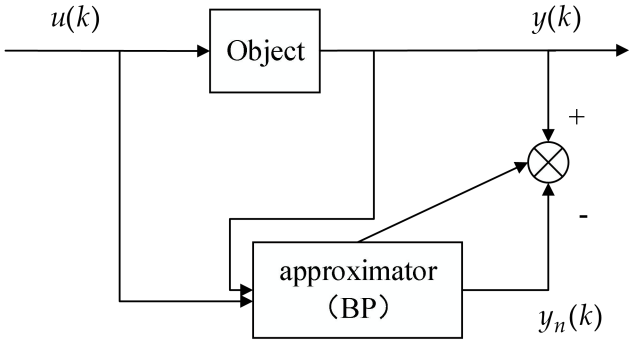


Figure 2.12: BP Network Approximation Structure Diagram

The training process of the BP network is as follows: forward propagation refers to the transmission of input signals from the input layer through the hidden layer to the output layer. If the output layer obtains the expected output, the learning algorithm ends; Otherwise, proceed to back propagation.

BP neural network is a multi-layer feed forward neural network trained according

to the error back propagation algorithm, which continuously adjusts the neuron weights through gradient descent method to approach the minimum error. Compared to RBF (Radical Basis Function) neural networks, their network structure is relatively simple, with fewer hidden layer neurons and less computational complexity. Assuming the number of nodes in the input layer is n, the number of nodes in the hidden layer is *l*, and the number of hidden layers is *l*, it is necessary to repeatedly try to obtain the optimal value to minimize the approximation error, and the number of nodes in the output layer is m. The weight from input layer to hidden layer, the weight from hidden layer to output layer is v_{ij}, the offset from input layer to hidden layer is a_j, and the offset from hidden layer to output layer is bk. The learning rate is η , and the excitation function is *g(x)*. The excitation function is *g(x)*, taking the sigmoid function.

The form is:

$$f(x) = \frac{1}{1+e^{-x}} \qquad \text{Equation 2.22}$$

For BP neural networks, the hidden layer output H_j is:

$$H_j = g(\sum_{i=1}^{n} \upsilon_{ij} x_i + a_j) \qquad \text{Equation 2.23}$$

The output layer output O_k is:

$$O_k = \sum_{j=1}^{l} H_j \upsilon_{jk} + b_k \qquad \text{Equation 2.24}$$

Train the BP neural network using the gradient descent method, set the expected output as Y_k, and take the error formula as:

$$E = \frac{1}{2}\sum_{k=1}^{m}(Y_k - O_k)^2 \qquad \text{Equation 2.25}$$

If Y_k-O_k=e_k, then E can be expressed as:

$$E = \frac{1}{2}\sum_{k=1}^{m} e_k{}^2 \qquad \text{Equation 2.26}$$

In the above formula, $i = 1\cdots n, j = 1\cdots l, k = 1\cdots m.$

The training process of neural networks uses the gradient descent method to adjust the network connection weights, so that the output error gradually decreases. Therefore, the weights from the hidden layer to the output layer are corrected as follows:

$$\begin{cases} \upsilon_{ij} = \upsilon_{ij} + \eta H_j(1-H_j)x_i\sum_{k=1}^{m}\upsilon_{jk}e_k \\ \upsilon_{jk} = \upsilon_{jk} + \eta H_j e_k \end{cases} \qquad \text{Equation 2.27}$$

The advantages of BP neural network are as follows:

i. As long as there are enough hidden layers and hidden layer nodes, BP network can approximate any flying thorn dark star mapping relationship.

ii. The learning algorithm of BP network belongs to the global approximation algorithm and has strong generalization ability.

iii. The correlation information between the input and output of the BP network is distributed and stored in the connection weights of the network. The damage of individual neurons only has a small impact on the input and output relationships, so the BP network has good fault tolerance.

The drawbacks of BP neural network are as follows:

i. There are many parameters to be optimized and the convergence speed is slow.

ii. The objective function has multiple extreme points, and learning by gradient descent method can easily fall into local minima.

iii. It is difficult to determine the number of hidden layers and hidden layer nodes. At present, there is no good way to determine the specific network structure based on specific problems, and it still needs to be tried based on experience.

Due to its excellent approximation properties and generalization ability, BP networks can be used for the design of neural network controllers. However, due to the slow convergence speed of the BP neural network, it is difficult to adapt to the requirements of real-time control.

2.7 Optimal theory

The theory of quadratic optimal control is one of the most important research achievements in modern control theory research. The mathematical expression of its quadratic performance index has distinct practical physical significance. Moreover, its optimal control quantity can be expressed as a linear form of state feedback quantity and expected value, with a simple mathematical expression. Closed loop control can be achieved through state feedback. The form of state feedback control is simple and easy to implement in engineering applications. Therefore, the theory of quadratic optimal control is of great significance for optimal control problems in engineering (Fuhrer & Fuica, 2024).

For a linear system:

$$\dot{x} = Ax + Bu \qquad \text{Equation 2.28}$$

Where, x is an n-dimensional state vector, u is an m-dimensional state vector, A is an $n \times n$ dimensional state coefficient matrix, B is an $n \times m$ dimensional control coefficient matrix. The matrix A and B satisfy the following condition: the rank r of the matrix $D = \left[B \middle| AB \middle| A^2 B \middle| \cdots \middle| A^{n-1} B \right]$ is n, which means that the system is completely controllable. Then, the quadratic objective function can be established as:

$$J = \frac{1}{2} \int_0^\infty \left(x^T Q x + u^T R u \right) dt \qquad \text{Equation 2.29}$$

Where, Q a is positive definite or semi-positive-definite $n \times n$ dimensional weighted state matrix, Q is usually a diagonal constant matrix, and the elements on the diagonal Q_{ii} represent the degree of importance attached to the corresponding error component x_i. The more important the error component is, the smaller it is hoped to be, and correspondingly, the larger its weighting coefficient Q_{ii} should be achieved. R is a positive definite $m \times m$ weighting matrix represents the constraints or requirements for control in dynamic processes.

The purpose of optimal control is to minimize the performance index J to the minimum value J_{min}, and its essence lies in using minimal control to maintain small errors, thus achieving the goal of comprehensive optimization of energy and error. When J reaches J_{min}, the control vector u is

$$u = -Kx \qquad \text{Equation 2.30}$$

Where, K is the optimal feedback gain matrix, and:

$$K = R^{-1} B^T P \qquad \text{Equation 2.31}$$

Where, R is the weight coefficient, P is the solution to the Riccati equation:

$$A^T P + PA - PBR^{-1}B^T P + Q = 0 \qquad \text{Equation 2.32}$$

2.8 H-infinity theory

In the early 1980s, Zames et al. proposed the H-infinity optimization control theory (Liu, 2021). He introduced the H-infinity norm as the objective function in his paper to optimize the design of the system, unveiling the prelude to the H-infinity control theory. In 1982, renowned American scholar Doyle invented a tool called singular value structure to verify the robustness of H-infinity norm performance indicators. Subsequently, the H-infinity control theory achieved significant development. In 1988, Doyle et al. published their famous DGKF paper at the American Conference on Control, first proposing a simplified state space solution formula for H-infinity control problems, which became a milestone in the field of H-infinity control problems. The results of this paper indicate that only two Riccati equations need to be solved to obtain the solution of the H-infinity controller, which greatly promotes the development of H-infinity control theory.

Linear time invariant continuous time system：

$$\begin{aligned} \dot{x}(t) &= Ax(t) + Bw(t) \\ z(t) &= Cx(t) + Dw(t) \end{aligned} \qquad \text{Equation 2.33}$$

Where, $x \in R^n$ is the state of the system, is the tuned output of the interested system, and $w \in R^q$ is the external disturbance input. If the tuned output *z(t)* of the system always remains "small" for a certain type of external disturbance signal *w(t)*, then a system with such performance is considered to have "good" performance. In fact, this indicates that external disturbances have a minimal impact on the system, thus reflecting the system's ability to suppress external disturbances (Bortoff et al., 2022 & Song et al., 2022). A

standard method for quantifying system performance is to consider the gain Γ of the system:

$$\Gamma = \sup_{w \neq 0} \frac{\text{size}(z)}{\text{size}(w)} \qquad \text{Equation 2.34}$$

Where, size(z) represents a certain measure of the size of signal z. Γ measures the size of the system output signal z corresponding to the worst-case disturbance input under zero initial conditions. Therefore, the smaller the system gain, the better the system performance.

For equation (2.33), its transfer function is $\boldsymbol{T}(s) = \boldsymbol{C}(s\boldsymbol{I} - \boldsymbol{A})^{-1}\boldsymbol{B} + \boldsymbol{D}$. The H-infinity norm of is defined as:

$$\left\|\boldsymbol{T}(s)\right\|_\infty = \sup_w \sigma_{\max}(\boldsymbol{T}(jw)) \qquad \text{Equation 2.35}$$

The peak value of the maximum singular value of the system frequency response.

For EE (Energy to Energy) gain Γ_{ee} :

$$\Gamma_{ee} = \sup_{\|w\|_2 \leq 1} \|z\|_2 \qquad \text{Equation 2.36}$$

There is an explanation in the frequency domain: it happens to be equal to the H-infinity norm of the transfer function matrix $\boldsymbol{T}(s)$, that is, $\Gamma_{ee} = \left\|\boldsymbol{T}(s)\right\|_\infty$. For a given constant $\gamma > 0$, the system is asymptotically stable and $\left\|\boldsymbol{T}(s)\right\|_\infty < \gamma$, if and only if a symmetric matrix P exists, so that matrix inequality holds. This conclusion is the famous bounded real lemma.

$$\begin{bmatrix} \boldsymbol{A}^T\boldsymbol{P}+\boldsymbol{P}\boldsymbol{A} & \boldsymbol{P}\boldsymbol{B} & \boldsymbol{C}^T \\ \boldsymbol{B}^T\boldsymbol{P} & -\gamma\boldsymbol{I} & \boldsymbol{D}^T \\ \boldsymbol{C} & \boldsymbol{D} & -\gamma\boldsymbol{I} \end{bmatrix} < \boldsymbol{0} \qquad \text{Equation 2.37}$$

By solving optimization problems

$$\begin{aligned} &\min \gamma \\ \text{s.t.} \quad &\begin{bmatrix} \boldsymbol{A}^T\boldsymbol{P}+\boldsymbol{P}\boldsymbol{A} & \boldsymbol{P}\boldsymbol{B} & \boldsymbol{C}^T \\ \boldsymbol{B}^T\boldsymbol{P} & -\gamma\boldsymbol{I} & \boldsymbol{D}^T \\ \boldsymbol{C} & \boldsymbol{D} & -\gamma\boldsymbol{I} \end{bmatrix} < \boldsymbol{0} \\ &\boldsymbol{P} > \boldsymbol{0} \end{aligned} \qquad \text{Equation 2.38}$$

Then the solution for the optimal H-infinity performance analysis of the system can be obtained. The optimal value of problem (2.38) is the optimal H-infinity performance index of equation (2.33). The standard H-infinity control problem is shown in Figure 2.13.

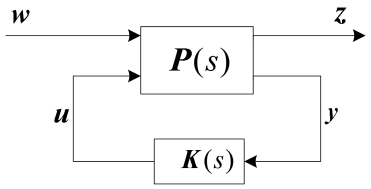


Figure 2.13: Standard H-infinity Control

$P(s)$ is a linear time-invariant system described by the following state space:

$$\begin{aligned} \dot{x} &= Ax + B_1 w + B_2 u \\ z &= C_1 x + D_{11} w + D_{12} u \\ y &= C_2 x + D_{21} w + D_{22} u \end{aligned} \qquad \text{Equation 2.39}$$

Where, $x \in R^n$ is the state vector, $u \in R^m$ the control input, $y \in R^p$ the measurement output, $z \in R^r$ the modulated output, $\omega \in R^q$ the external disturbance, and $K(s)$ is the controller. A, B_1, B_2, C_1, D_{11}, D_{12}, C_2, D_{21}, D_{22} is the constant matrices, and $A \in R^{n\times n}$, $B_1 \in R^{n\times q}$, $B_2 \in R^{n\times m}$, $C_1 \in R^{r\times n}$, $D_{11} \in R^{r\times q}$, $D_{12} \in R^{r\times m}$, $C_2 \in R^{p\times q}$, and $D_{22} \in R^{p\times m}$. From input signal w, u to output

signal z, the object represented by the transfer function $K(s)$ of y is the augmented controlled object, which includes the actual controlled object and the weighting function set to describe the indicators, etc.

For equation (2.39), if $C_2=I$, $D_{21}=D_{22}=0$, then when the system meets the following conditions:

i. $(\boldsymbol{A}, \boldsymbol{B}_2)$ can be stable and detectable;

ii. $\boldsymbol{D}_{12} = \boldsymbol{0}$;

iii. $\boldsymbol{D}^T_{11}[\boldsymbol{C}_1 \quad \boldsymbol{D}_{11}] = [\boldsymbol{0} \quad \boldsymbol{I}]$

Then this system must be able to introduce a state feedback H-infinity controller

$$\boldsymbol{u} = \boldsymbol{K}\boldsymbol{x} \qquad \text{Equation 2.40}$$

so that the corresponding closed-loop system (2.41) is asymptotically stable, and the transfer function of this closed-loop system $T_{zw}(s)$ satisfies equation (2.42).

$$\begin{aligned} \dot{x} &= (A + B_2K)x + B_1w \\ z &= (C_1 + D_{12}K)x + D_{11}w \end{aligned} \qquad \text{Equation 2.41}$$

$$\left\| \boldsymbol{T}_{zw}(s) \right\|_\infty = \left\| (\boldsymbol{C}_1 + \boldsymbol{D}_{12}\boldsymbol{K})[s\boldsymbol{I} - (\boldsymbol{A} + \boldsymbol{B}_2\boldsymbol{K})]^{-1}\boldsymbol{B}_1 + \boldsymbol{D}_{11} \right\|_\infty < \gamma \qquad \text{Equation 2.42}$$

In the above equation, a positive number as small as possible is selected to reduce the adverse impact of disturbances on the system.

To solve the feedback gain matrix of this system, first obtain the positive definite solution P of the Riccati equation (2.43), and then obtain the control gain of this system based on Equation (2.40) (Bortoff et al., 2022 & Song et al., 2022).

$$\boldsymbol{A}^T\boldsymbol{P}+\boldsymbol{P}\boldsymbol{A}-\boldsymbol{P}(\boldsymbol{B}_2\boldsymbol{B}_2{}^T-\gamma^{-2}\boldsymbol{B}_1\boldsymbol{B}_1{}^T)\boldsymbol{P}+\boldsymbol{C}_1{}^T\boldsymbol{C}_1=\boldsymbol{0} \quad \text{Equation 2.43}$$

$$\boldsymbol{K}=-\boldsymbol{B}_2{}^T\boldsymbol{P} \quad \text{Equation 2.44}$$

2.9 Review of WTGS Control Strategies

There are many control strategies used for wind turbine control currently, including traditional PID control and fuzzy control. There is also optimal control, artificial neural network control, adaptive control, sliding mode control, *etc*. There is also hybrid control that combines multiple control methods.

2.9.1 PID Control

The PID controller is the most widely used and mature control strategy in the industrial field, and it is also the most used control strategy in variable pitch control of wind power generation. PID control plays a good role in the control process because of its simple design, good stability and accuracy. Its biggest advantage is that it does not depend on the precise model of the wind power generation system. Through debugging to determine the parameters, it plays a certain control role and can suppress the vibration of the wind turbine. However, its disadvantages are also obvious. When the control system has higher order, more variables, coupling and uncertain factors, the control effect is not ideal. Liu and Gao (2016) adopted PID control to ensure the control effect at the linear operating point, but its overall effect is not good, and it cannot effectively deal with random interference.

In order to achieve better control results, PID is often combined with other control strategies. Yuan et al. (2019) combined PID with artificial bee colony (ABC) algorithm, then conducted an optimization study on the parameters of the pitch controller for large

wind turbines. Cheng (2021) and Zhang et al. (2022) have combined PID technology with fuzzy control, fuzzify all data, select power error e and power deviation change rate ec as inputs for fuzzy inference, adjust and correct the three parameters of the PID controller in real-time according to fuzzy rules, and finally use the center of gravity method for fuzzy resolution. This control method can ensure the stable operation of wind turbines when performing constant rate control on wind turbines, but it has not simulated the actual wind speed, nor considered the three-dimensional model of wind speed and tower shadow effect, resulting in certain limitations. Fan and Mu (2022) incorporates an adaptive neuron fuzzy inference system for wind speed evaluation on the basis of fuzzy PID, using input rotor speed and pitch angle as inputs to the neural network and wind speed as output parameters, thus effectively estimating wind speed to adjust the control system.

2.9.2 Fuzzy Control

Fuzzy control describes the dynamic characteristics and performance indexes of a system by using fuzzy language and language rules. Fuzzy control does not need accurate mathematical model, which avoids the difficulty of establishing system model and has strong practical engineering significance. In the process of wind turbine control, because the wind speed and direction change all the time, it is often difficult to set up the rule base empirical values of the dynamic load of the system. As a result, the fuzzy control is very difficult to control the dynamic load of the wind turbine, and the optimization effect of the dynamic load of the wind turbine is not very obvious.

Through a detailed analysis of the control system of the wind power generator, Kong and Wang (2008) designed the fuzzy controller of the system with the output power deviation as the input value of the system control and the variation of the pitch angle and

wind wheel speed as the output value. Bustan and Moodi (2022) proposes an adaptive interval 2 fuzzy controller suitable for variable speed variable pitch wind turbines. This control method can ignore wind speed estimation, thereby reducing computational complexity. Cao (2023) constructs a new T-S fuzzy model through model reconstruction, using piece-wise linear approximation theory and sector nonlinear modeling principles. The error generated by piece-wise linear approximation is used as a prerequisite variable for constructing the T-S fuzzy model. This method can approach error information faster, stabilize the controlled object quickly, reduce conservatism, and enhance robustness. Although the model reconstruction method can further introduce membership function information, as the number of fuzzy system rules increases, the computational complexity will further increase.

In order to achieve better control results, fuzzy control is often combined with other control methods. In addition to PID control mentioned in 2.9.1, fuzzy control can also be combined with neural networks, genetic algorithms, etc. to improve control effectiveness. Civelek (2020) adopted advanced intelligent genetic algorithm (AIGA) to optimize the fuzzy controller, which eliminates the inaccuracies that may occur when converting binary to decimal, thus avoiding errors. This controller can better achieve the control of wind turbine pitch angle, improve the stability of wind turbine output power, and provide a more stable power supply for the power grid.

2.9.3 Optimal Control

The optimal control method mainly relies on the mathematical model of the wind turbine control system, and finds the optimal solution of the system by using the state space analysis method, the extreme value principle and dynamic programming. The design

of the optimal power controller of wind turbine usually uses the weighted quadratic function of the state output value and the control input value as the performance index of the control object. At the same time, it must consider the dynamic performance and economic index of wind turbine. At present, in the application of optimal control in wind turbine control system, the output power is mainly optimized by controlling pitch angle, wind turbine torque, speed and generator torque (Yao et al., 2009). Optimal control is applied to the regulation of variable propeller control system of wind turbine to keep the output power constant (Khezami, 2012).

2.9.4 Artificial Neural Network Control

Neural network control strategy is a kind of intelligent control algorithm which simulates human neural behavior characteristics to carry out distributed parallel information processing. According to the complexity of the system network, it analyzes the interconnection relationship between each node in the neural network, so as to realize the purpose of processing system information (Valle et al., 2024). Neural network control has good self-learning and adaptive ability, which can analyze and calculate the potential rules between the two nodes through the input and output data corresponding to each other provided by the system. Finally, according to these potential rules, the new input data of the system is used to train and analyze the output value. The neural network can calculate the nonlinear mathematical model of the controlled system through the control law, and constantly update the output deviation value of the controlled object, so that it is infinitely close to any system nonlinear model, so that the uncertain model of the controlled object becomes more accurate, which is very suitable for use in the nonlinear time-varying and uncertain problems of wind turbine.

Zhu et al. (2023) used the self-learning and self-adaptive ability of neural network to identify and estimate the generator output power of wind turbine, and optimizes the output power in real time. In order to achieve dual control of wind turbine power and speed, BP neural networks were used to adaptive control the pitch angle and generator speed respectively (Chen, 2022). The two controllers controlled the wind turbine speed to maintain the optimal speed at low wind speeds and the generator speed to maintain constant power at medium wind speeds. The two controllers were independent and complementary, and were able to maintain constant wind turbine operation at different wind speed stages. This control method has good advantages in facing the complexity of wind turbines, but the BP neural network itself has some defects, which are prone to faults and falling into a dead zone.

Neural network algorithms can be used alone to design control systems, or combined with other control methods to form an intelligent control system with strong learning ability. For example, in combination with PID mentioned in 2.9.1 and fuzzy control mentioned in 2.9.2, neural networks can also be combined with other algorithms such as expert systems. Taghavipour (2012) has applies cerebellar model articulation controller (CMAC) and Radial Basis Function (RBF) neural network to the optimal control strategy of a split parallel hydraulic hybrid electric vehicle. Due to the limited training frequency, fast calculation speed, and better generalization ability of CMAC, compared with RBF neural networks, this controller has better control performance, and the CMAC network can maintain good sensitivity when facing multiple correlation factors.

2.9.5 Adaptive Control

Adaptive control is a control method that combines model identification and control design of a system. Predict the current state of the system based on its previous output and state values. Calculate the difference between the current output of the system and the expected value, predict the next output value of the controller, and change the parameters and structure of the control system at any time to ensure that the system remains in the optimal operating state. The main advantage of adaptive control is that it is less sensitive to changes in the parameters of the controlled object and unknown system states, making it very suitable for application in complex nonlinear time-varying systems. When the parameters of the controlled object change, the adaptive control system can ensure that the performance indicators initially set by the control system remain at the optimal value by adjusting the relevant parameters of the control system in real time.

Yang (2020) designed an L_1 adaptive controller. Construct an L_1 adaptive controller for this non affine and nonlinear system, which consists of three elements: state predictor, adaptive law, and control law. It can achieve constant power output of the system without the need for precise system dynamics models and wind speed measurements. Lasheen (2020) studied the design of a discrete-time L_1 adaptive pitch controller, which introduces the L_1 adaptive controller in discrete-time to eliminate errors caused by tracking reference signals and improve the steady-state performance of wind power systems. Based on this, Chen (2019) and Chen (2022) have combined disturbance estimation with feedback linearization, which can be used to adaptive compensate for actual disturbances and achieve adaptive feedback linearization control of the original nonlinear system. This control scheme has smaller tracking error and better dynamic performance, and has higher

robustness to wind power system parameter uncertainty, disturbance torque, and generator actuator faults.

2.9.6 Sliding Mode Control

Sliding mode control provides an effective way to solve the problem of system model imprecision and parameter perturbation. Sliding mode variable structure control can be regarded as discontinuous switching control, simple design, can realize the switch of the state of the control system like a switch, limit the state of the control system to the movement of the sliding mode surface, through the movement of the sliding mode tends to the origin, is not sensitive to parameter change and interference, and can achieve good control effect.

Huang et al. (2023) have designed an efficient sliding mode controller to limit the energy capture of the fan when the fan was operating in the high wind speed section. Ma (2020) has used high-order sliding mode control to improve the robustness of wind power systems and reduce bucket vibration phenomena, and estimates rotor speed and system disturbances using high-gain observers and disturbance observers respectively, in order to achieve maximum power point tracking of the wind turbine. At the same time, the combination of sliding mode variable structure control with other control methods, especially with fuzzy control and neural network intelligent control methods has become a new development direction.

2.9.7 Hybrid Control

The current development trend of wind power control technology is to combine various control algorithms to design a better controller. Liu et al. (2015) have designed the pitch controller based on the H_2/H-infinity hybrid optimization. Jiao et al. (2019) have

designed a variable-pitch controller based on the adaptive continuous neural theory. Ren et al. (2020) have combined back-propagation (BP) neural network and PID theory, then proposed a BP-PID pitch-controller. Yarmohammadi et al. (2020) have adopted the Gain Scheduling (GS) control algorithm to achieve the maximum power tracking of the wind turbine, and effectively adjust the pitch angle of the blades. The controller took the pitch angle as the control input and can adjust the rotor speed to the rated value even if the model of the wind turbine was uncertain (Colombo et al., 2020). Chen et al. (2020) combined an actor-critic structure and a Temporal-Difference (TD) algorithm to design an adaptive dynamic programming (ADP) controller that enabled real-time online learning. In the high wind speed area, the wind energy utilization coefficient was indirectly adjusted by changing the pitch angle, and the stable rotation speed of the rotor was maintained near the rated value. Yang et al. (2020) designed a novel L_1 adaptive controller, which controlled the fan pitch angle of the wind turbine to achieve stable output of generator speed and power under random wind speeds. Fan et al. (2022) combined fuzzy logic control theory with adaptive neuron-fuzzy theory to design a novel nonlinear hybrid control method, to adjust the pitch angle of wind turbines to make the captured wind energy constant. Tian et al. (2021) used the fuzzy cuckoo algorithm to tune the parameters of Active Disturbance Rejection Control (ADRC), which improved the applicability and implementability of the ADRC algorithm, and was successfully applied to the gradually dominant permanent magnet synchronous wind turbine. Asghar et al. (2022) have proposes a robust sliding mode method that uses blade pitch as the control input to adjust the rotor speed to a fixed rated value in the presence of uncertainty characterizing the wind turbine model to ensure that the wind turbine can operate at the specified value in high wind speed regions.

2.10 Research Gap

From the above literature, it can be seen that previous researchers have done a lot of research on pitch angle control, but there are still some problems.

i. Although some algorithms have good control effects, they are very complex and require accurate mathematical models of wind turbines. This is difficult to achieve in practical engineering applications.

ii. Although some algorithms are simple, they have poor control effects, such as long response time and large overshoot, or the control effect can only be good at certain points, but poor at other operating points.

Therefore, designing a controller with uncomplicated algorithms and excellent control effects is the research gap now.

T-S fuzzy theory or BP neural network have been introduced into the design of controllers to improve control effectiveness. T-S fuzzy control method is a very effective nonlinear control method. Its greatest advantage is that a complex nonlinear system is represented as a weighted sum of a group of simple linear subsystems, that is, a complex nonlinear problem is transformed into a linear problem on several small segments. When the system has some uncertainties, system parameters are unknown or human factors change, the control system can still achieve the desired characteristics. Formally, this approach is similar to the typical piece-wise linear model approach to nonlinear systems, and also similar to the approach of some locally linear smooth models to compound through the membership function that describes the global characteristics, but it is still a nonlinear dynamic system in essence.

Ma et al. (2019), Shi and Zhang (2019), Liu et al. (2019), Liu et al. (2021) and Wang and Li (2019) have introduced the specific application of T-S fuzzy model in nonlinear system stability control. The research results show that T-S fuzzy theory is indeed applicable to nonlinear dynamic systems with large variation range. Wind power system is a multi-variable and nonlinear time-varying strong coupling dynamic system. Meanwhile, because of the randomness of wind energy, when the wind speed changes greatly, the traditional control methods cannot achieve good control effect in the full wind speed range. At this point, the T-S fuzzy theory mentioned above is very applicable.

BP neural network also can be applied to the controller design to improve the global control effect. It is a multi-layer feed-forward neural network trained according to the error back-propagation algorithm, which continuously adjusts the neuron weights through gradient descent to approach the minimum error. Due to its excellent ability to approximate nonlinear mappings, the BP neural network has a wide range of applications in fields such as pattern recognition, image processing, system identification, function fitting, optimization calculation, optimal prediction, and adaptive control, so BP neural network is also suitable for nonlinear WTGS.

By combining T-S fuzzy theory with optimal control or H-infinity control, combining BP neural network with optimal control theory, hybrid high-performance controller can be designed.

2.11 Chapter Summary

This chapter reviews the types of wind turbines, as well as the structure and principles of wind turbines. And the working principle of the main subsystems of the wind turbine is introduced in detail, and mathematical models of each subsystem and wind speed

are established. This chapter also reviews the development of fuzzy control, as well as the characteristics and composition of T-S fuzzy models, and elaborates on the stability theory of T-S fuzzy systems. The basic principle of BP neural network is also introduced in this chapter. At the same time, several control methods for variable pitch systems are introduced, research gaps are identified, and new control strategies are proposed.

CHAPTER 3

METHODOLOGY

3.1 Introduction

This chapter presents methodology that is set out to achieve the stated objectives. The main objective of this research is to design novel high-performance hybrid variable pitch controller that can achieve minimal fluctuation in output power of WTG above the rated wind speed. When the wind speed changes, it is required to make corresponding changes in the pitch angle and wind energy utilization coefficient, while maintaining the rotor speed and output power at the rated values. Meanwhile, the controller should respond as quickly as possible and the overshoot should be as small as possible. The methodology main flowchart is shown in Figure 3.1.

From the main flowchart, it can be seen that the first main step is linearization. The detailed sub-steps are shown in Figure 3.2. The first sub-step is to process the wind turbine nonlinear mathematical model into standard form, the second sub-step is to get different linear matrix using partial derivatives at different operating points, then the linear subsystems are obtained. Here the improvement is the number of linear subsystems. If the number is too large, the calculation is too difficult. If the number is too small, the control accuracy is insufficient. Based on the range of wind speed changes, selecting six operating points are most suitable. They are: V_1=11 m/s, V_2=13 m/s, V_3=15 m/s, V_4=17 m/s, V_5=19 m/s and V_6=21 m/s.

The second main step is to design hybrid controllers based on the linear subsystems from the previous step.

Figure 3.3 shows the detailed steps of T-S optimal controller designing. The first sub-step is to determine the value of Q and R after testing many times. The second sub-step is to obtain the value of P by solving a Riccati equation. The third sub-step is to calculate the optimal feedback gain K_i, then get the sub-controller u_i. Then optimize the controller using T-S fuzzy theory to obtain a hybrid optimal controller. Here the improvement is using T-S fuzzy theory to optimize the controller.

Figure 3.4 shows the detailed steps of T-S H-infinity controller designing. The first sub-step is to determine the value of γ after testing many times. The second sub-step is to obtain the value of P by solving a Riccati equation. The third sub-step is to calculate the optimal feedback gain K_i, then get the sub-controller u_i. Then optimize the controller using T-S fuzzy theory to obtain a hybrid H-infinity controller. Here the improvement is using T-S fuzzy theory to optimize the controller.

Figure 3.5 shows the detailed steps of BP neural network optimal controller designing. The first sub-step is to determine the value of Q and R after testing many times. The second sub-step is to obtain the value of P by solving a Riccati equation. The third sub-step is to calculate the optimal feedback gain K_i. Then use wind speed, rotor speed, pitch angle as inputs, and use controller gain as output. Learn the mapping rules of input and output by using the BP neural network to optimize the controller. Here the improvement is Learning the mapping rules of input and output by using the BP neural network to optimize the controller.

The third main step is to analyse the performance of the proposed controller using critical parameters such as rotor speed and output power, then identify the controller with the fastest response time and lowest overshoot.

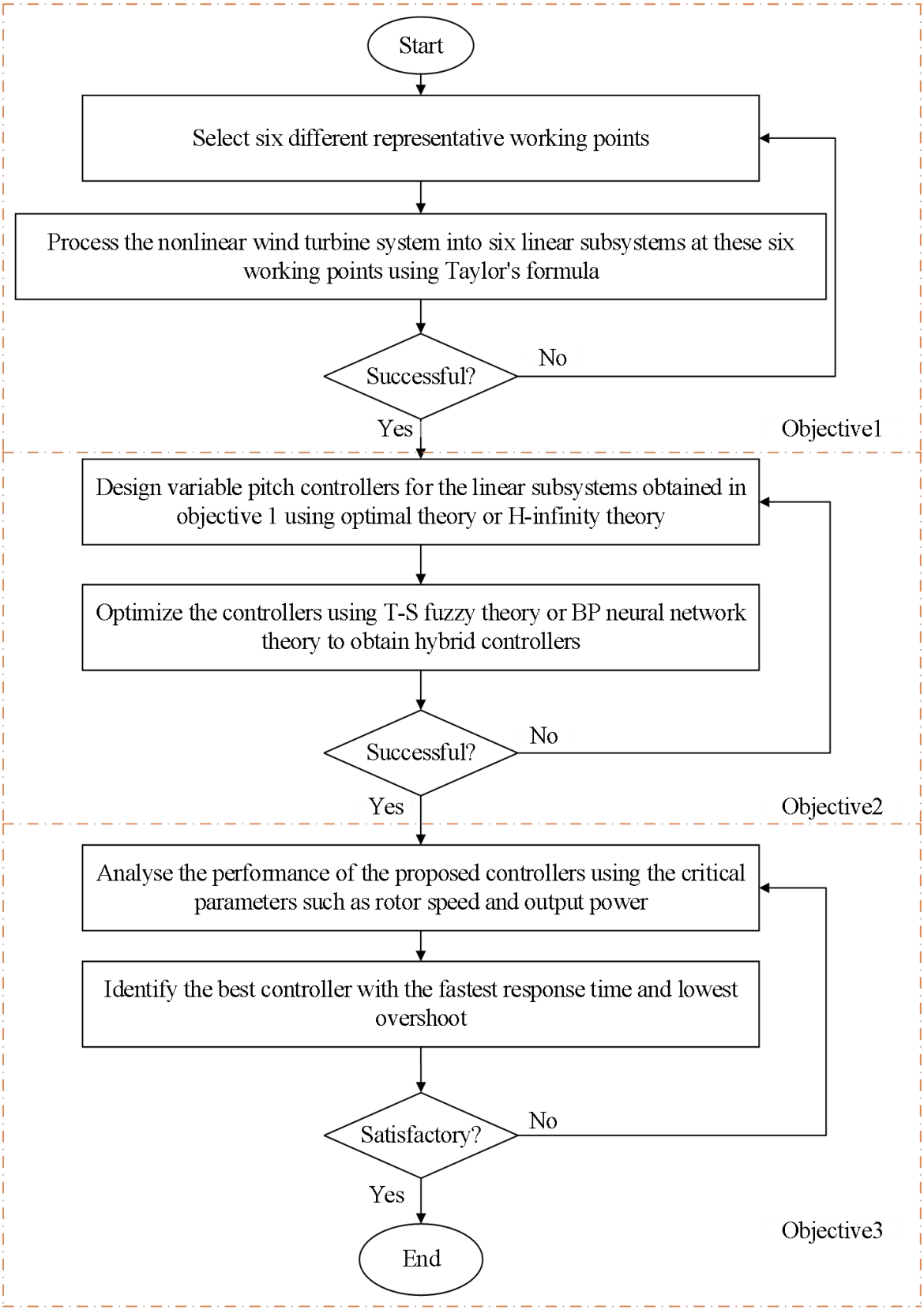


Figure 3.1: Methodology Flow Chart of the Hybrid Controller Designing

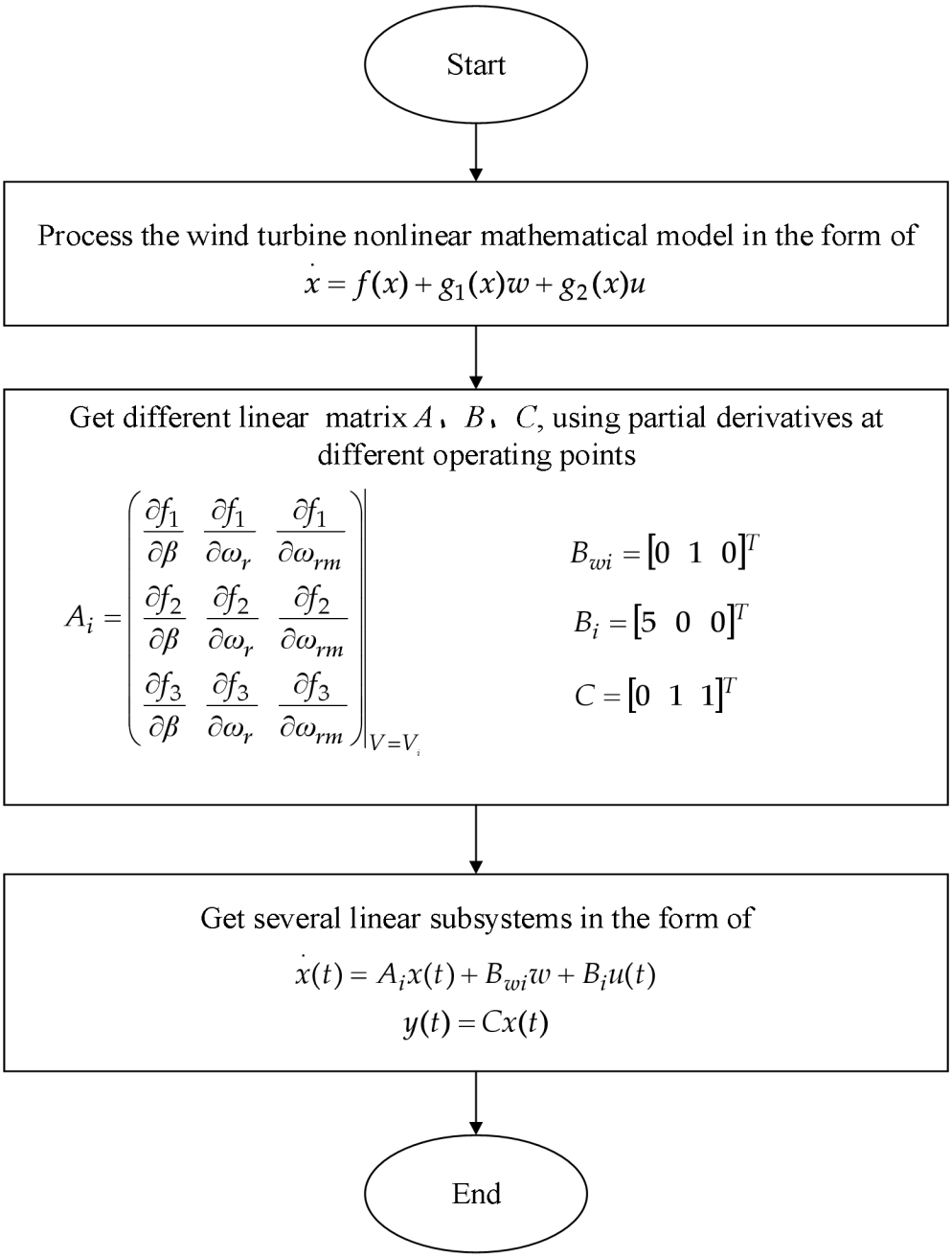


Figure 3.2: Sub Flow Chart for Linearizing the WTS in Objective 1

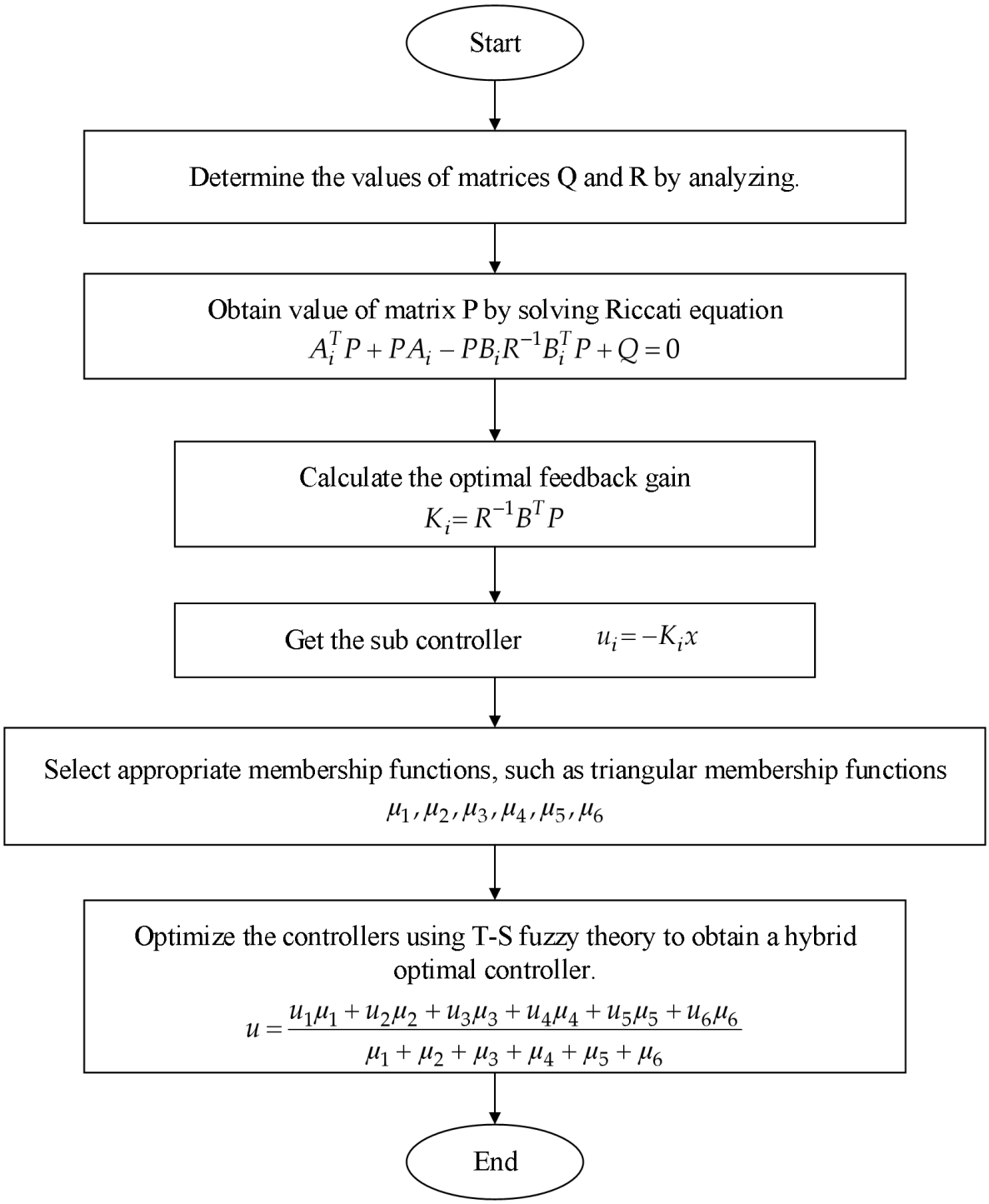


Figure 3.3: Design Flow Chart of T-S Optimal Controller in Objective 2

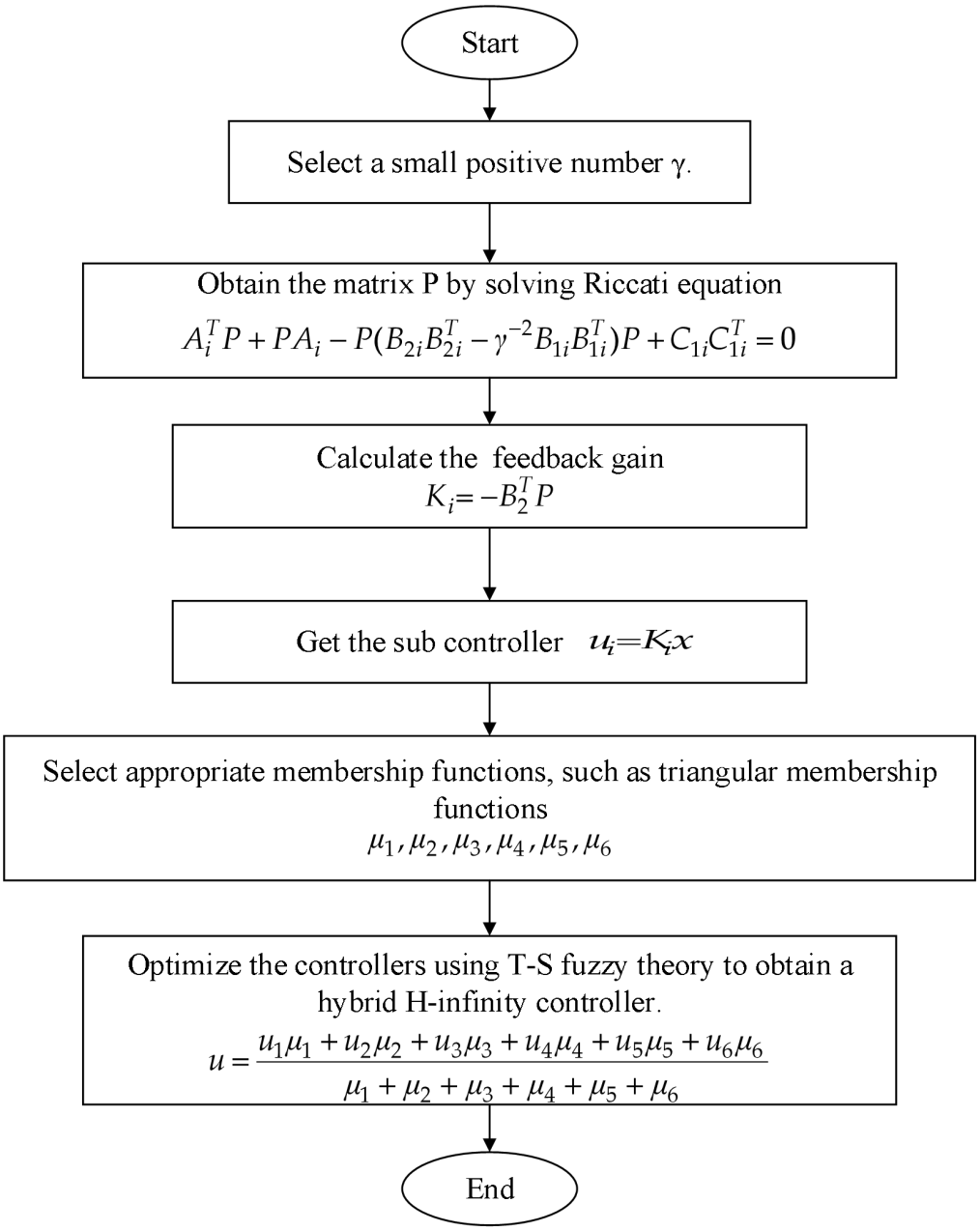


Figure 3.4: Design Flow Chart of T-S H-infinity Controller in Objective 2

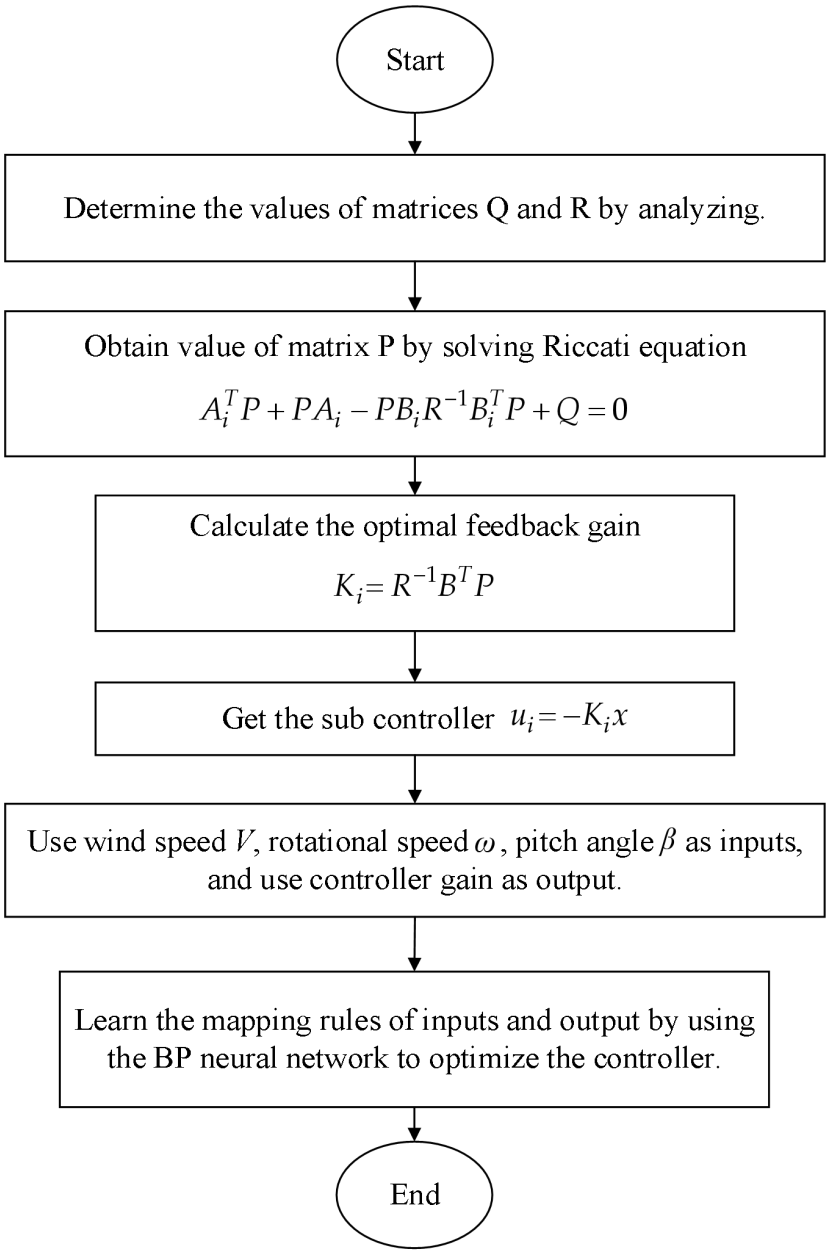


Figure 3.5: Design Flow Chart of BP Neural Network Optimal Controller in Objective 2

From Figures 3.3 and 3.4, it can be seen that the steps in the latter half of the controller design are the same, both using T-S fuzzy theory to integrate the sub controllers into one controller. The difference lies in the first half. Figure 3.3 adopts the optimal theory to design the sub controller, while Figure 3.4 adopts the H-infinity theory to design the sub controller. From Figures 3.3 and 3.5, it can be seen that the first half of the controller design steps for these two controllers are the same, both using optimal theory to design sub controllers. However, the theory used for integrating the sub controllers is different. Figure 3.3 adopts T-S fuzzy theory while Figure 3.5 adopts BP neural network theory. The design concepts of Figure 3.3 and Figure 3.5 are completely different and will not be compared here.

Taking the design of T-S optimal controller as an example, introduce the design principle of the controller.

Firstly, linearize the nonlinear wind power system at six operating points into a linear model, every linear model is

$$\dot{x} = A_i x + B_i u + B_{wi} w \qquad \text{Equation 3.1}$$

Secondly, the pitch controller for each subsystem is designed using H-infinity control theory, the subsystem controller is

$$u_i = K_i x \qquad \text{Equation 3.2}$$

Thirdly, by connecting the sub controllers through membership functions, the global pitch controller of the system is obtained, the global pitch controller is

$$u = -\sum_{i=1}^{l} h_i(x) u_i \qquad \text{Equation 3.3}$$

Under the action of the controller, the output power of the fan can be stabilized at the rated value no matter how the input wind speed changes. Compared with precise feedback linearization, the advantage of this method is its simple algorithm and low requirements for mathematical models. If the number of linearization points is sufficient and the membership function is appropriate, the system can approach the original nonlinear system infinitely, thereby effectively improving the modeling accuracy.

Next, the techniques, equations, and algorithms required for this study will be discussed. In Section 3.2, the Taylor formula is described, and then the nonlinear system of the wind turbine is processed into multiple linear subsystems at six operating points using the Taylor formula. In Section 3.3, optimal controllers are designed for each linear subsystem obtained in Section 3.2 using optimal control theory. In Section 3.4, H-infinity sub controllers are designed for each linear subsystem obtained in Section 3.2 using H-infinity control theory. In Section 3.5, utilizing T-S fuzzy theory and incorporating membership functions, several optimal sub controllers from Section 3.3 are integrated into a global hybrid T-S optimal controller. The same method can integrate several H-infinity sub controllers in Section 3.4 into a global hybrid T-S H-infinity controller. In Section 3.6, the BP neural network theory is combined with several optimal sub controllers from Section 3.3 to form a global hybrid BP neural network optimal controller. Finally, concluding remarks are given in Section 3.7.

3.2 Linearization

3.2.1 Taylor Formula

Taylor's formula is a very important content in higher mathematics, widely used in various fields such as differential calculus, quantum mechanics, engineering applications,

image processing and neural networks (Liu, 2022). The Taylor formula has the function of "simplifying complexity", which approximates some complex nonlinear functions as simple polynomial functions. The Taylor formula's function of simplifying complexity makes it a powerful tool for analyzing and researching many mathematical problems. Taylor expansion is one of the commonly used formulas for locally linearizing functions. However, from a geometric perspective, it uses tangent approximation instead of curve approximation, which is relatively rough and only near the balanced point can it have high accuracy and significance.

The system has a balanced operating point $(\boldsymbol{x}_0, \boldsymbol{u}_0)$, which satisfies

$$\boldsymbol{F}(\boldsymbol{x}_0, \boldsymbol{u}_0) = 0 \qquad \text{Equation 3.4}$$

The linear model of the system can be obtained using the Taylor series expansion method

$$\Delta\dot{\boldsymbol{x}} = \boldsymbol{A}\Delta\boldsymbol{x} + \boldsymbol{B}\Delta\boldsymbol{u} \qquad \text{Equation 3.5}$$

where, $\Delta\boldsymbol{x} = \boldsymbol{x} - \boldsymbol{x}_0$, $\Delta\boldsymbol{u} = \boldsymbol{u} - \boldsymbol{u}_0$, $\boldsymbol{A} = \left.\frac{\partial \boldsymbol{F}}{\partial \boldsymbol{x}}\right|_{\substack{\boldsymbol{x}=\boldsymbol{x}_0 \\ \boldsymbol{u}=\boldsymbol{u}_0}}$, $\boldsymbol{B} = \left.\frac{\partial \boldsymbol{F}}{\partial \boldsymbol{u}}\right|_{\substack{\boldsymbol{x}=\boldsymbol{x}_0 \\ \boldsymbol{u}=\boldsymbol{u}_0}}$.

3.2.2 Linearization of Wind Turbines

The nonlinear model of wind turbines is

$$\begin{cases} \dot{\beta} = \dfrac{1}{T_\beta}\left(\beta_r - \beta\right) \\ \dot{\omega}_r = \dfrac{1}{J}\left(T_{\text{aero}}\left(\beta, \omega_r\right) - T_{gen}\right) \\ \dot{\omega}_{rm} = \dfrac{1}{T_\omega}\left(\omega_r - \omega_{rm}\right) \end{cases} \qquad \text{Equation 3.6}$$

Where, β is the pitch angle, T_β is the time constant, β_r is the controlled quantity of pitch angle, ω_r is the turbine speed, J is the total rotation inertia of the fan and the generator, T_{aero} is the pneumatic torque of the fan, T_{gen} is the electromagnetic torque of the generator, ω_{rm} is the angular speed of the fan measured by speed sensor, T_ω is a time constant.

The above nonlinear mathematical model of the WTGS can be written in the form of equation 3.7

$$\dot{x} = f(x) + g_1(x)w + g_2(x)u \qquad \text{Equation 3.7}$$

x, $f(x)$, $g_1(x)$, $g_2(x)$ and u are shown in the following equations.

$$x = \begin{bmatrix} \beta & \omega_r & \omega_{rm} \end{bmatrix}^{\mathrm{T}} \qquad \text{Equation 3.8}$$

$$f(x) = \begin{bmatrix} -\dfrac{1}{T_\beta}\beta \\ \dfrac{1}{J}\left(T_{\text{aero}}\ (\beta, \omega_r) - T_{gen}\right) \\ \dfrac{1}{T_\omega}\left(\omega_r - \omega_{rm}\right) \end{bmatrix} \qquad \text{Equation 3.9}$$

$$g_1(x) = \begin{bmatrix} 0 & 1 & 0 \end{bmatrix}^{\mathrm{T}} \qquad \text{Equation 3.10}$$

$$g_2(x) = \begin{bmatrix} 1/T_\beta & 0 & 0 \end{bmatrix}^{\mathrm{T}} \qquad \text{Equation 3.11}$$

$$u = \beta_r \qquad \text{Equation 3.12}$$

The linearized linear model using Taylor's formula is as follows:

$$\begin{aligned} \dot{x}(t) &= Ax(t) + B_w w + Bu(t) \\ y(t) &= Cx(t) \end{aligned} \qquad \text{Equation 3.13}$$

If the system is linearized at multiple different working condition points *i*, multiple different linear models, that is, different coefficient matrices A、B_W、B、C, will be obtained.

$$A_i = \left[\begin{array}{ccc} \frac{\partial f_1}{\partial \beta} & \frac{\partial f_1}{\partial \omega_r} & \frac{\partial f_1}{\partial \omega_{rm}} \\ \frac{\partial f_2}{\partial \beta} & \frac{\partial f_2}{\partial \omega_r} & \frac{\partial f_2}{\partial \omega_{rm}} \\ \frac{\partial f_3}{\partial \beta} & \frac{\partial f_3}{\partial \omega_r} & \frac{\partial f_3}{\partial \omega_{rm}} \end{array} \right] \Bigg|_{V=V_i} \qquad \text{Equation 3.14}$$

$B_w = \begin{bmatrix} 0 & 1 & 0 \end{bmatrix}^T$, $B = \begin{bmatrix} 5 & 0 & 0 \end{bmatrix}^T$ and $C = \begin{bmatrix} 0 & 1 & 1 \end{bmatrix}^T$.

The wind turbine used here is the test prototype CART (controls advanced research turbine) from the National Renewable Energy Laboratory (NREL) in the United States. The main parameters are as follows: the wind turbine type is horizontal axis and upwind direction, the rated power is 600 kW, the rated wind speed is 11 m/s, the rated rotor speed is 41.5 r/min, which is 4.35 rad/s, the diameter of the wind turbine is 43.3 m, the rotational inertia of the fan is 2.58×10^5 kg·m^2, the rotational inertia of the generator is 6.41×10^4 kg·m^2, the operating speed of the variable pitch motor is -10-10 °/s, the displacement of the pitch motor is 0-30 °, the time constant of the variable pitch is 0.2 seconds.

Six working points are selected for linearization here. If too many points are selected, the calculation difficulty will increase. If too few points are selected, the control accuracy will be insufficient. The wind speed range in the research region is 11 m/s to 21 m/s, so these six points selected are: V_1=11 m/s, V_2=13 m/s, V_3=15 m/s, V_4=17 m/s, V_5=19 m/s and V_6=21 m/s, then the system is locally linearized into six linear sub-systems, the values of each element of the A_i matrix can be calculated from equation 3.14: A_{11}=-5, A_{12}=0,

A_{13}=0, A_{23}=0, A_{31}=0, A_{32}=10, A_{33}=-10. The values of elements A_{21} and A_{22} are shown in Table 3.1.

Table 3.1: Values of Elements A_{21} and A_{22}

V（m/s）	A_{21}	A_{22}
11	-0.0168	-0.0885
13	-0.0288	-0.1570
15	-0.0441	-0.2342
17	-0.0631	-0.3209
19	-0.0861	-0.4170
21	-0.1137	-0.5222

The six subsystems are:

Subsystem 1:
$$\begin{bmatrix} \dot{\beta} \\ \dot{\omega}_r \\ \dot{\omega}_{rm} \end{bmatrix} = \begin{bmatrix} -5 & 0 & 0 \\ -0.0168 & -0.0885 & 0 \\ 0 & 0 & 0 \end{bmatrix} \begin{bmatrix} \beta \\ \omega_r \\ \omega_{rm} \end{bmatrix} + \begin{bmatrix} 0 \\ 1 \\ 0 \end{bmatrix} w + \begin{bmatrix} 5 \\ 0 \\ 0 \end{bmatrix} u$$

Subsystem 2:
$$\begin{bmatrix} \dot{\beta} \\ \dot{\omega}_r \\ \dot{\omega}_{rm} \end{bmatrix} = \begin{bmatrix} -5 & 0 & 0 \\ -0.0288 & -0.1570 & 0 \\ 0 & 0 & 0 \end{bmatrix} \begin{bmatrix} \beta \\ \omega_r \\ \omega_{rm} \end{bmatrix} + \begin{bmatrix} 0 \\ 1 \\ 0 \end{bmatrix} w + \begin{bmatrix} 5 \\ 0 \\ 0 \end{bmatrix} u$$

Subsystem 3:
$$\begin{bmatrix} \dot{\beta} \\ \dot{\omega}_r \\ \dot{\omega}_{rm} \end{bmatrix} = \begin{bmatrix} -5 & 0 & 0 \\ -0.0441 & -0.2342 & 0 \\ 0 & 0 & 0 \end{bmatrix} \begin{bmatrix} \beta \\ \omega_r \\ \omega_{rm} \end{bmatrix} + \begin{bmatrix} 0 \\ 1 \\ 0 \end{bmatrix} w + \begin{bmatrix} 5 \\ 0 \\ 0 \end{bmatrix} u$$

Subsystem 4:
$$\begin{bmatrix} \dot{\beta} \\ \dot{\omega}_r \\ \dot{\omega}_{rm} \end{bmatrix} = \begin{bmatrix} -5 & 0 & 0 \\ -0.0631 & -0.3209 & 0 \\ 0 & 0 & 0 \end{bmatrix} \begin{bmatrix} \beta \\ \omega_r \\ \omega_{rm} \end{bmatrix} + \begin{bmatrix} 0 \\ 1 \\ 0 \end{bmatrix} w + \begin{bmatrix} 5 \\ 0 \\ 0 \end{bmatrix} u$$

Subsystem 5:
$$\begin{bmatrix} \dot{\beta} \\ \dot{\omega}_r \\ \dot{\omega}_{rm} \end{bmatrix} = \begin{bmatrix} -5 & 0 & 0 \\ -0.0861 & -0.4170 & 0 \\ 0 & 0 & 0 \end{bmatrix} \begin{bmatrix} \beta \\ \omega_r \\ \omega_{rm} \end{bmatrix} + \begin{bmatrix} 0 \\ 1 \\ 0 \end{bmatrix} w + \begin{bmatrix} 5 \\ 0 \\ 0 \end{bmatrix} u$$

Subsystem 6:
$$\begin{bmatrix} \dot{\beta} \\ \dot{\omega}_r \\ \dot{\omega}_{rm} \end{bmatrix} = \begin{bmatrix} -5 & 0 & 0 \\ -0.1137 & -0.5222 & 0 \\ 0 & 0 & 0 \end{bmatrix} \begin{bmatrix} \beta \\ \omega_r \\ \omega_{rm} \end{bmatrix} + \begin{bmatrix} 0 \\ 1 \\ 0 \end{bmatrix} w + \begin{bmatrix} 5 \\ 0 \\ 0 \end{bmatrix} u$$

3.3 Design of Optimal Controller

The linear model of the wind turbine has been obtained in the previous section. Here, linear optimal control theory can be used to design its controller, which can be treated as a quadratic optimal output tracking control problem.

For a linear system:

$$\dot{x} = Ax + Bu \qquad \text{Equation 3.15}$$

According to optimal theory, the control vector u is

$$u = -Kx \qquad \text{Equation 3.16}$$

Where, K is the optimal feedback gain matrix, and:

$$K = R^{-1}B^T P \qquad \text{Equation 3.17}$$

Where, R is the weight coefficient, P is the solution to the Riccati equation:

$$A^T P + PA - PBR^{-1}B^T P + Q = 0 \qquad \text{Equation 3.18}$$

According to equation 3.16, 3.17, 3.18, and combined with the linear subsystem obtained in section 3.2.2, the optimal controller can be designed for each linear subsystem.

i. Optimal controller design under the first operating condition

When the wind speed is 11 *m/s*, select appropriate weight values $Q_1 = 520$, $Q_2 = 15$, and according to equation 3.16 and 3.17, the value of K can be calculated as:

$$K_1 = [4.6 \quad 0.079]$$

Then the optimal controller u_1 for this subsystem is

$$u_1 = 4.6 \times \omega_r - 0.079 \times \beta - 23 \qquad \text{Equation 3.19}$$

ii. Optimal controller design under the second operating condition

When the wind speed is 13 *m/s*, select appropriate weight values $Q_1 = 2900$, $Q_2 = 6$, and according to equation 3.16 and 3.17, the value of K can be calculated as:

$$K_2 = [16.69 \quad 0.091]$$

Then the optimal controller u_2 for this subsystem is

$$u_2 = 16.69 \times \omega_r - 0.091 \times \beta - 64.015 \qquad \text{Equation 3.20}$$

iii. Optimal controller design under the third operating condition

When the wind speed is 15 *m/s*, select appropriate weight values $Q_1 = 5800$, $Q_2 = 6$, and according to equation 3.16 and 3.17, the value of K can be calculated as:

$$K_3 = [25.25 \quad 0.202]$$

Then the optimal controller u_3 for this subsystem is

$$u_3 = 25.25 \times \omega_r - 0.202 \times \beta - 92.23 \qquad \text{Equation 3.21}$$

iv. Optimal controller design under the fourth operating condition

When the wind speed is 17 *m/s*, select appropriate weight values $Q_1 = 11400$, $Q_2 = 7$, and according to equation 3.16 and 3.17, the value of *K* can be calculated as:

$$K_4 = [33.83 \quad 0.36]$$

Then the optimal controller u_4 for this subsystem is

$$u_4 = 33.83 \times \omega_r - 0.36 \times \beta - 120.38 \qquad \text{Equation 3.22}$$

v. Optimal controller design under the fifth operating condition

When the wind speed is 19*m/s*, select appropriate weight values $Q_1 = 15300$, $Q_2 = 6$, and according to equation 3.16 and 3.17, the value of *K* can be calculated as:

$$K_5 = [43.09 \quad 0.57]$$

Then the optimal controller u_5 for this subsystem is

$$u_5 = 43.09 \times \omega_r - 0.57 \times \beta - 150.8 \qquad \text{Equation 3.23}$$

vi. Optimal controller design under the sixth operating condition

When the wind speed is 21 *m/s*, select appropriate weight values $Q_1 = 19800$, $Q_2 = 5$, and according to equation 3.16 and 3.17, the value of *K* can be calculated as:

$$K_6 = [54.52 \quad 0.86]$$

Then the optimal controller u_6 for this subsystem is

$$u_6 = 54.52 \times \omega_r - 0.86 \times \beta - 188.28 \qquad \text{Equation 3.24}$$

3.4 H-infinity Controller Design

In section 3.3, optimal controllers were designed for each of the six linear subsystems obtained in section 3.2. This section will use H-infinity control theory to design H-infinity controllers for the six linear subsystems obtained in section 3.2.

For a linear system:

$$\begin{aligned} \dot{x} &= Ax + B_1 w + B_2 u \\ z &= C_1 x + D_{11} w + D_{12} u \\ y &= C_2 x + D_{21} w + D_{22} u \end{aligned} \qquad \text{Equation 3.25}$$

A state feedback H-infinity controller is as follows.

$$u = Kx \qquad \text{Equation 3.26}$$

Where, K can be calculated by the following equation.

$$K = -B_2^T P \qquad \text{Equation 3.27}$$

Where, P is the solution to the following equation.

$$\boldsymbol{A}^T \boldsymbol{P} + \boldsymbol{P}\boldsymbol{A} - \boldsymbol{P}(\boldsymbol{B}_2 \boldsymbol{B}_2^T - \gamma^{-2} \boldsymbol{B}_1 \boldsymbol{B}_1^T)\boldsymbol{P} + \boldsymbol{C}_1^T \boldsymbol{C}_1 = \boldsymbol{0} \qquad \text{Equation 3.28}$$

According to equation 3.26, 3.27, 3.28, and combined with the linear subsystem obtained in section 3.2.2, an H-infinity controller is designed for each linear subsystem.

i. H-infinity controller Design under the first operating condition

When the wind speed is 11 *m/s*, according to Equation 3.27 and Equation 3.28, the K_1 value can be calculated as:

$$K_1 = [-4.55 \quad 4444.28]$$

According to Equation 3.26, the H-infinity controller u_1 of this subsystem is

$$u_1 = 4444.28 \times \omega_r - 4.55 \times \beta - 19342 \quad \text{Equation 3.29}$$

ii. H-infinity controller Design under the second operating condition

When the wind speed is 13 *m/s*, according to Equation3.27 and Equation3.28, the K_2 value can be calculated as:

$$K_2 = [-6.22 \quad 4432.8]$$

According to Equation 3.26, the H-infinity controller u_2 of this subsystem is

$$u_2 = 4432.8 \times \omega_r - 6.22 \times \beta - 19226 \quad \text{Equation 3.30}$$

iii. H-infinity controller Design under the third operating condition

When the wind speed is 15 *m/s*, according to Equation3.27 and Equation3.28, the K_3 value can be calculated as:

$$K_3 = [-7.89 \quad 4429.2]$$

According to Equation 3.26, the H-infinity controller u_3 of this subsystem is

$$u_3 = 4429.2 \times \omega_r - 7.89 \times \beta - 19118 \quad \text{Equation 3.31}$$

iv. H-infinity controller Design under the fourth operating condition

When the wind speed is 17 *m/s*, according to Equation3.27 and Equation3.28, the K_4 value can be calculated as:

$$K_4 = [-9.61 \quad 4418.2]$$

According to Equation 3.26, the H-infinity controller u_4 of this subsystem is

$$u_4 = 4418.2 \times \omega_r - 9.61 \times \beta - 19011 \quad \text{Equation 3.32}$$

v. H-infinity controller Design under the fifth operating condition

When the wind speed is 19 *m/s*, according to Equation3.27 and Equation3.28, the

K_5 value can be calculated as:

$$K_5 = [-11.37 \quad 4412.24]$$

According to Equation 3.26, the H-infinity controller u_5 of this subsystem is

$$u_5 = 4412.24 \times \omega_r - 11.37 \times \beta - 18870 \qquad \text{Equation 3.33}$$

vi. H-infinity controller Design under the sixth operating condition

When the wind speed is 21 *m/s*, according to Equation3.27 and Equation3.28, the K_6 value can be calculated as:

$$K_6 = [-13.19 \quad 4406.95]$$

According to Equation 3.26, the H-infinity controller u_6 of this subsystem is

$$u_6 = 4406.95 \times \omega_r - 13.19 \times \beta - 18783 \qquad \text{Equation 3.34}$$

3.5 Hybrid Controller Design Based on T-S Fuzzy Theory

3.5.1 T-S Fuzzy Theory

According to section 2.5, for the following nonlinear systems:

$$\dot{\boldsymbol{x}} = \boldsymbol{F}(\boldsymbol{x}, \boldsymbol{u}) = \boldsymbol{f}(\boldsymbol{x}) + \boldsymbol{g}(\boldsymbol{x})\boldsymbol{u} \qquad \text{Equation 3.35}$$

the fuzzy formula model of this nonlinear system can be described as:

R_p^i： *If* $x_1(t)$ is M_1^i and…and *if* $x_n(t)$ is M_n^i， *Then*

$$\dot{\boldsymbol{x}}(t) = \boldsymbol{A}_i\boldsymbol{x}(t) + \boldsymbol{B}_i\boldsymbol{u}(t) \qquad \text{Equation 3.36}$$

i=1，2，…，l

Then, the equation of the whole nonlinear system can be expressed as follows:

$$\dot{\boldsymbol{x}}(t)=\sum_{i=1}^{l}h_i(\boldsymbol{x})[\boldsymbol{A}_i\boldsymbol{x}(t)+\boldsymbol{B}_i\boldsymbol{u}(t)] \qquad \text{Equation 3.37}$$

Where, $h_i(\boldsymbol{x})=\mu^i(\boldsymbol{x})/\sum_{j=1}^{l}\mu^j(\boldsymbol{x})$, $\mu^j(\boldsymbol{x})=\prod_{j=1}^{n}\mu_j^i(\boldsymbol{x})$ and it is the membership function of x belonging to M^i, and also represents the applicability of the rule i.

At present, there is no mature and effective method for establishing membership functions, and most of them are still based on experience and experiments. For the same fuzzy concept, different people will establish different membership functions. Although the forms are not completely the same, as long as they can reflect the same fuzzy concept, they can still achieve the same goal in solving and processing actual fuzzy information (Saini & Thakur, 2022).

The conclusion of the T-S model is that the fuzzy posterior is described using linear equations, which facilitates the design of relevant controllers using traditional linear control strategies. Tanaka et al. used the Parallel Distributed Compensation (PDC) method to design controllers, which involves designing a local linear state feedback controller for each linear subsystem. Pole placement design methods or linear quadratic optimal controller design methods can be used. The PDC controller design is as follows:

R_p^i : *if* $x_1(t)$ is M_1^i and$\cdots$and *if* $x_n(t)$ is M_n^i, *then* $\boldsymbol{u}_i(t)=-\boldsymbol{K}_i\boldsymbol{x}(t)$

According to the PDC approach, the control law of the entire system is the weighted sum of local feedback control for each subsystem, that is

$$\boldsymbol{u}(t)=\sum_{i}^{l}u_i(t)=-\sum_{i}^{l}h_i(x)\boldsymbol{K}_i\boldsymbol{x}(t) \qquad \text{Equation 3.38}$$

Where, $h_i(\boldsymbol{x})=\mu^i(\boldsymbol{x})/\sum_{j=1}^{l}\mu^j(\boldsymbol{x})$.

3.5.2 Design of T-S Optimal Hybrid Controller

According to the previous section, to design a T-S hybrid optimal controller, first the T-S fuzzy dynamic model of the system should be determined, then appropriate membership functions should be selected, and finally several optimal sub controllers will be integrated into a hybrid global controller through PDC method.

The T-S fuzzy dynamic model is:

Rule1: *If* V_1 = 11 m/s, β is about -2.6°, *then* $\dot{\boldsymbol{x}} = \boldsymbol{A}_1 x(t) + \boldsymbol{B}_1 u(t) + \boldsymbol{B}_{w1} w$, and $u_1 = K_1 x$

Rule2: *if* V_2 = 13 m/s, β is about 7.9°, *then* $\dot{\boldsymbol{x}} = \boldsymbol{A}_2 x(t) + \boldsymbol{B}_2 u(t) + \boldsymbol{B}_{w2} w$, and $u_2 = K_2 x$

Rule3: *if* V_3 = 15 m/s, β is about 14.6°, *then* $\dot{\boldsymbol{x}} = \boldsymbol{A}_3 x(t) + \boldsymbol{B}_3 u(t) + \boldsymbol{B}_{w3} w$, and $u_3 = K_3 x$

Rule4: *if* V_4 = 17 m/s, β is about 19.5°, *then* $\dot{\boldsymbol{x}} = \boldsymbol{A}_4 x(t) + \boldsymbol{B}_4 u(t) + \boldsymbol{B}_{w4} w$, and $u_4 = K_4 x$

Rule5: *if* V_5 = 19 m/s, β is about 23.3°, *then* $\dot{\boldsymbol{x}} = \boldsymbol{A}_5 x(t) + \boldsymbol{B}_5 u(t) + \boldsymbol{B}_{w5} w$, and $u_5 = K_5 x$

Rule6: *if* V_6 = 21 m/s, β is about 26.2°, *then* $\dot{\boldsymbol{x}} = \boldsymbol{A}_6 x(t) + \boldsymbol{B}_6 u(t) + \boldsymbol{B}_{w6} w$, and $u_6 = K_6 x$

A triangular membership function is adopted here. The equations based on the correspondence between wind speed, pitch angle, and membership function are as follows. The curve is shown in Figure 3.8.

When V_1 = 11 m/s, the pitch angle is about -2.6°, $\mu_1 = \begin{cases} \dfrac{7.9 - \beta}{7.9} & -2.6^\circ \le \beta \le 7.9^\circ \\ 0 & else \end{cases}$

When V_2 = 13 m/s, the pitch angle is about 7.9°, $\mu_2 = \begin{cases} \dfrac{\beta}{7.9} & 0^\circ \le \beta \le 7.9^\circ \\ \dfrac{14.6-\beta}{14.6-7.9} & 7.9^\circ \le \beta \le 14.6^\circ \\ 0 & else \end{cases}$

When V_3=15 m/s, the pitch angle is about 14.6°, $\mu_3 = \begin{cases} \dfrac{\beta-7.9}{14.6-7.9} & 7.9^\circ \le \beta \le 14.6^\circ \\ \dfrac{19.5-\beta}{19.5-14.6} & 14.6^\circ \le \beta \le 19.5^\circ \\ 0 & else \end{cases}$

When V_4=17 m/s, the pitch angle is about 19.5°, $\mu_4 = \begin{cases} \dfrac{\beta-14.6}{19.5-14.6} & 14.6^\circ \le \beta \le 19.5^\circ \\ \dfrac{23.2-\beta}{23.2-19.5} & 19.5^\circ \le \beta \le 23.2^\circ \\ 0 & else \end{cases}$

When V_5=19 m/s, the pitch angle is about 23.2°, $\mu_5 = \begin{cases} \dfrac{\beta-19.5}{23.2-19.5} & 19.5^\circ \le \beta \le 23.2^\circ \\ \dfrac{26.2-\beta}{26.2-23.2} & 23.2^\circ \le \beta \le 26.2^\circ \\ 0 & else \end{cases}$

When V_6=21 m/s, the pitch angle is about 26.2°, $\mu_6 = \begin{cases} \dfrac{\beta-23.2}{26.2-23.2} & 23.2^\circ \le \beta \le 26.2^\circ \\ 0 & else \end{cases}$

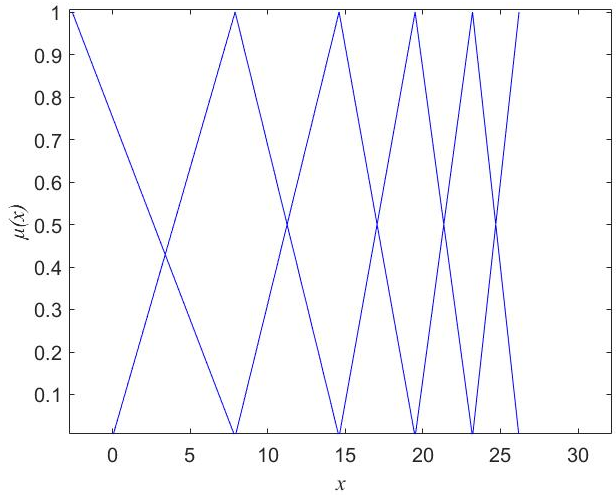


Figure 3.6: Curve of Membership Function

Finally, the pitch angle controllers of each linear subsystem are added up through the membership function to form the controller of the entire system:

$$u = \frac{\mu_1 u_1 + \mu_2 u_2 + \mu_3 u_3 + \mu_4 u_4 + \mu_5 u_5 + \mu_6 u_6}{\mu_1 + \mu_2 + \mu_3 + \mu_4 + \mu_5 + \mu_6} \qquad \text{Equation 3.39}$$

At this point, the design of the hybrid optimal controller based on the T-S fuzzy model is done.

3.5.3 Design of T-S H-infinity Hybrid Controller

The design process of the T-S H-infinity hybrid controller is identical to that of the T-S optimal hybrid controller. That is, firstly, the T-S fuzzy dynamic model of the system is determined, then the appropriate membership function is selected, and finally several sub controllers is integrated into a hybrid global controller through PDC method. In order to compare the control effects of the two controllers, the T-S fuzzy dynamic model and membership function of T-S H-infinity controller are the same as those of the T-S optimal controller. So the final format of the global controller obtained is still as shown in Equation

3.39, but it should be noted that the six sub controllers u_1, u_2, u_3, u_4, u_5 and u_6 are different from the optimal control. The flow chart is shown in Figure 3.4.

Hence, the design of the H-infinity controller based on the T-S theory is done.

3.6 Design of Global Controller Based on BP Neural Network

3.6.1 BP Neural Network Controller

According to the different roles of neural networks in controllers, neural network controllers can be divided into two categories: one is neural network control, which is an independent intelligent control system formed based on neural networks; Another type is neural network hybrid control, which utilizes the learning and optimization capabilities of neural networks to improve traditional hybrid control methods.

Neural network hybrid control is an intelligent control system that integrates the advantages of various branches of artificial intelligence and combines neural network technology with fuzzy control, expert control and so on. It has strong learning ability. Among them, a fuzzy neural network is formed by combining neural networks with fuzzy control, and a neural network expert system is formed by combining neural networks with expert systems. Neural network hybrid control can enable the system to have learning, reasoning, and decision-making capabilities simultaneously. This research combines neural networks with optimal control to form a neural network optimal control system.

3.6.2 Design of Hybrid BP Neural Network Optimal Controller

The control parameters of the BP global controller in this research are obtained based on the parameters of the six sub controllers in Section 3.3.2, and then by the BP

artificial neural network adaptive prediction model. The diagram of the controller parameter setting is shown in Figure 3.7.

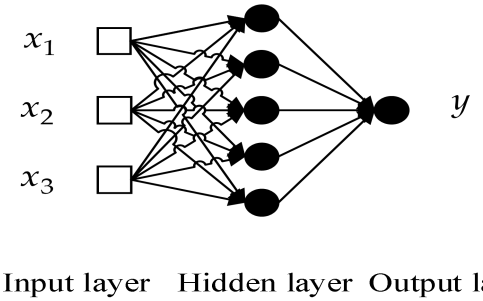


Figure 3.7: BP Neural Network Structure Diagram

When using the neural network toolbox to establish a BP neural network in MATLAB, it is necessary to normalize the training data obtained from the optimal controller. To avoid overestimating high amplitude data, it is necessary to standardize the data before training. This standardization method scales the data to its absolute maximum range and maintains the zero mean characteristic of structural vibration, limiting the data to the range of [0,1]. After standardization is completed, the data is divided into training sets, validation sets, and testing sets. Among them, the training set is used for network learning and training; The validation set is used to ensure that over fitting does not occur; The test set is used to evaluate the trained network model. The gradient descent method is used to achieve the learning and training of neural networks, and to establish a mapping relationship between input vectors and output quantities. By inputting gradient wind parameter vectors and random wind parameter vectors to provide information to the BP neural network, the optimal controller gain can be autonomously adjusted to adapt to changes in wind speed, and it has real-time prediction ability.

For this system, three input layer units, one output layer unit, and five hidden layer units are designed. The training frequency is set to 2000 times, with an error range of

0.000006 and a learning rate of 0.01. The input is the input wind speed, wind turbine speed, and pitch angle parameters, while the output is the optimal controller control parameter.

$$\begin{cases} x_1 = \omega_r \\ x_2 = \beta \\ x_3 = V \end{cases} \quad \text{Equation 3.40}$$

By combining the six sub controllers of Section 3.3.2, the BP hybrid controller can be designed.

For the wind turbine model, the basic system parameters are imported into the system to obtain the corresponding wind turbine speed and pitch angle parameters. Through continuous data collection, 200 sets of training data for the wind turbine speed, pitch angle, and optimal controller parameters at the corresponding wind speed are obtained for training the BP neural network. If there are too many data sets, it will slow down the training speed, and if there is too little data sets, it will be inaccurate, so 200 sets are very suitable. The training data is shown in Figure 3.8.

R^2 represents the proportion of data variance that the model can explain, and is typically used to compare the performance of different models. Generally speaking, the range of R^2 determination coefficient values is [0,1]. When R^2 is 1, it indicates that the model has perfectly predicted the data; From the above figure, it can be seen that the regression fitting curve has good goodness of fit and can effectively predict data.

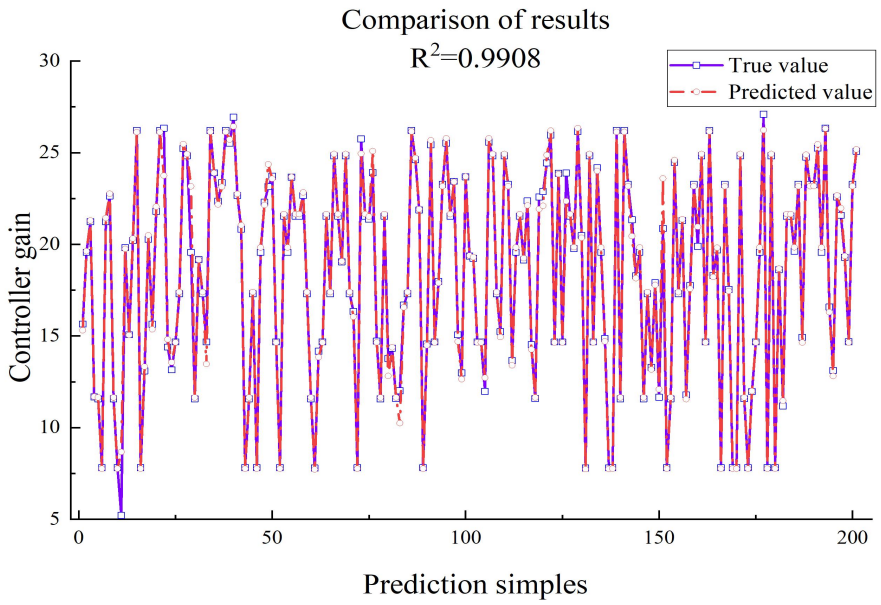


Figure 3.8: Data-set Prediction Chart

The trained BP neural network is loaded into the system, and real-time wind speed is input into the system. According to the system control transformation of wind speed and pitch angle, the controller gains corresponding to the wind speed and pitch angle values are obtained. In this way, the adjustment of the blade angle is completed, keeping the wind turbine in a stable state.

3.7 Modeling and Simulation in MATLAB/Simulink

The previous sections designed various variable pitch controllers based on different control algorithms. In order to verify the control effect of the controller, it is necessary to model and simulate the wind turbine model with the controllers in MATLAB. Modeling in MATLAB/Simulink is shown below. Figure 3.9 shows the overall model, Figure 3.10 shows the wind speed module, Figure 3.11 shows the wind turbine module, Figure 3.12 shows the overall controller module, Figure 3.13 shows the T-S Optimal controller module, Figure 3.14 shows the T-S H-infinity controller module, and Figure 3.15 shows the BP

neural network controller module. After modeling, simulation is carried out with different controllers under different wind conditions.

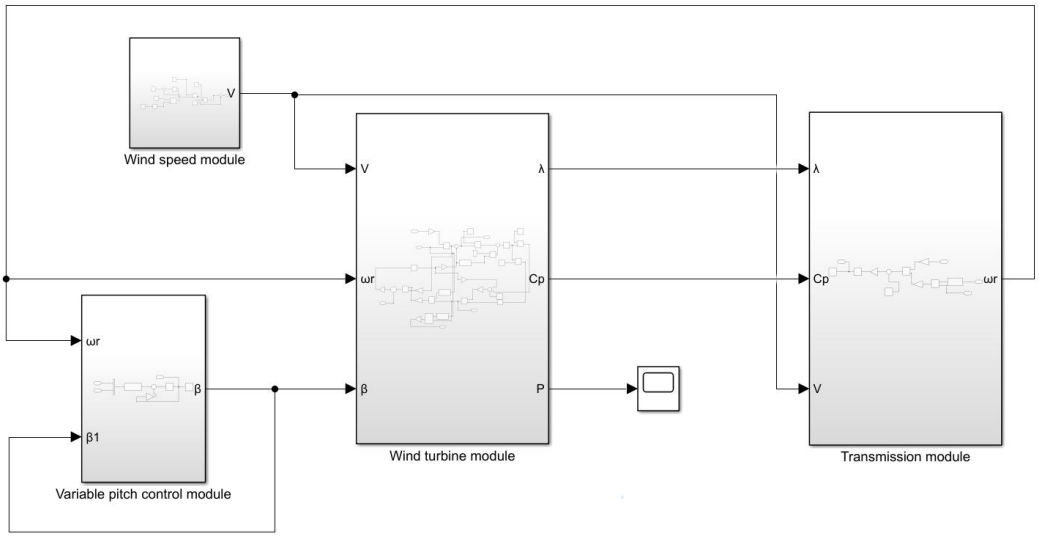


Figure 3.9: Overall model

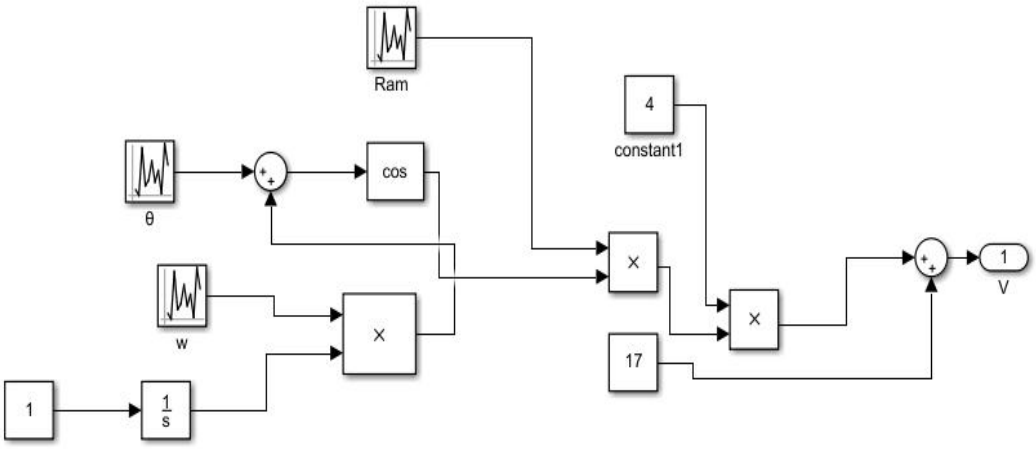


Figure 3.10: Wind speed module

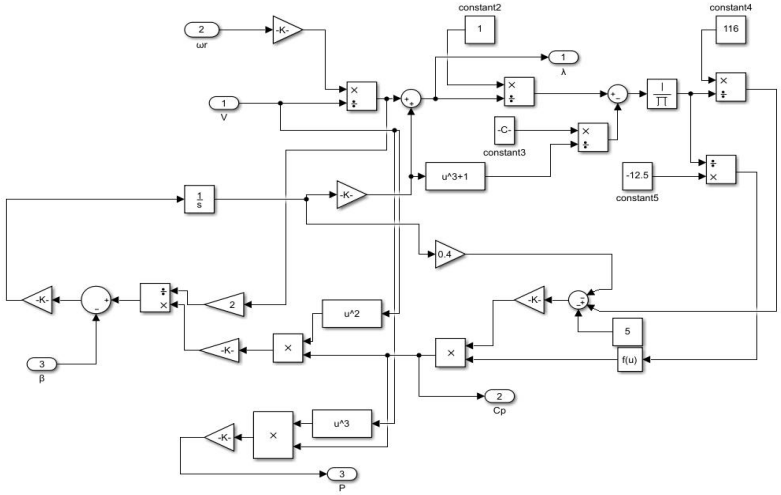


Figure 3.11: Wind turbine module

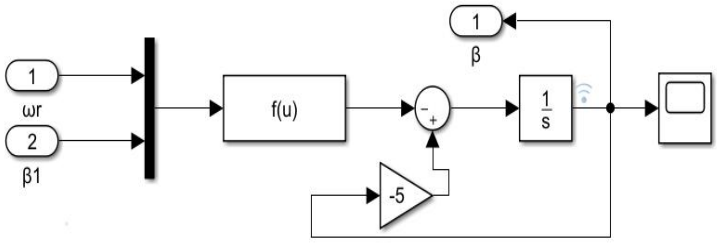


Figure 3.12: Overall controller module

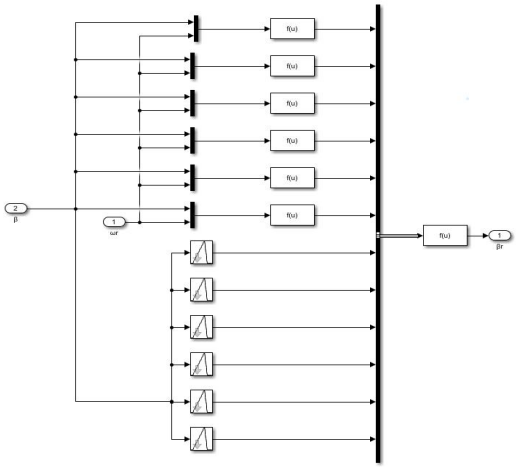


Figure 3.13: T-S Optimal controller module

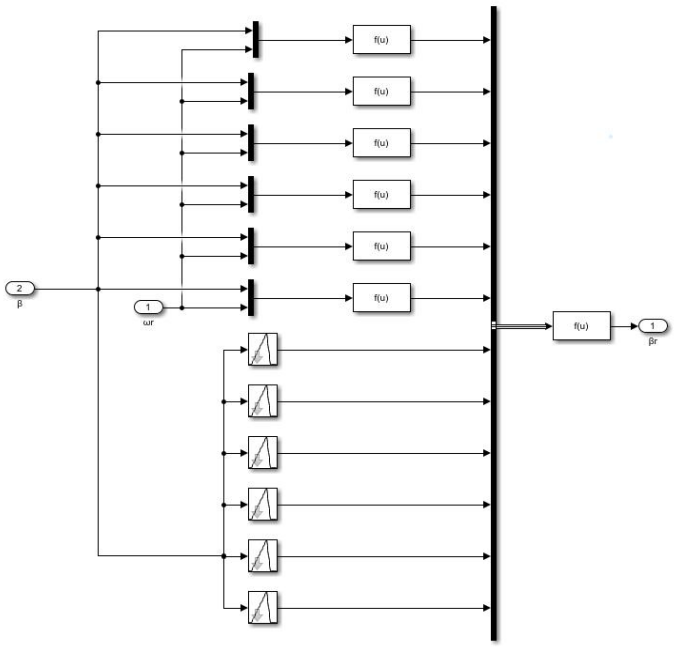


Figure 3.14: T-S H-infinity controller module

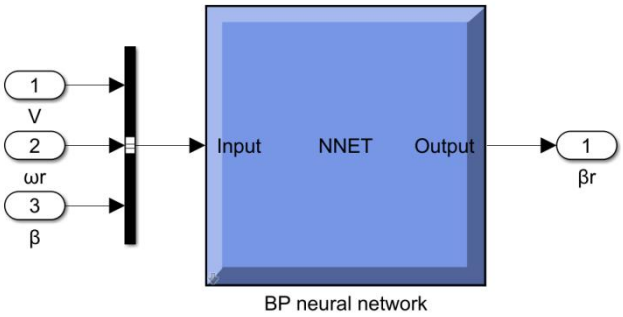


Figure 3.15: BP neural network controller module

3.8 Chapter Summary

This chapter mainly introduces three different design methods for controllers. They are the design of the optimal global controller based on the T-S fuzzy model, the design of the H-infinity global controller based on the T-S fuzzy model, and the design of the optimal global controller based on the BP neural network. Finally, modeling and simulation are carried out in MATLAB/Simulink.

CHAPTER 4

RESULTS AND DISCUSSION

The previous chapter elaborated on the design process of the controller and introduced modeling and simulation in MATLAB/Simulink. This chapter will present simulation results, analyze and compare the control performance of each controller, and identify the best controller.

4.1 Introduction

Section 4.2 shows the response curve of pitch angle, wind energy utilization coefficient, rotor speed, and output power when the wind speed changes without any variable pitch controller.

Section 4.3 shows the response curves of pitch angle, wind energy utilization coefficient, rotor speed, and output power under the action of T-S optimal hybrid controller when wind speed changes. These curves are analyzed and compared with the response curves under the PID controller.

Section 4.4 shows the response curves of pitch angle, wind energy utilization coefficient, rotor speed, and output power under the action of T-S H-infinity hybrid controller when wind speed changes. These curves are analyzed and compared with the response curves under the PID controller.

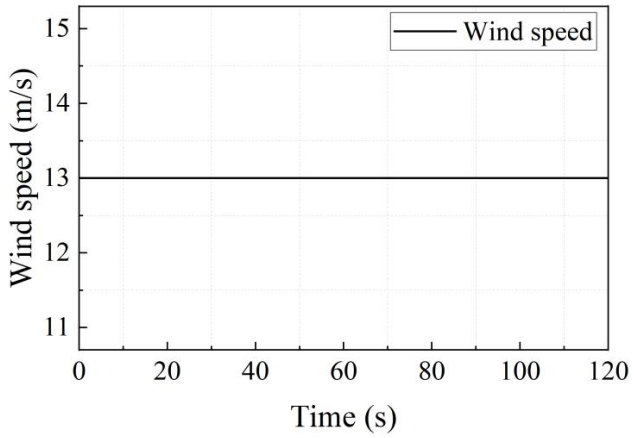
Section 4.5 shows the response curves of pitch angle, wind energy utilization coefficient, rotor speed, and output power under the action of BP neural network optimal

hybrid controller when wind speed changes. These curves are analyzed and compared with the response curves under the PID controller.

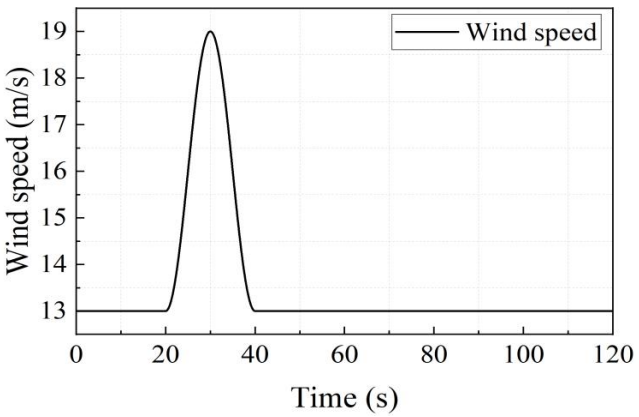
In Section 4.6, the curves under the three controllers are put together for comparison to identify the one with the best control effect.

4.2 Simulation results of WTGS without Controller

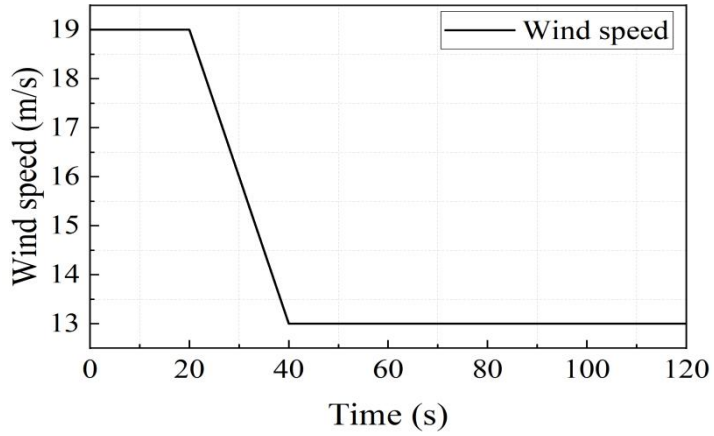
From the equations in Section 2.4, the profiles of each wind speed component and composite wind speed can be obtained, as shown in Figure 4.1.



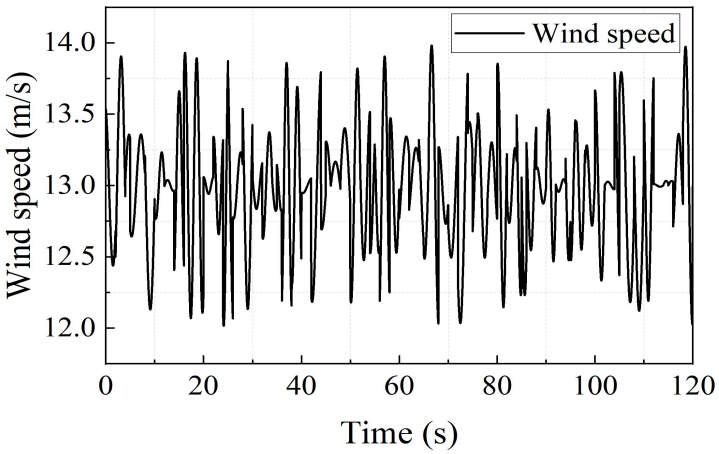
(a)Basic wind speed profile



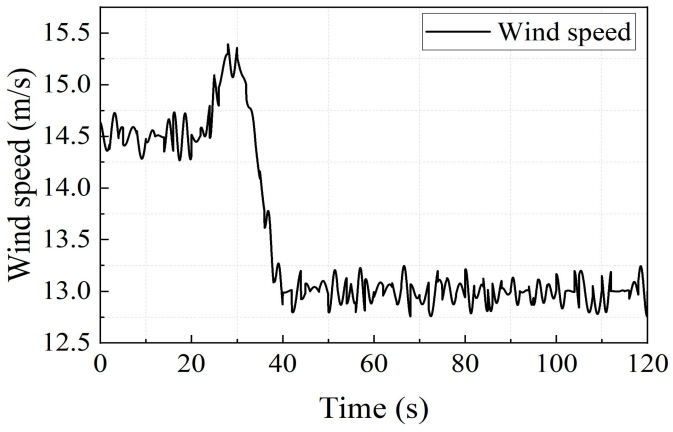
(b) Gust wind speed profile



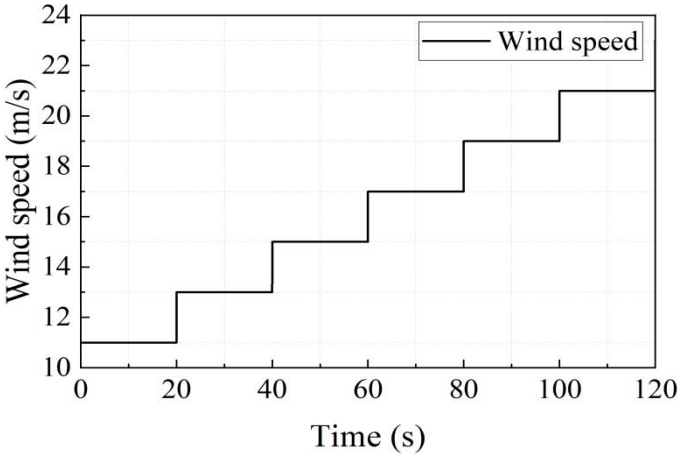
(c) Gradient wind speed profile



(d) Random wind speed profile



(e) Combined wind speed of multiple wind speed components

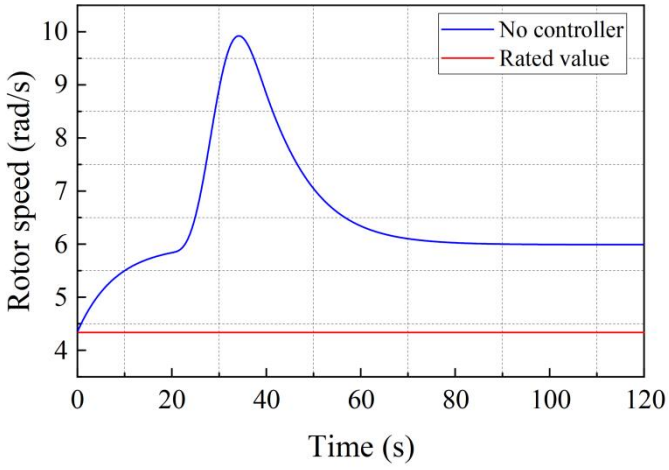


(f) Step wind speed profile

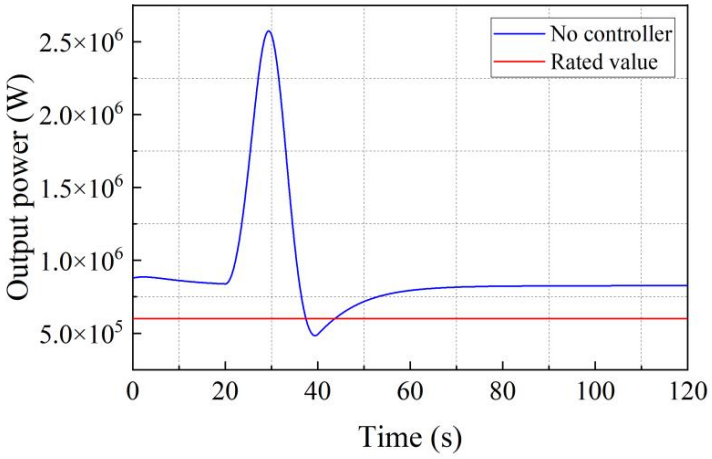
Figure 4.1: Wind Speed Profile

If there is no controller, the rotor speed and output power of the WTGS under different wind speed components are shown in the blue curves of Figure 4.2. The red curves in Figure 4.2 represent the rated value.

i. Gust wind

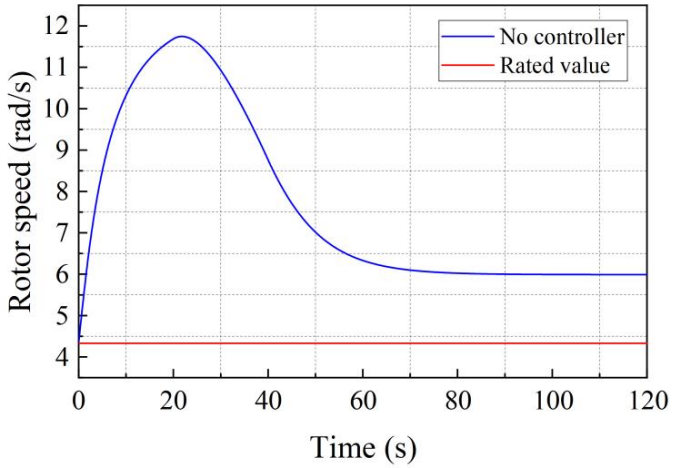


(a) Rotor speed variation during gust wind

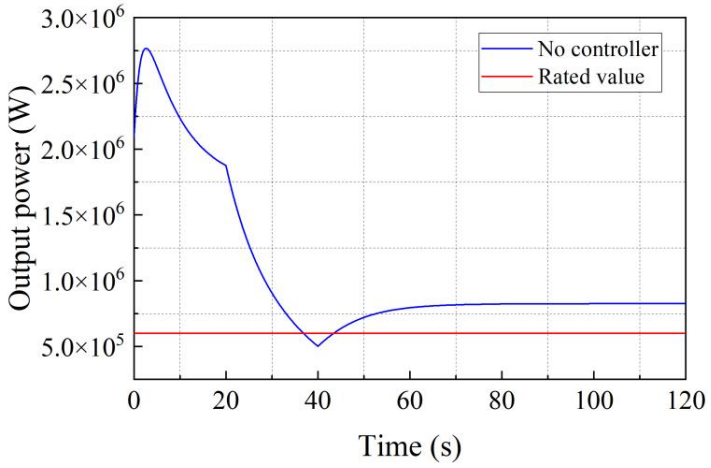


(b) Output power variation during gust wind

ii. Gradient wind

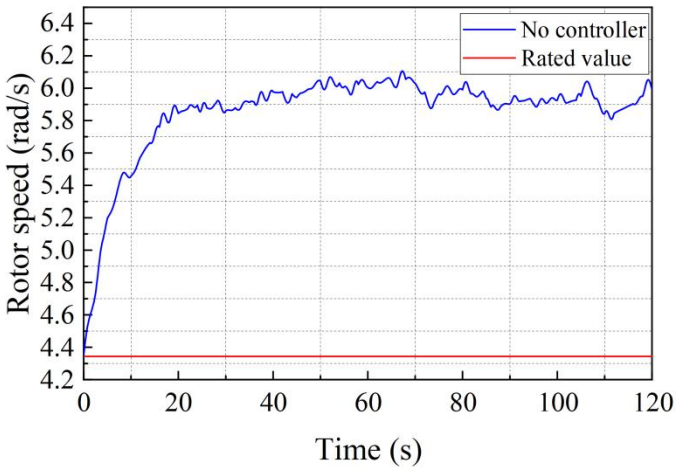


(c) Rotor speed variation during gradient wind

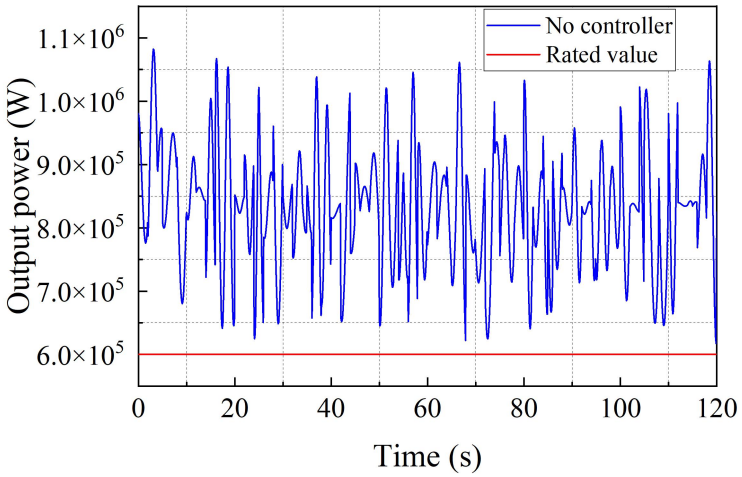


(d) Output power variation during gradient wind

iii. Random wind

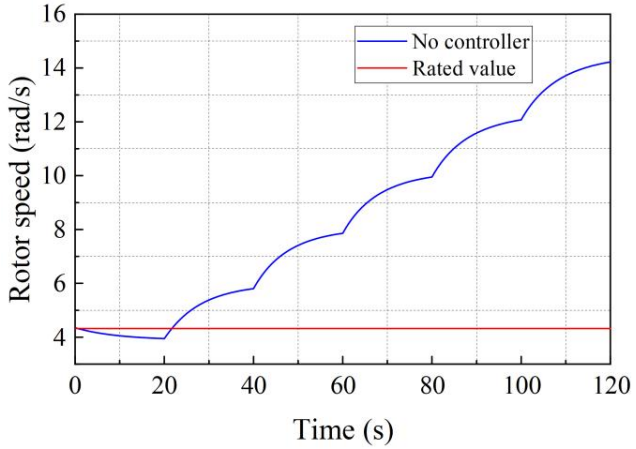


(e) Rotor speed variation during random wind

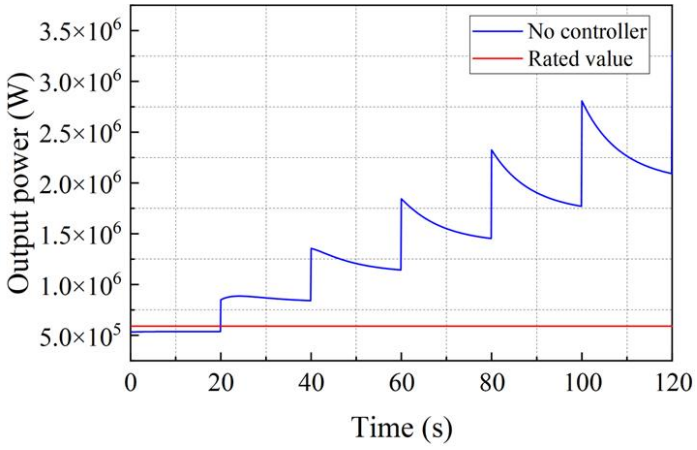


(f) Output power variation during random wind

iv. Step wind of 11 m/s-21 m/s

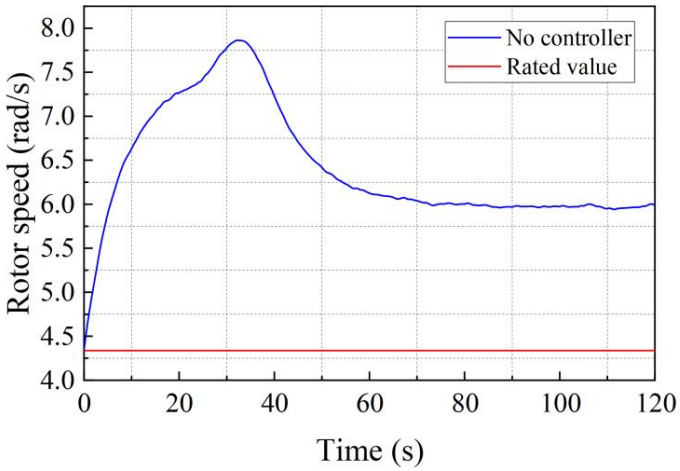


(g) Rotor speed variation during step wind of 11 m/s-21 m/s

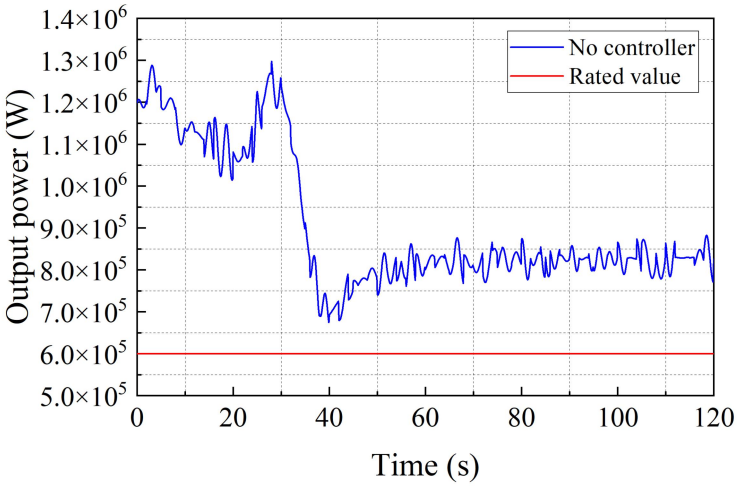


(h) Output power variation during step wind of 11m/s-21m/s

v. Combined wind speed of multiple wind speed components



(i) Rotor speed variation during combined wind speed



(j) Output power variation during combined wind speed

Figure 4.2: Response Curves of WTGS without Controller

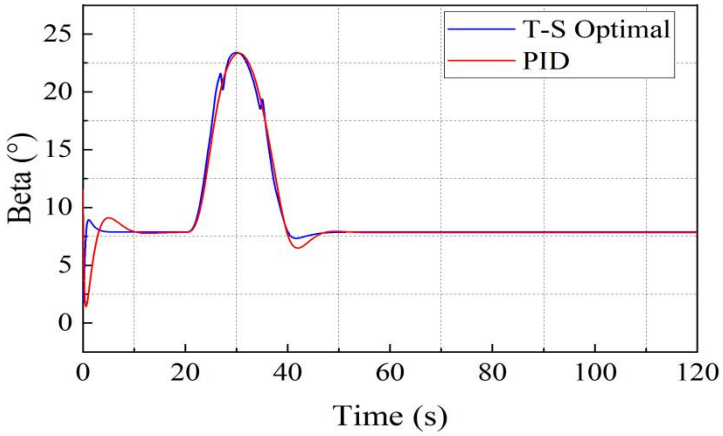
From the above results, it can be seen that when there is no controller in the WTGS, the rotor speed and output power both cannot be maintained near the rated value, so a controller must be designed to achieve constant power output of the WTGS.

4.3 Simulation Results and Analysis with Hybrid T-S Optimal Controller

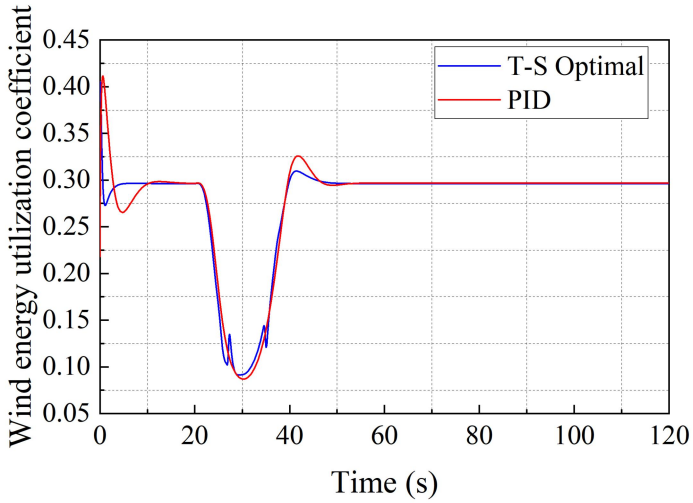
The simulation results under different wind speeds with T-S optimal hybrid controller are shown in Figure 4.3, Figure 4.4, Figure 4.5, Figure 4.6, and Figure 47. To demonstrate the control effect of the T-S Optimal controller, the response curves of the T-S Optimal controller and the PID controller are presented together for comparison and analysis.

4.3.1 Simulation Results and Analysis of Gust Wind

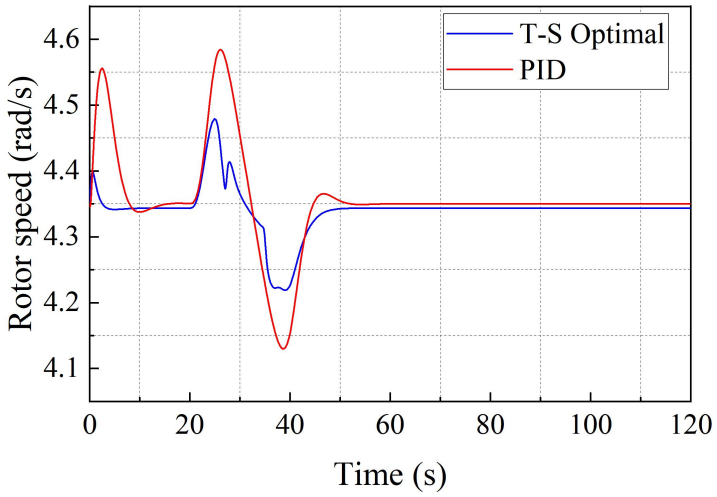
Figure 4.3 shows the response curves of pitch angle, wind energy utilization coefficient, rotor speed, and output power to gust wind.



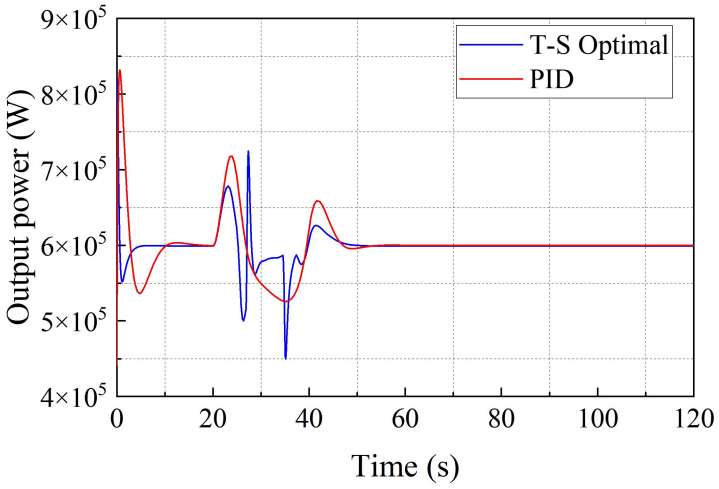
(a) Pitch angle



(b)Wind energy utilization coefficient



(c) Rotor speed



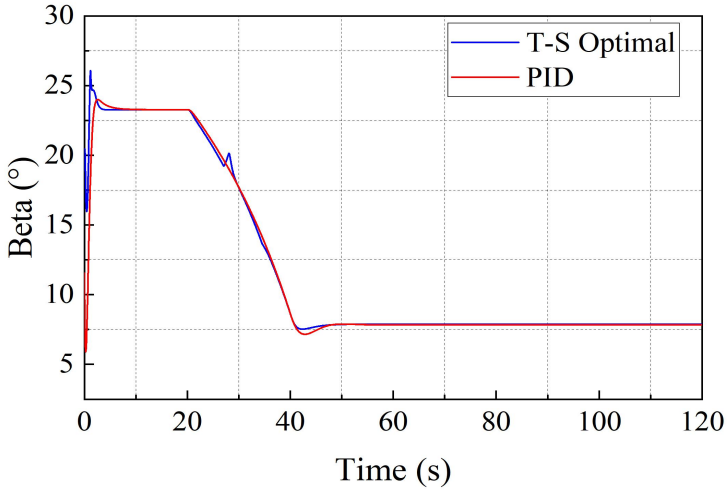
(d) Output power

Figure 4.3: Responses of the WTGS to Gust Wind

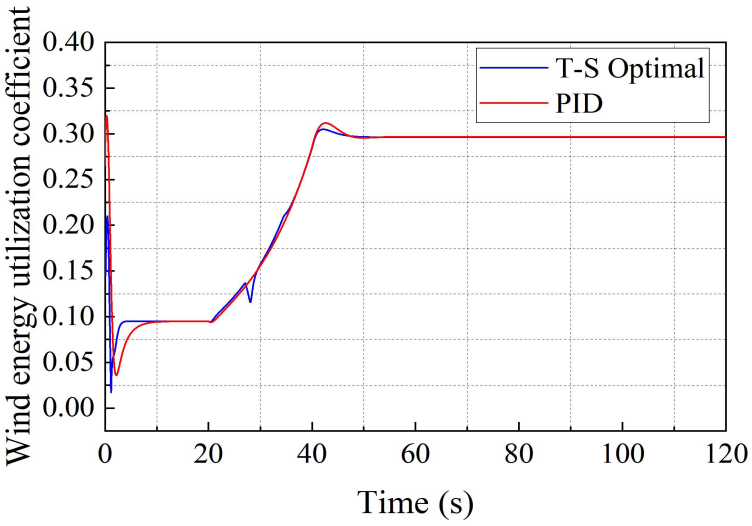
In this simulation, the wind speed remains 13 m/s unchanged for the first 20 seconds, the rotor speed and output power can be maintained unchanged. At 20s, the WTGS is encountered with a gust wind, the gust amplitude is 19 m/s and the duration is 20s. The wind speed profile involving a gust is described in Figure 4.1 (a). In order to eliminate the impact of this gust on the WTGS, the pitch angle will be changed under the action of the controller, thereby changing the wind energy utilization coefficient and maintaining the rotor speed and output power at the rated value. From the above figure, it can be seen that between 20 s and 40 s, the pitch angle and wind energy utilization coefficient did indeed change, thus maintaining the rotor speed at the rated value of 4.35 rad/s and the output power at around 600 kW. From Figure 4.3 (c), it can be seen that when the wind speed changes, the maximum rotor speed is 4.47 rad/s and the minimum is 4.22 rad/s, so the maximum overshoot is 2.76%, and the response time is 10s longer than the wind speed changing time. As shown in Figure 4.5 (d), the maximum output power is 750 kW and the minimum output power is 450 kW. The power overshoot reaches 25%, and the response time is also 10 s longer than the wind speed changing time. Overall, when gust wind comes, the controller can achieve basic control effects, although there are drawbacks such as long response time, large overshoot of power, and insufficient smoothness of the response curve.

4.3.2 Simulation Results and Analysis of Gradient Wind

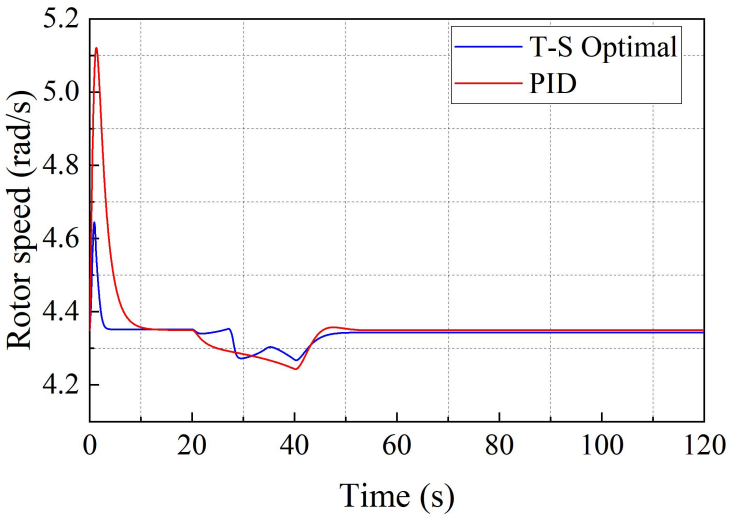
Figure 4.4 shows the response curves of pitch angle, wind energy utilization coefficient, rotor speed, and the output power when WTGS encountering gradient wind.



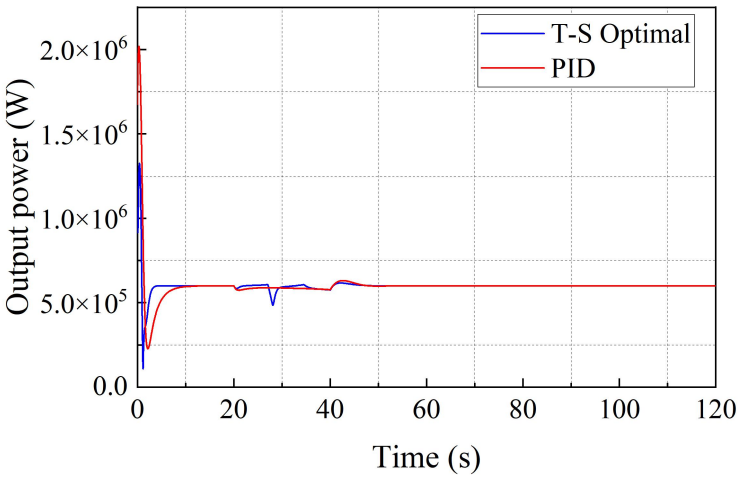
(a) Pitch angle



(b) Wind energy utilization coefficient



(c) Rotor speed



(d) Output power

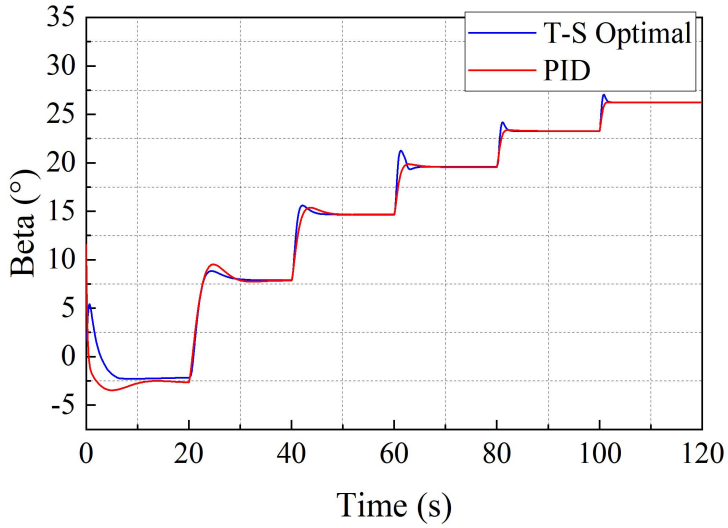
Figure 4.4: Responses of the WTGS to Gradient Wind Speed

In this simulation case, the wind speed remains 13 m/s unchanged for the first 20 seconds, the rotor speed and output power can remain unchanged. At 20 s, the WTGS is encountered with a gradient wind. From the 20th to the 40th second, the wind speed plummeted from 19 m/s to 13 m/s. The wind speed profile involving a gradient wind is described in Figure 4.1 (b). In order to counteract the impact of gradient wind on the WTGS, the controller begins to operate, thereby changing the angle of the pitch angle, thereby changing the wind energy utilization coefficient, and maintaining the rotor speed and output power at a constant value. From the above figure, it can be seen that between 20 seconds and 40 seconds, the pitch angle and wind energy utilization coefficient did indeed change, thus maintaining the rotor speed at the rated value of 4.35 rad/s and the output power at around 600 kW. As shown in Figure 4.4 (c), when the wind speed changes, the maximum value of the rotor speed is 4.42 rad/s, and the minimum value is 4.27 rad/s. Therefore, the maximum overshoot is 1.84%, and the response time is 10 seconds longer than the wind speed change time. Meanwhile, as shown in Figure 4.3 (d), the maximum output power is 610 kW and the minimum output power is 500 kW. The power overshoot reaches 16.7%, and the response time is about 5 seconds longer than the wind speed

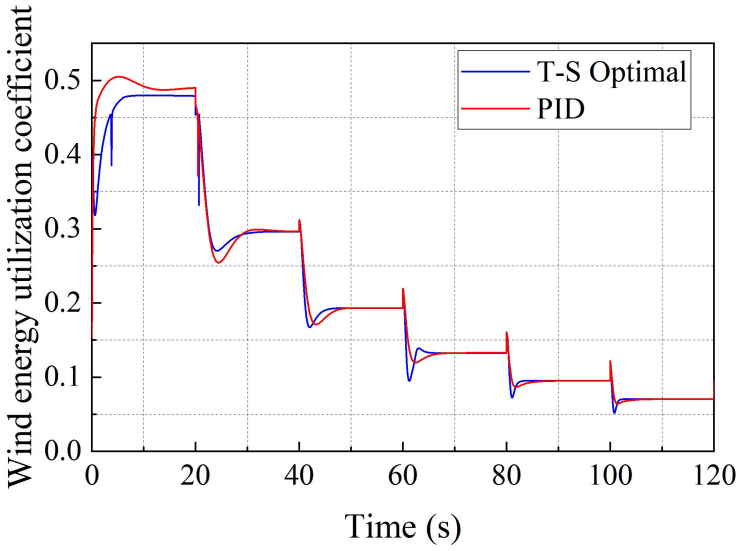
change time. Overall, when the gradient wind approaches, the controller can achieve basic control effects, although there are drawbacks such as long response time, large overshoot of power, and insufficient smoothness of the response curve.

4.3.3 Simulation Results and Analysis of Step Wind Speeds

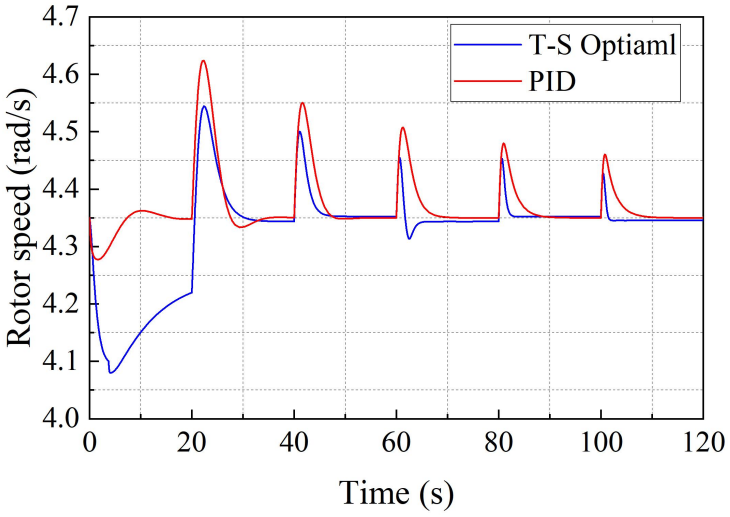
Figure 4.5 shows the WTGS response curves as the wind speed undergoes step wind changes from 11 m/s to 21 m/s.



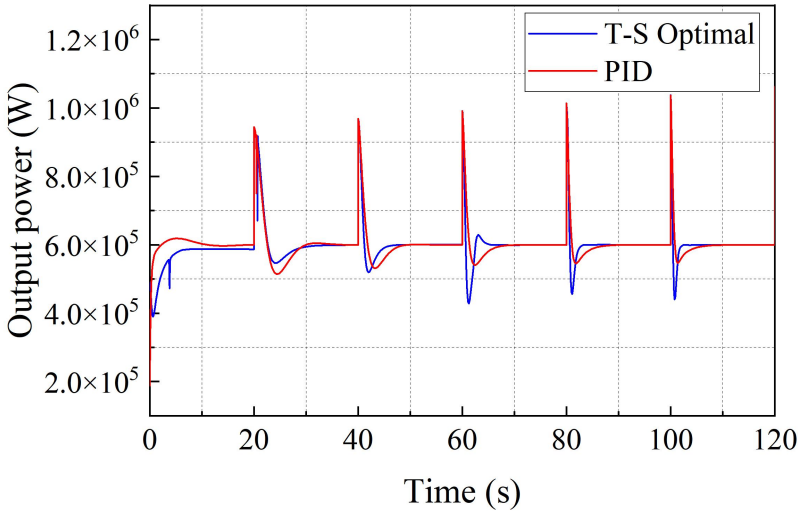
(a) Pitch angle



(b)Wind energy utilization coefficient



(c) Rotor speed



(d) Output power

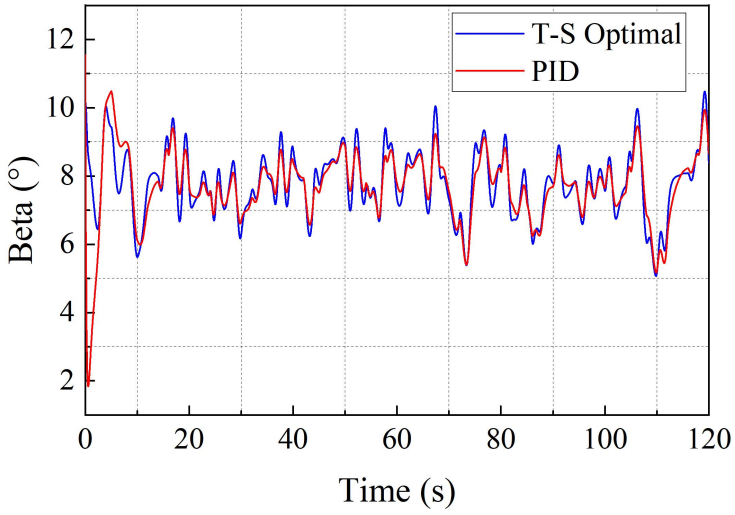
Figure 4.5: Responses of WTGS to Step Wind

As shown in Figure 4.5, the wind speed steps up by 2 m/s every 20 seconds. At 20 s, the wind speed jumps from 11 m/s to 13 m/s, the pitch angle of the wind turbine blades increases from -2.5° to about 8°, and the wind energy utilization coefficient decreases from 0.48 to about 0.3. At 40 s, the wind speed jumps from 13 m/s to 15 m/s, the pitch angle of the wind turbine blades increases from 8° to about 15°, and the wind energy utilization coefficient decreases from 0.3 to about 0.2. At 60 seconds, the wind speed jumps from 15 m/s to 17 m/s, the pitch angle of the wind turbine blades increases from 15° to about 20°,

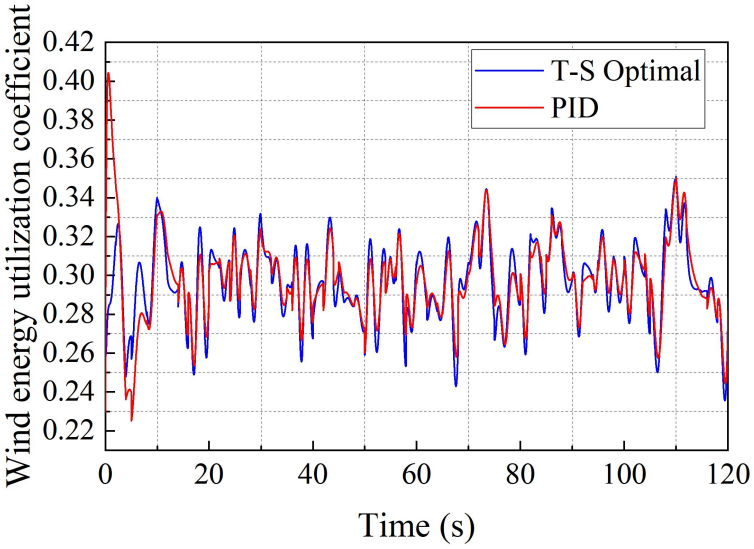
and the wind energy utilization coefficient decreases from 0.19 to about 0.13. At 80 seconds, the wind speed jumps from 17 m/s to 19 m/s, the pitch angle of the wind turbine blades increases from 20° to about 23°, and the wind energy utilization coefficient decreases from 0.13 to about 0.1. At 100s, the wind speed jumps from 19 m/s to 21 m/s, the pitch angle of the wind turbine blades increases from 23° to about 26°, and the wind energy utilization coefficient decreases from 0.1 to about 0.07. It can be seen that in the process of continuously increasing wind speed, in order to limit the energy obtained by the WTGS, it is necessary to reduce the wind energy utilization coefficient by increasing the pitch angle, so as to maintain the rotor speed at 4.35 rad/s, and the output power of the WTGS can be stabilized at the rated power of 600 kW. In addition, as shown in Figure 4.5 (c), the maximum speed reaches 4.55rad/s, with an overshoot of 4.60%. And after 80 seconds, even under steady-state conditions, the speed deviated from the rated value. From Figure 4.5 (d), it can be seen that the maximum power reaches 1000 kW, with an overshoot of 66.7%. However, the corresponding time is short, and the output power can be maintained at the rated value in steady-state. Overall, when the wind speed continuously increases in steps, the controller can continuously adjust the pitch angle to stabilize the speed and output power near the rated value. However, excessive power overshoot is an issue that cannot be ignored.

4.3.4 Simulation Results and Analysis of Random Wind

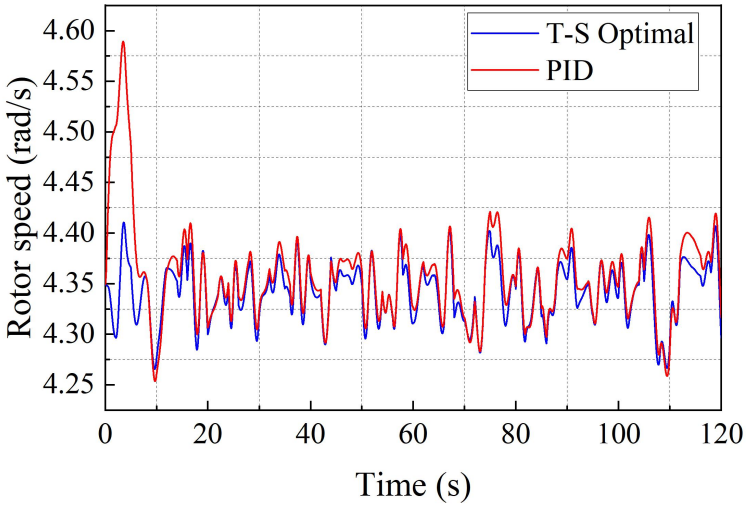
Figure 4.6 shows the WTGS response curves as the wind speed changes randomly between 13 m/s and 15 m/s.



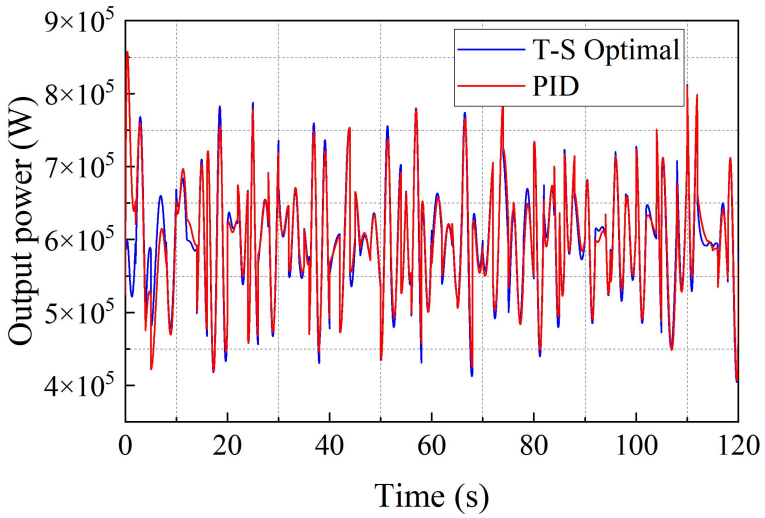
(a) Pitch angle



(b) Wind energy utilization coefficient



(c) Rotor speed



(d) Output power

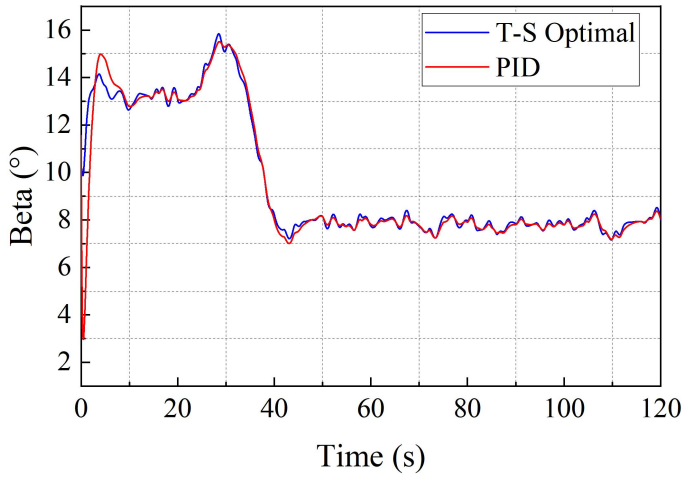
Figure 4.6: Responses of the WTGS to Random Wind

From the above figure, it can be seen that when the wind speed randomly changes between 13 m/s and 15 m/s, the pitch angle of the WTGS also undergoes corresponding changes under the action of the controller, and the wind energy utilization coefficient also changes accordingly. The rotor speed and output power remain relatively stable. The speed mainly varies randomly between 4.0 rad/s and 4.6 rad/s, with a maximum overshoot of 8.05%. The output power mainly varies randomly between 0 and 1500 kW, with a maximum overshoot of 150%. It can be seen that the designed controller has poor adaptability to wind speed for this model, especially due to the large overshoot of power, and the control effect is not ideal.

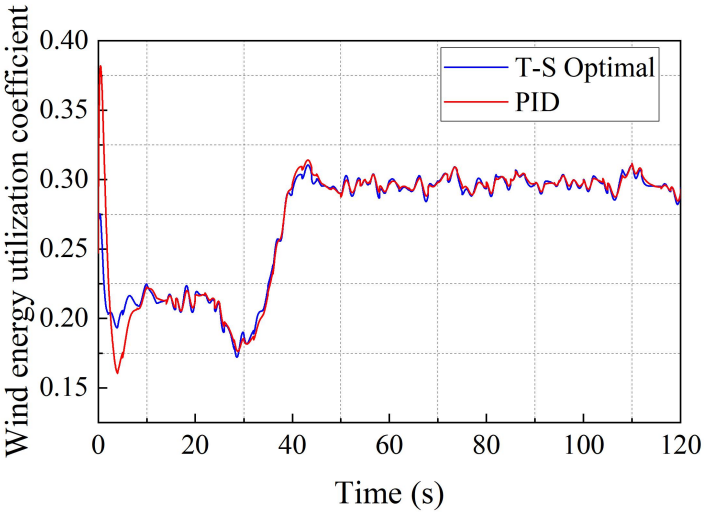
4.3.5 Simulation Results and Analysis of Combined Wind Speed

The actual wind speed is often the superposition of multiple wind components. In order to verify the effectiveness of the controller in natural wind conditions, it is necessary to simulate this composite wind speed. Figure 4.7 shows the response curves of the pitch angle, wind energy utilization coefficient, rotor speed, and output power to the combined

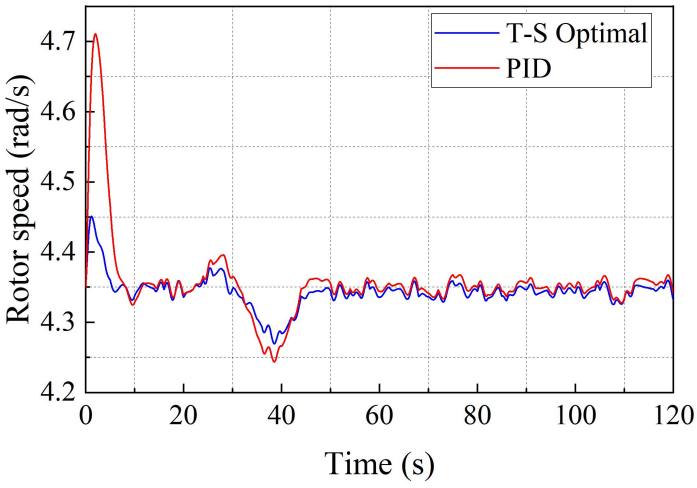
wind speed combined with each wind speed component.



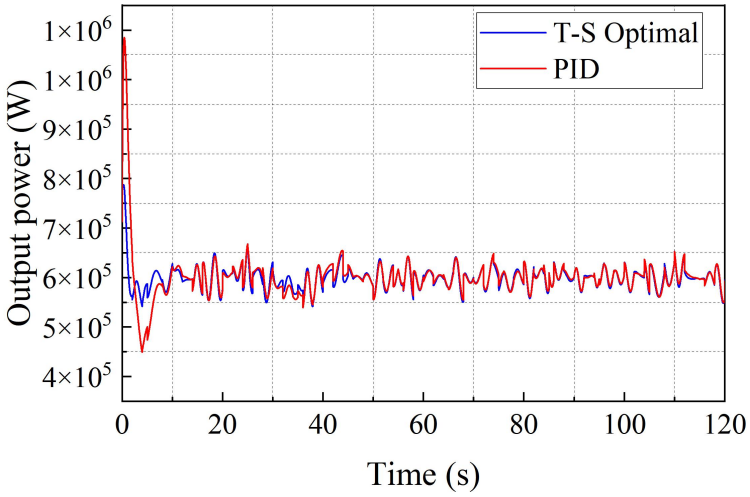
(a) Pitch angle



(b)Wind energy utilization coefficient



(c) rotor speed



(d) Output power

Figure 4.7: Responses to Superposition of Multiple Wind Components

The wind speed model is based on the superposition of gradient wind, gust wind, and step wind on the basis of random wind. From Figure 4.7 (a) and Figure 4.7 (b), it can be seen that when the wind speed changes, the pitch angle changes correspondingly under the action of the controller, thereby changing the wind energy utilization coefficient. As shown in Figure 4.7 (c), the variation range of the speed is between 4.1 rad/s and 4.55 rad/s, with a maximum overshoot of 5.75%. As shown in Figure 4.9 (d), the variation range of output power is mainly between 400 kW and 800 kW, with a maximum overshoot of 33.33%. From these data, it can be seen that the controller can achieve a certain control effect under natural wind speed, but the main problem is that the power overshoot is too large.

4.3.6 Conclusions

This section conducted simulation tests on WTGS containing a T-S optimal controller. The simulation results showed that the controller has certain control effects to different wind speed components and natural wind conditions, and can maintain the rotor speed and output power near the rated value. However, the control effects of this controller

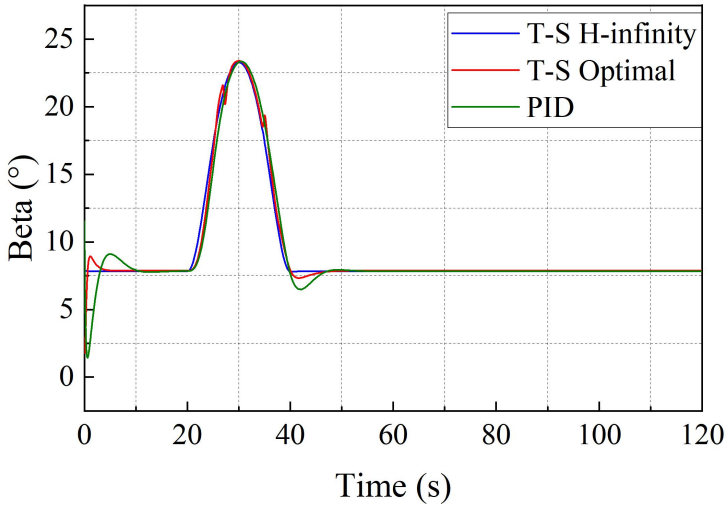
are different to different wind speeds, resulting in issues such as long response time and excessive overshoot. Compared with the waveform of PID, the fluctuation range of T-S optimal curve is slightly smaller, indicating that the control performance of T-S optimal is slightly better than that of traditional PID. The essence of T-S optimal control is to extend the optimal control theory of linear systems to nonlinear systems. Its core advantage lies in utilizing the nonlinear mapping capability of T-S fuzzy to compensate for the linear limitations of optimal, while ensuring the control accuracy of each local region through the optimality of optimal, ultimately achieving high-performance control on a global scale. This combination of "theoretical rigor" and "engineering adaptability" demonstrates significant advantages in complex system control. PID performs well in simple systems, but its control effect is not good enough in strong nonlinear or high-precision control scenarios, because its "linear, fixed parameter, pure feedback" control mechanism is not suitable for the "nonlinear, time-varying, multi-variable" characteristics of actual complex systems.

4.4 Simulation and Results Analysis with Hybrid T-S H-infinity Controller

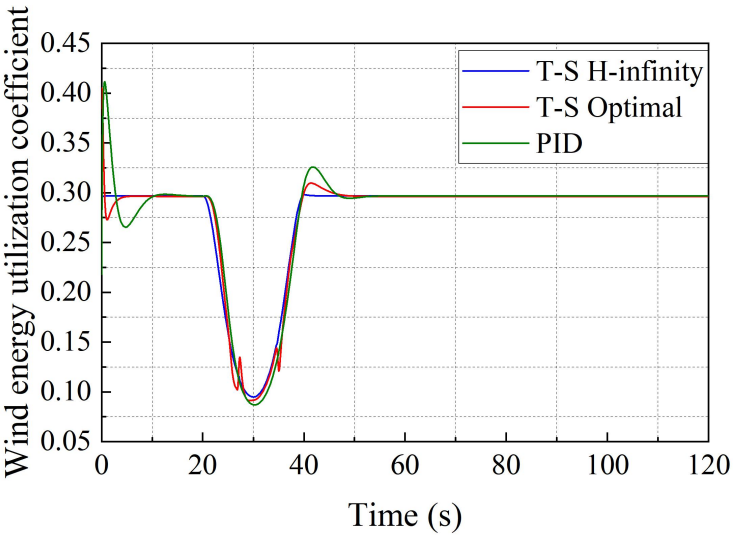
The proposed T-S H-infinity controller is applied to WTGS, and the simulation results at different wind speeds are shown in Figure 4.8, Figure 4.9, Figure 4.10, Figure 4.11, and Figure 4.12. To demonstrate the control effect of the T-S H-infinity controller, the response curves of the T-S H-infinity controller, T-S Optimal controller and PID controller are presented together for comparison and analysis.

4.4.1 Simulation Results and Analysis of Gust Wind

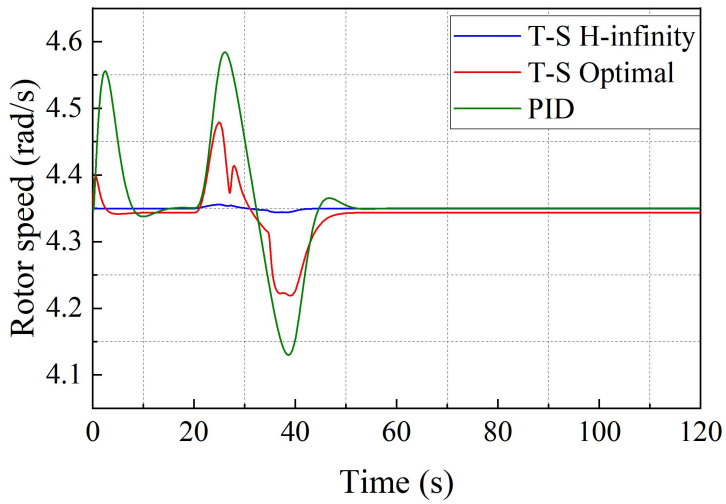
Figure 4.8 shows the response curves of pitch angle, wind energy utilization coefficient, wind turbine speed, and output power under gust wind.



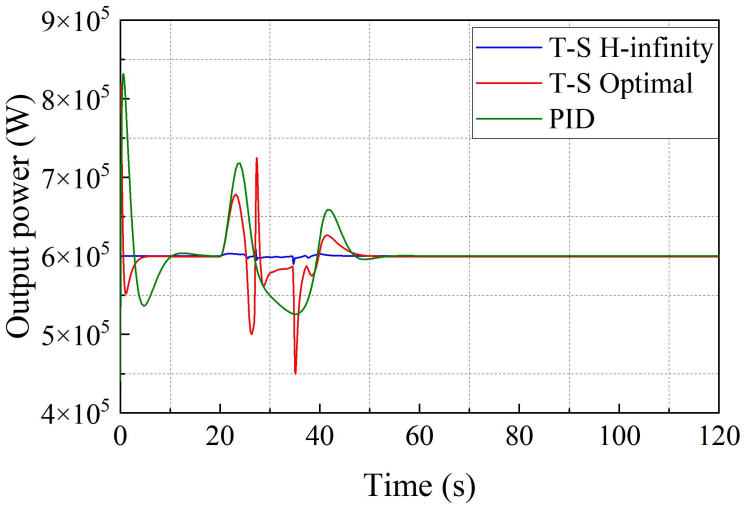
(a) Pitch angle



(b)Wind energy utilization coefficient



(c) rotor speed



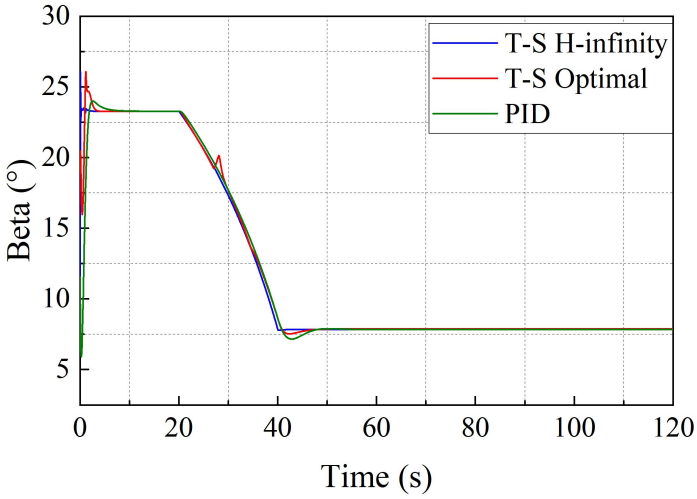
(d) Output power

Figure 4.8: Responses to Gust Wind

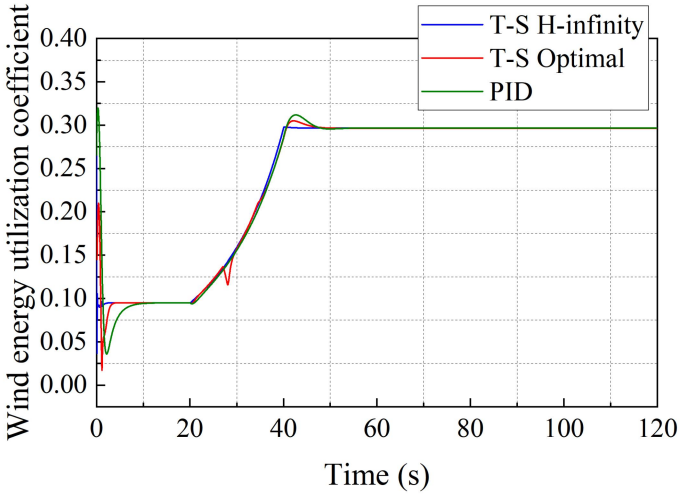
This set of curves displays the response curves of various parameters when the WTGS encounters gust. The gust curve is shown in Figure 4.1 (a). From Figure 4.8, it can be seen that the pitch angle and wind energy utilization coefficient can change with the changes of wind speed, thereby maintaining the rotor speed and output power around the rated values. Compared with the response curve of the T-S optimal controller and PID controller, the response curve of the T-S H-infinity controller is smoother, its response time is shorter, and the overshoot is much smaller, indicating that the control effect of this controller is far superior to the former.

4.4.2 Simulation Results and Analysis of Gradient Wind

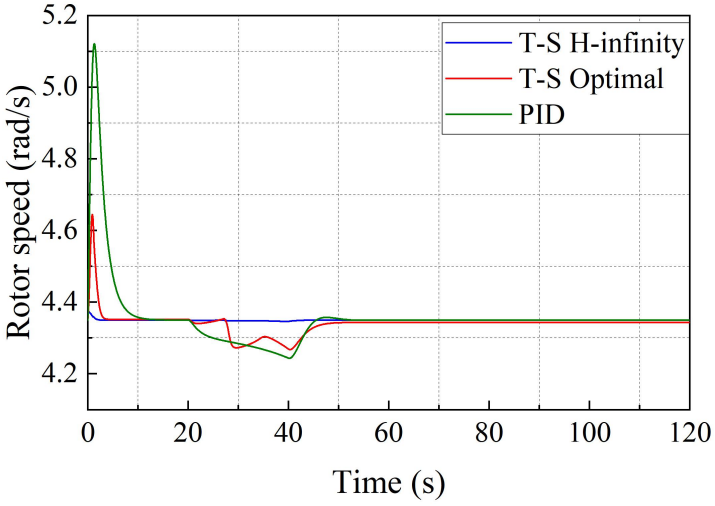
Figure 4.9 shows the response curves of pitch angle, wind energy utilization coefficient, wind turbine speed, and output power of the WTGS under gradient wind conditions.



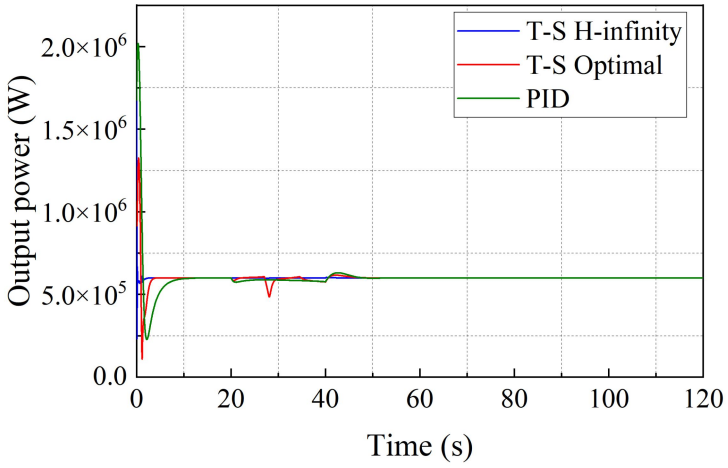
(a) Pitch angle



(b)Wind energy utilization coefficient



(c) rotor speed



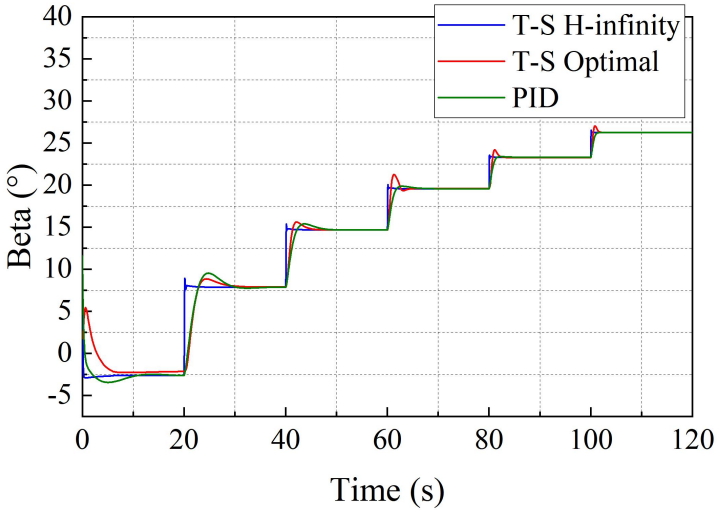
(d) Output power

Figure 4.9: Responses to Gradient Wind

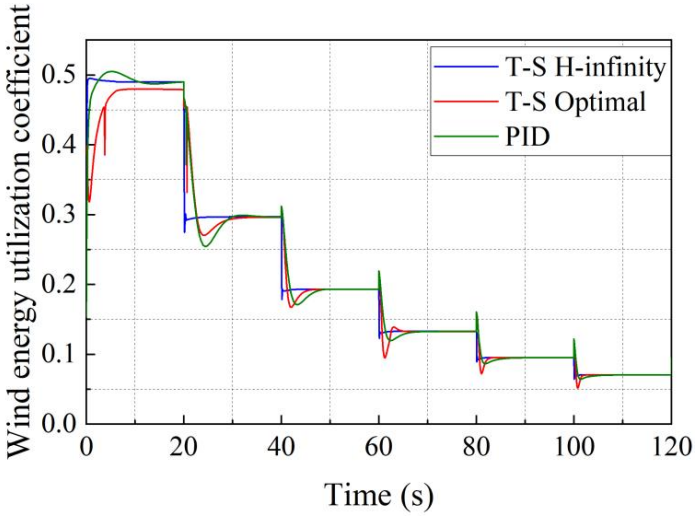
This set of curves shows the response of various parameters when the WTGS encounters gradient wind. The gradient wind curve is shown in Figure 4.2 (b). From Figure 4.9, it can be seen that the pitch angle and wind energy utilization coefficient can change with changes of wind speed, thereby maintaining the speed and power around the rated values. Compared with the response curve of the T-S optimal controller and PID controller, the response curve of the T-S H-infinity controller at gradient wind is smoother, and its response time is shorter, and the overshoot is much smaller, so the control effect of this controller is much better than that of the former.

4.4.3 Simulation Results and Analysis of Step Wind Speeds

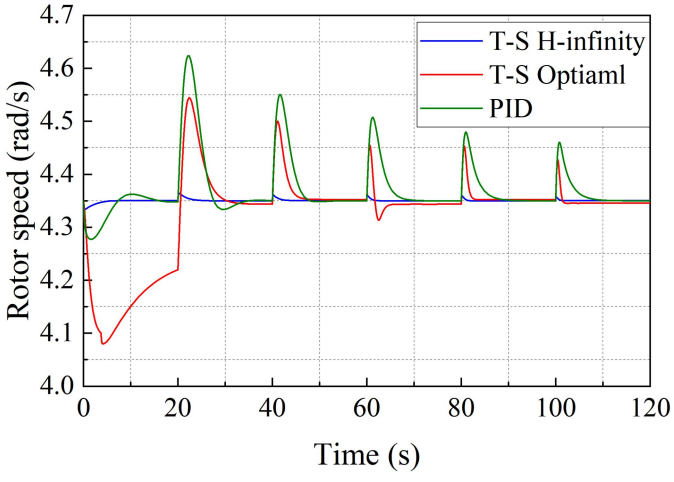
Figure 4.10 shows the response curves of a WTGS when the wind speed changes stepwise from 11 m/s to 21 m/s.



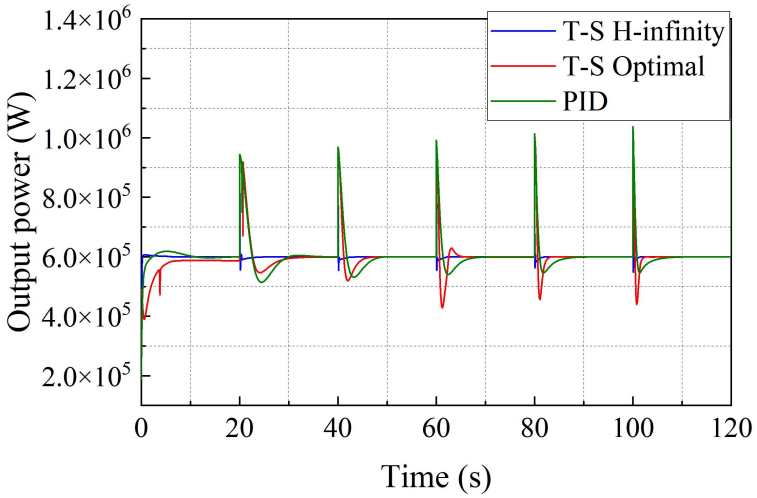
(a) Pitch angle



(b) Wind energy utilization coefficient



(c) Rotor speed



(d) Output power

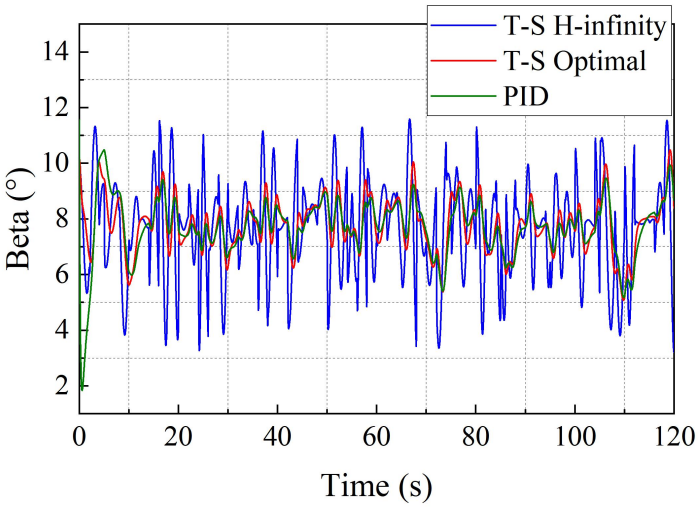
Figure 4.10: Response Curves to Step Wind

From the simulation in the figures above, we can see that when the wind speed changes from 11 m/s to 13 m/s at 20s, the blade pitch angle of the WTG increases from -2.5° to about 8°, and the rotor power coefficient drops from 0.49 to about 0.3. While the wind changes from 13 m/s to 15 m/s, the blade pitch angle increases from 8° to about 14.5°, and the rotor power coefficient decreases from 0.3 to about 0.19. While the wind changes from 15 m/s to 17 m/s at 60 s, the blade pitch angle of the WTG increases from 14.5° to about 19.5°, and the rotor power coefficient decreases from 0.19 to about 0.13. While the wind jumps from 17 m/s to 19 m/s at 80 s, the pitch angle increases from 19.5°to about 23.5°, and the rotor power coefficient decreases from 0.13 to about 0.1. At 100 s, the wind speed jumps from 19 m/s to 21 m/s, the blade pitch angle of the WTG increases from 23.5° to about 26°, and the rotor power coefficient decreases from 0.1 to about 0.07. It can be seen that in the process of wind speed increase, the pitch angle of the fans also increases, the wind energy utilization coefficient decreases, the rotor speed of the WTG can be maintained at 4.35 rad/s, and the output power of the WTG can be maintained at a rated power of 600 kW.

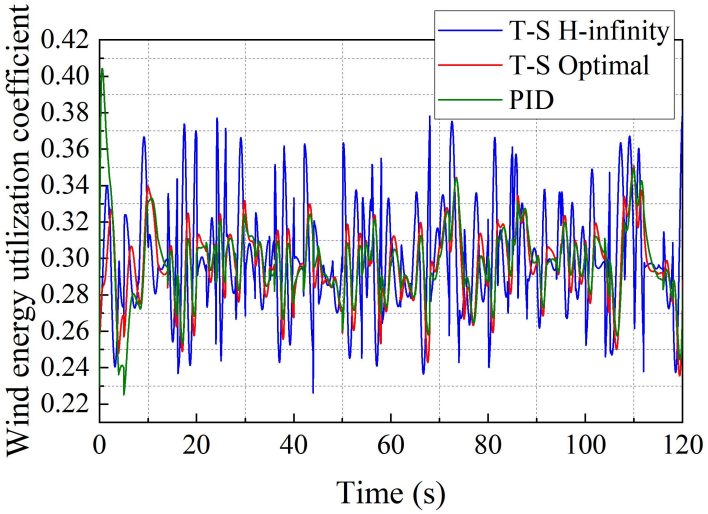
In addition, it can be seen from the series of curves in Figure 4.10 that, at the step wind speed, the proposed method here has a faster response speed and smaller overshoot than the T-S optimal controller and PID controller, and the response curves are smoother, which proves the effectiveness of the proposed method here.

4.4.4 Simulation Results and Analysis of Random Wind Speed

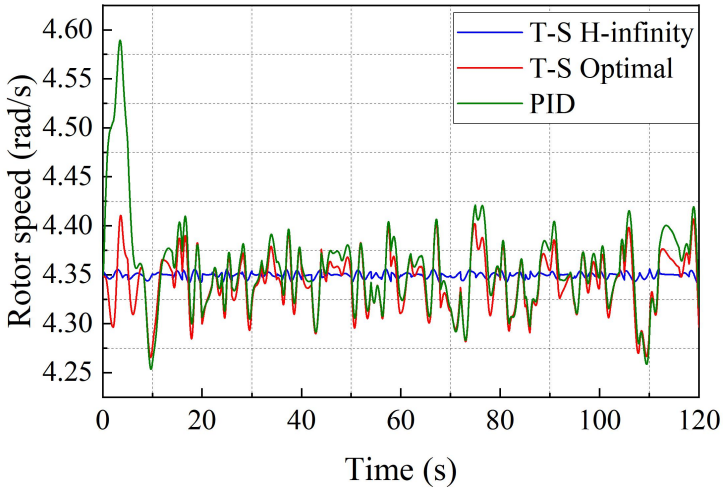
Figure 4.11 shows the response curves as the wind speed changes randomly between 13 m/s and 15 m/s.



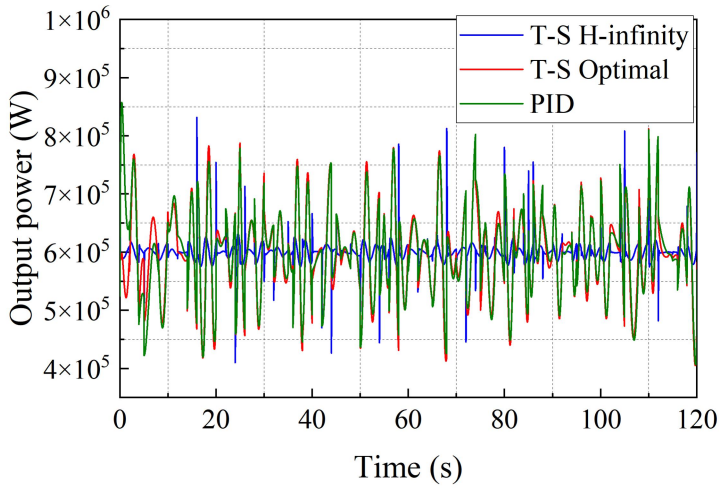
(a) Pitch angle



(b) Wind energy utilization coefficient



(c) rotor speed



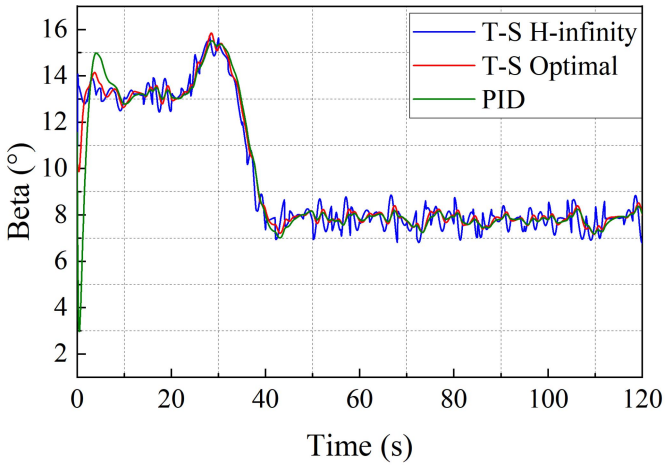
(d) Output power variation

Figure 4.11: Responses to Random Wind Speed

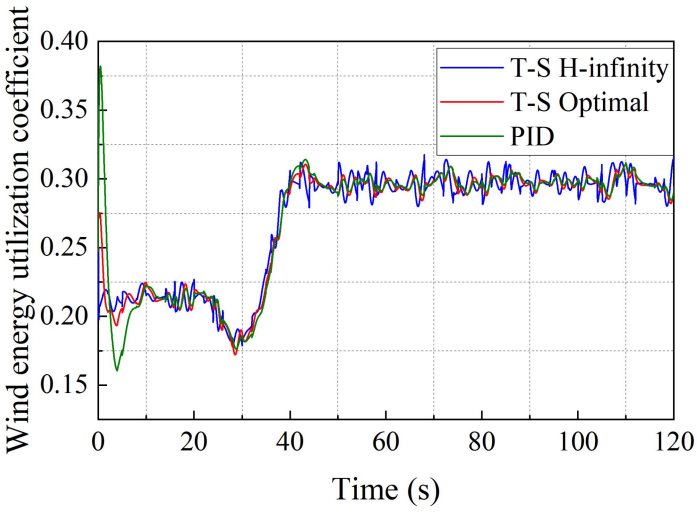
From the above figure, it can be seen that when the WTGS encounters random winds of 13 m/s to 15 m/s, the T-S H-infinity controller can maintain the rotor speed and output power near the rated value. Compared with the T-S optimal controller and PID controller, the controller proposed here has a smaller error between the rotor speed and the rated value, also smaller error between the output power and the rated output power, and the stability is larger. Although the wind speed changes randomly and the disturbance is large, the control effect of the proposed controller in this section is proper, so the controller has strong robustness.

4.4.5 Simulation Results and Analysis of Combined Wind Speeds

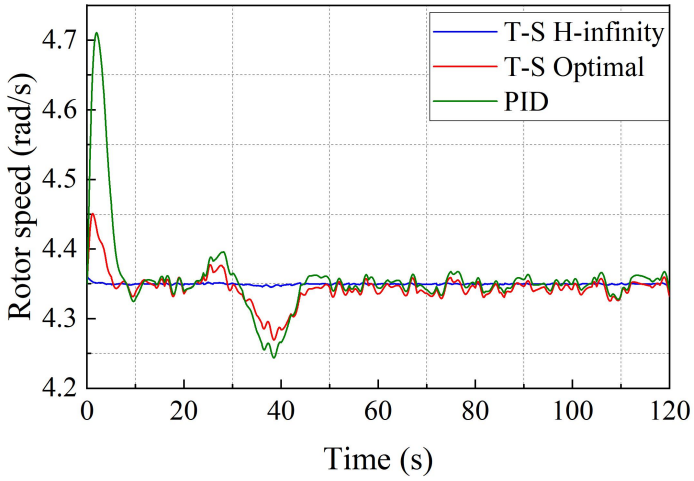
The curves of pitch angle, wind energy utilization coefficient, rotor speed, and output power under combined wind speed are shown in Figure 4.12.



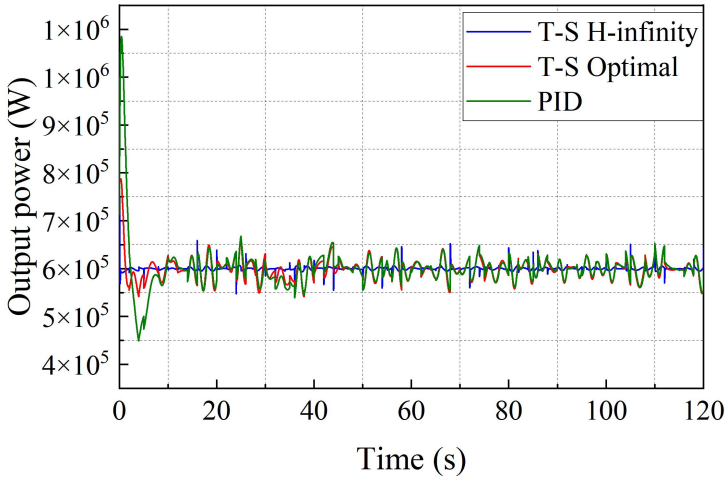
(a) Pitch angle



(b) Wind energy utilization coefficient



(c) Rotor speed



(d) Output power

Figure 4.12: Responses to Combined Wind Speed

When the wind speed encountered the superposition of multiple components, it can be seen from the curves in Figure 4.12 that the pitch angle changes with the change of wind speed under the action of the controller. In short, the pitch angle increases with the increase of wind speed, and decreases with the decrease of wind speed. It can be seen from Figure 4.12 that the rotor power efficiency also changes accordingly. Figure 4.12 also show that the rotor speed and output power can be stabilized near the rated value in, it indicates that the controller completes the desired control objectives. As shown from the red lines and the blue lines that, the proposed controller here provides the smaller tracking

error of the rotor speed and the output power, compared with the T-S optimal controller. The proposed controller here delivers a smoother output, and better maintain the rotor speed and the output power around the rated value.

4.4.6 Conclusions

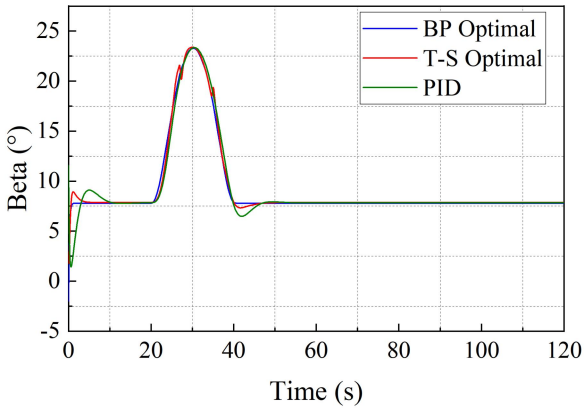
This section presents and analyzes the simulation results containing T-S H-infinity controller. The curve shows that regardless of the wind speed model, the controller can achieve good control effect, with small overshoot and response time. Moreover, the control performance of this controller is superior to other controllers. The T-S H-infinity controller performs better than the T-S optimal controller in complex systems due to the essential difference in their ability to handle system uncertainty. The optimal controller is designed based on an accurate system model and achieves optimal control by minimizing the quadratic performance index. However, this optimality highly depends on the accuracy of the model. When there are parameter perturbations or external disturbances in the system, the control performance may significantly decrease, and even lead to system instability. The H-infinity control theory, with robustness as its core design objective, essentially aims to optimize the worst-case system performance in the presence of model uncertainty and external disturbances, ensuring the stability and performance boundaries of the closed-loop system. It does not rely on an exact model, but rather expresses the uncertainty range by introducing weighting functions, transforming the control problem into an H-infinity norm minimization problem, thereby maintaining good control performance even when the model is inaccurate or the environment changes.

4.5 Simulation and Results Analysis with BP Neural Network Optimal Controller

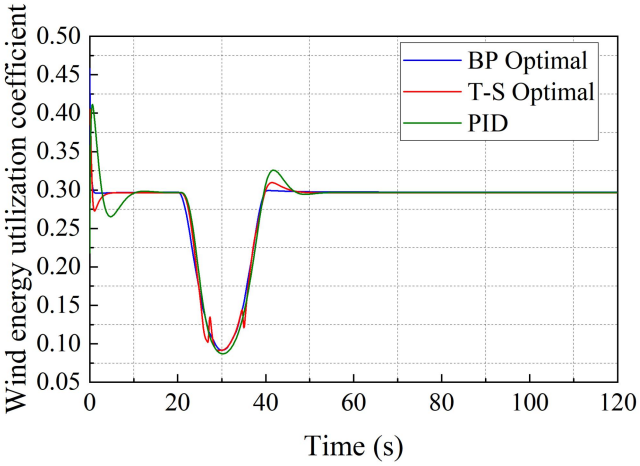
The proposed BP Neural Network Optimal controller is applied to WTGS, and the simulation results under different wind speeds are shown in Figure 4.13, Figure 4.14, Figure 4.15, Figure 4.16, and Figure 4.17. To demonstrate the control effect of BP Neural Network Optimal controller, the response curves of BP Neural Network Optimal controller, T-S Optimal controller and PID controller are presented together for comparison and analysis.

4.5.1 Simulation Results and Analysis of Gust Wind

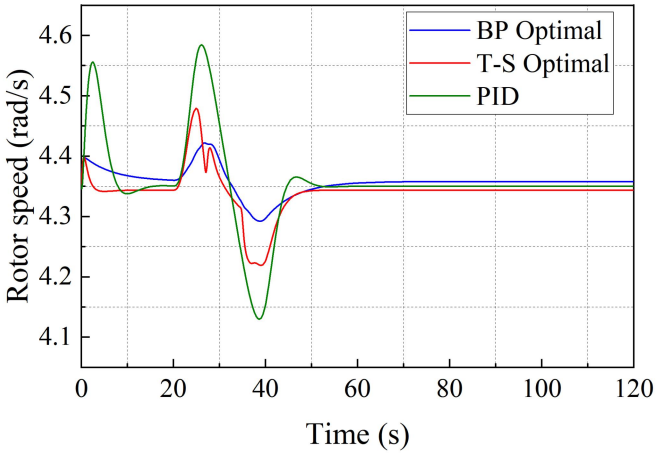
Figure 4.13 shows the response curves of pitch angle, wind energy utilization coefficient, rotor speed, and output power to gust wind.



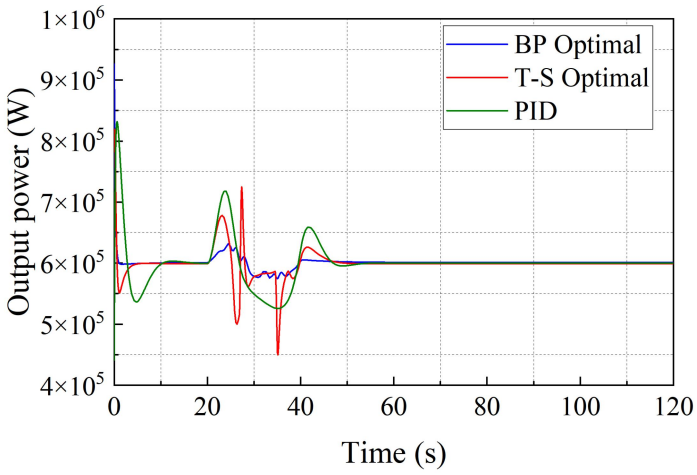
(a) Pitch angle



(b) Wind energy utilization coefficient



(c) Rotor speed



(d) Output power

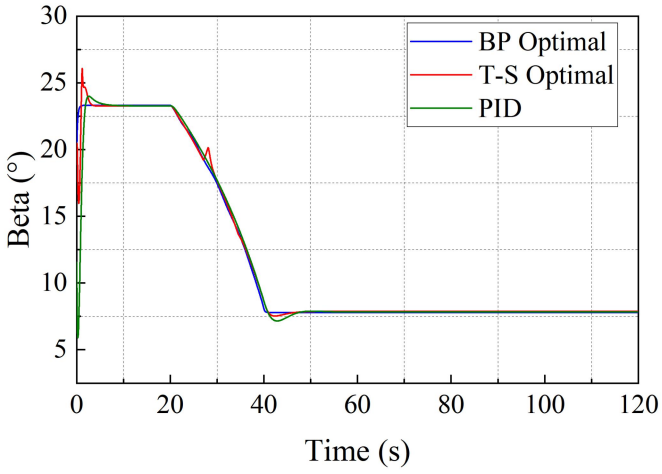
Figure 4.13: Responses to Gust Wind of the Two Controllers

In this simulation, WTGS encountered a gust of 20 seconds. In order to eliminate the impact of this gust on the WTGS, the pitch angle will be changed under the action of the controller, thereby changing the wind energy utilization coefficient and maintaining the rotor speed and output power at the rated value. From the above figure, it can be seen that between 20 s and 40 s, the pitch angle and wind energy utilization coefficient have indeed changed. The rotor speed increases with the increase of wind speed, while the wind energy utilization coefficient decreases with the increase of wind speed. Therefore, the rotor speed

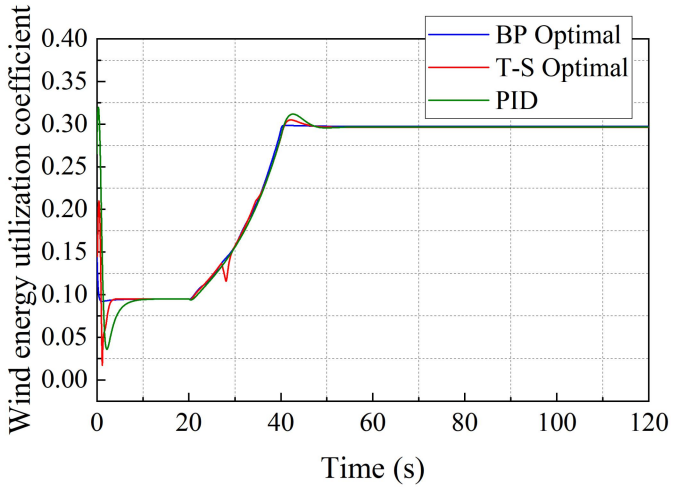
is maintained at the rated value of 4.35 rad/s and the output power is maintained at around 600 kW. As shown in Figure 4.13 (c), when the wind speed changes, the maximum rotor speed is 4.42 rad/s and the minimum is 4.29 rad/s, resulting in a maximum overshoot of 1.38%. However, under the T-S optimal controller, the maximum overshoot is 2.76%. Therefore, the proposed controller has better performance than the former. Meanwhile, as shown in Figure 4.13(d), the maximum output power is 620 kW and the minimum output power is 580 kW. The power overshoot is 3.33%, which is much smaller than the 25% under the T-S optimal controller. In practical applications it means that it can provide more stable electrical energy while protecting the wind turbine and may prolong the lifetime of the wind turbine too. Overall, when gusts come, this controller can achieve good control effect. Compared with the control effect of T-S optimal controller and PID controller, the overshoot of BP Neural Network Optimal controller is smaller and the curve is smooth.

4.5.2 Simulation Results and Analysis of Gradient Wind

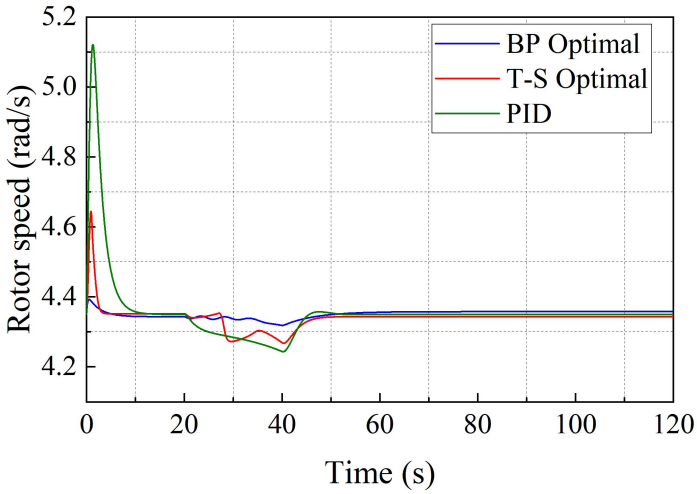
Figure 4.14 shows the response curves of wind turbine pitch angle, wind energy utilization coefficient, rotor speed, and output power under gradient wind conditions.



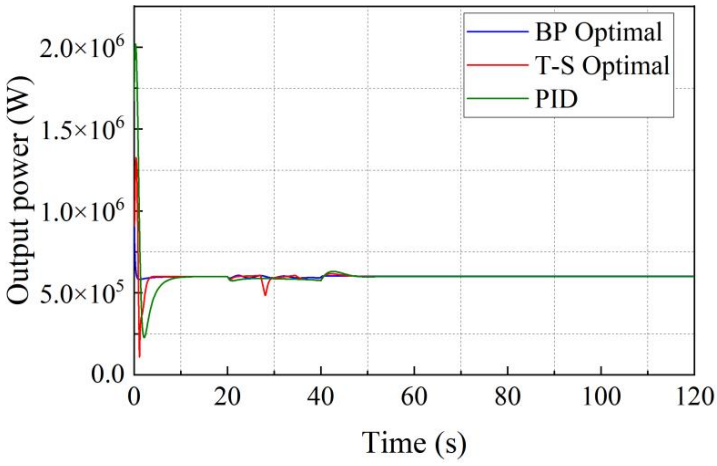
(a) Pitch angle



(b) Wind energy utilization coefficient



(c) Rotor speed



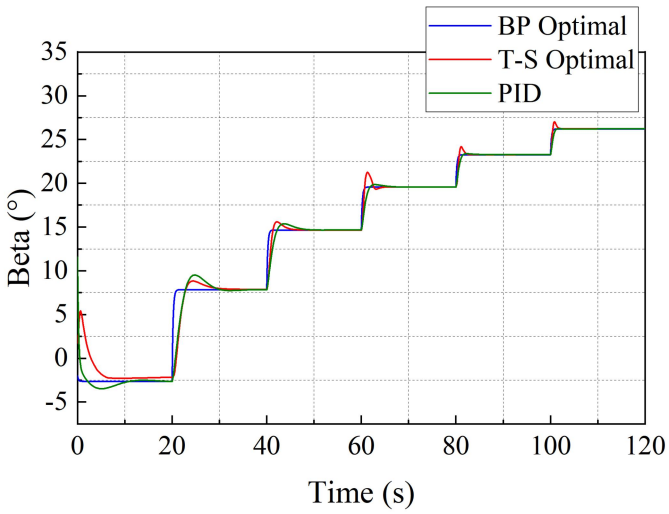
(d) Output power

Figure 4.14: Responses to Gradient Wind of the Two Controllers

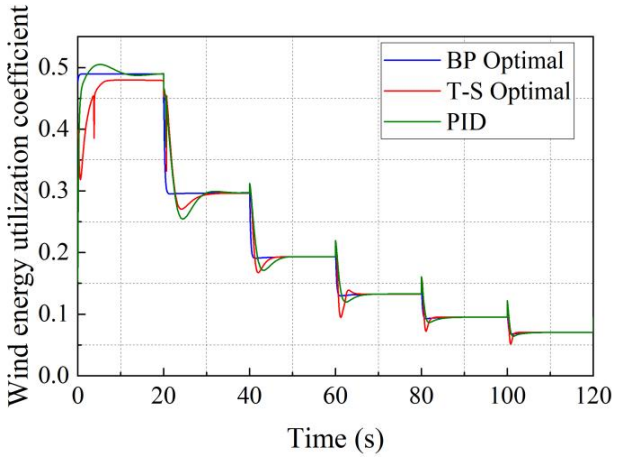
This set of curves displays the response curves of various parameters when the WTGS encounters a gradient wind. The gust curve is shown in Figure 4.1 (b). From Figure 4.14, it can be seen that the pitch angle and wind energy utilization coefficient can change with changes of wind speed, thereby maintaining the rotor speed and power near the rated values. Compared with the response curve of the T-S optimal controller and PID controller, the response curve of the BP Neural Network Optimal controller under gradient wind is smoother, its response time is shorter, and the overshoot is much smaller, indicating that the control effect of this controller is far superior to the former.

4.5.3 Simulation Results and Analysis of Step Wind Speed

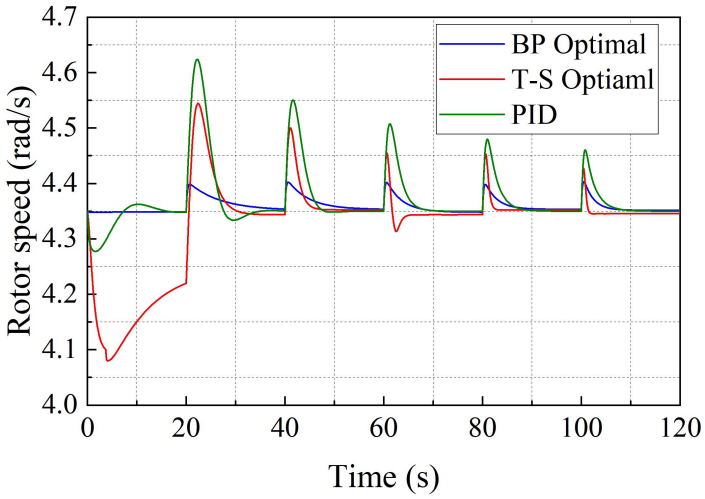
Figure 4.15 shows the response curves of WTGS when the wind speed changes stepwise from 11 m /s to 21 m/s.



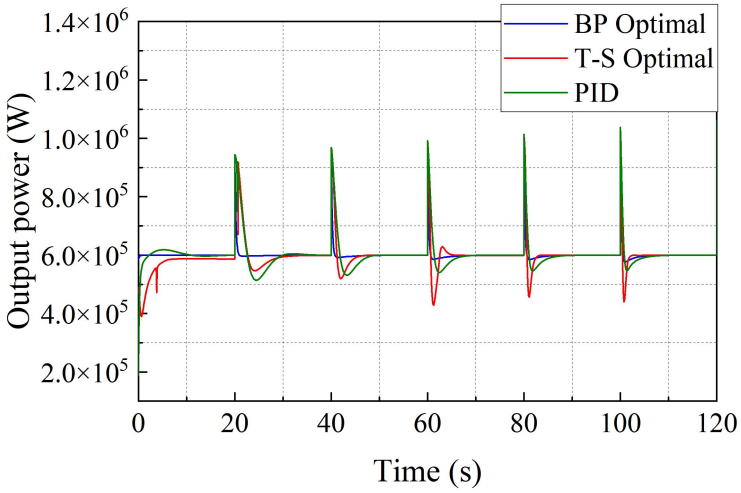
(a) Pitch angle



(b) Wind energy utilization coefficient



(c) Rotor speed



(d) Output power

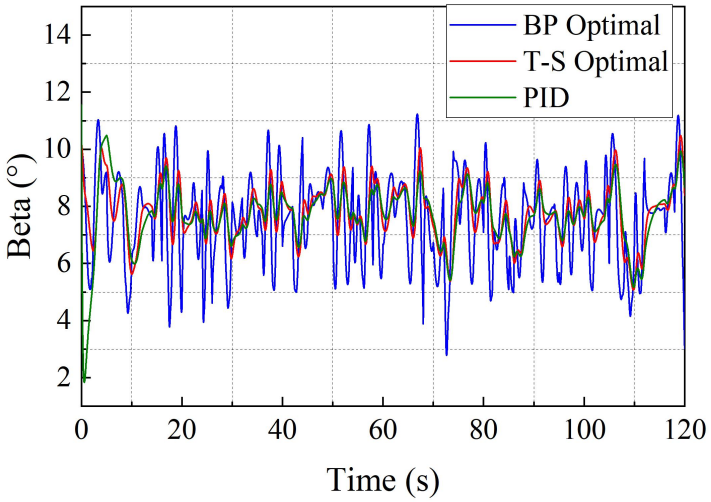
Figure 4.15: Response Curves to Step Wind

From the simulation in the figures above, we can see that under the action of the BP neural network optimal controller, when the wind speed steps up, the pitch angle also steps up, resulting in a step decrease in the wind energy utilization coefficient. Therefore, the rotor speed of the WTG can be maintained at about 4.35 rad/s, and the output power of the WTG can be maintained at a rated power of 600 kW.

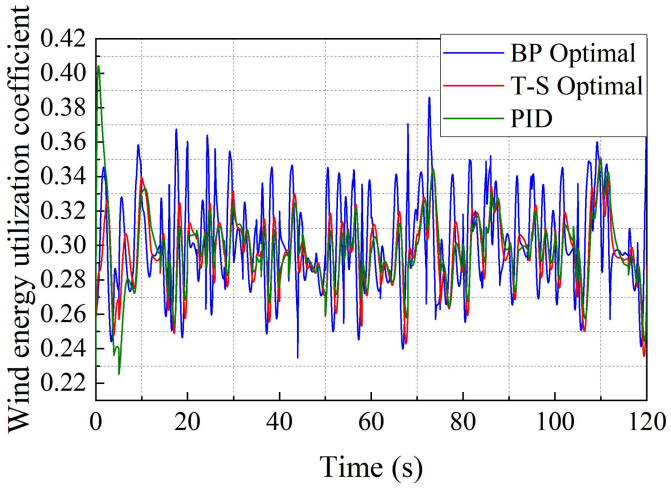
In addition, it can be seen from the series of curves in Figure 4.15 that, at the step wind speed, the proposed method here has a faster response speed and smaller overshoot than the T-S optimal controller and PID controller, and the response curves are smoother, which proves the effectiveness of the proposed method here.

4.5.4 WTGS Response Curves to Random Wind Speed

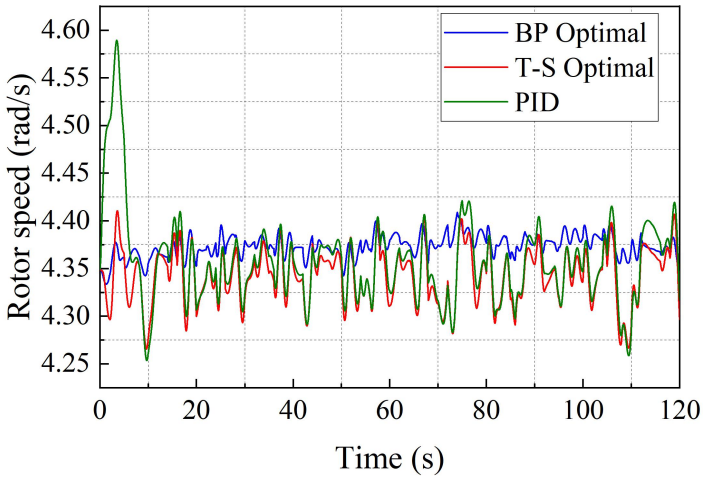
Figure 4.16 shows the WTGS response curves as the wind speed changes randomly between 13 m/s and 15 m/s.



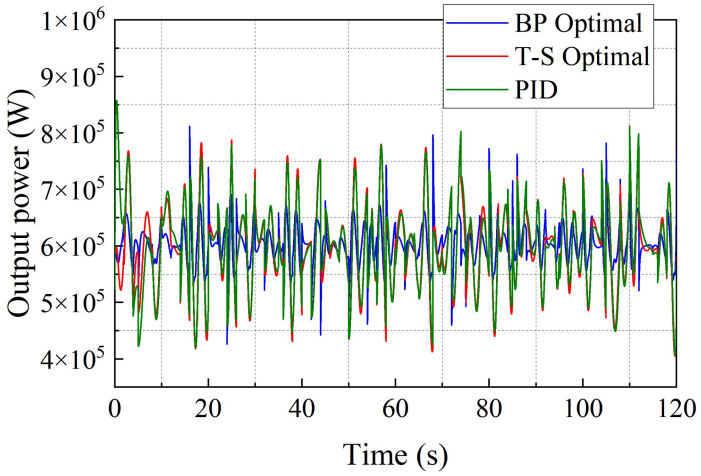
(a) Pitch angle variation



(b)Wind energy utilization coefficient



(c) Rotor speed



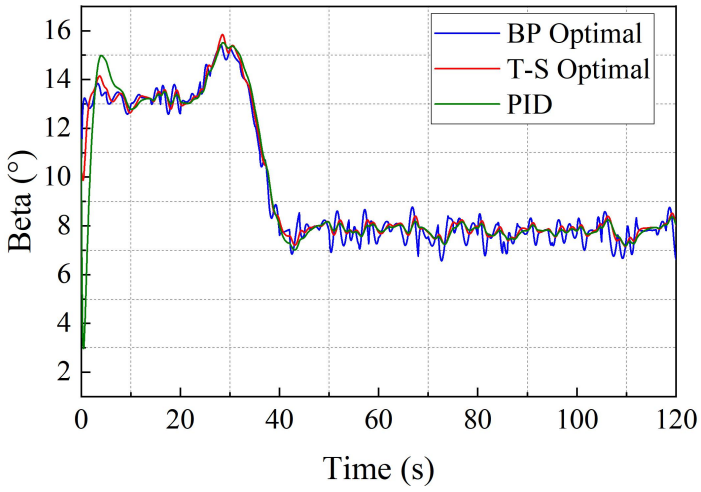
(d) Output power

Figure 4.16: Responses to Random Wind

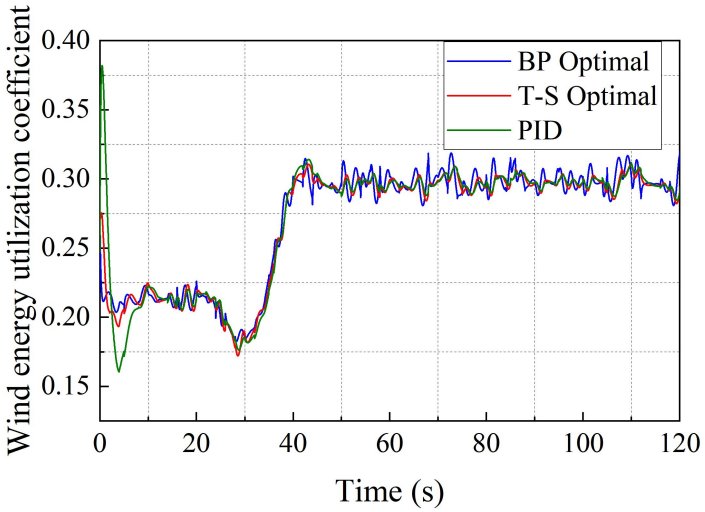
Under the random wind speeds of 13 m/s to 15 m/s, the constant power controller functioned well. The pitch angle and wind energy utilization coefficient were adjusted to minimize the change range of the output power of the fan, keeping the output power near the rated power. The simulation results show that under random wind conditions, the controller can effectively maintain the speed and output power at the rated values. Moreover, compared to the control effect of the T-S optimal controller, the curve under this controller is smoother and the control effect is better.

4.5.5 Response Curves to Combined Wind

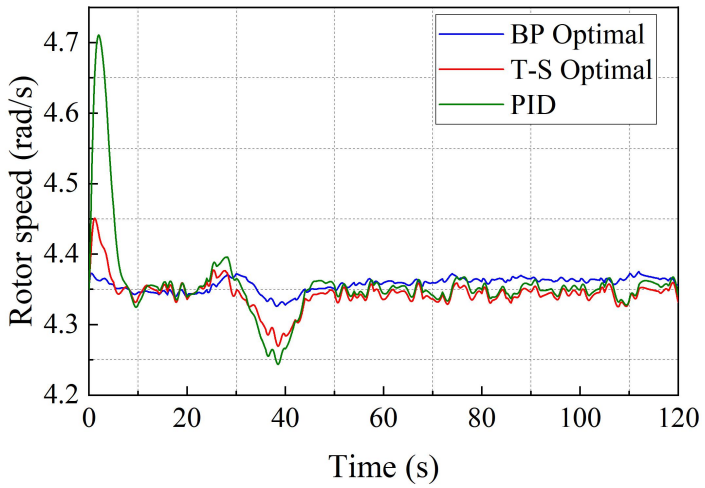
Figure 4.17 shows the response curves of WTGS When the wind speed is the superposition of four wind speed components.



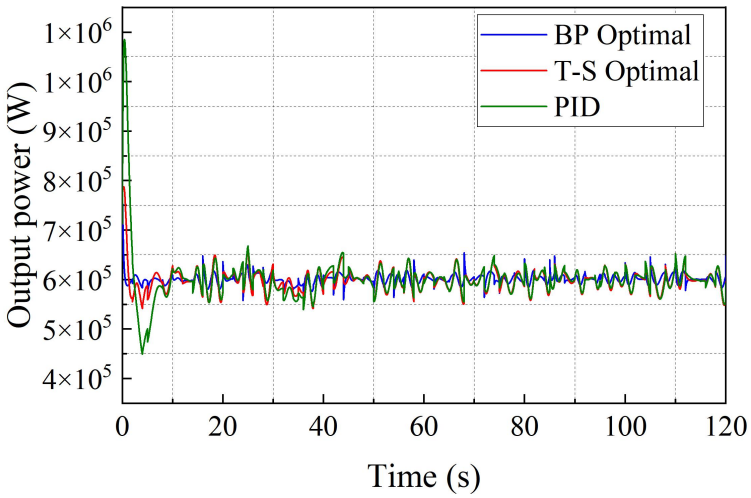
(a) Pitch angle



(b) Wind energy utilization coefficient



(c) Rotor speed



(d) Output power

Figure 4.17: Response Curves at Combined Wind Speed

When the WTGS encountered by the superposition of multiple wind components, it can be seen from the curves in Figure 4.17 that the pitch angle changes with the change of wind speed under the action of the controller. In short, the pitch angle increases with the increase of wind speed, and decreases with the decrease of wind speed. It can be seen from Figure 4.17 that the rotor power efficiency also changes accordingly. Figure 4.17 also show that the rotor speed and output power can be stabilized near the rated value in, it indicates that the controller completes the desired control objectives. As shown in this figure, the curves of the proposed controller have smaller fluctuation amplitude, compared with that of T-S optimal controller and PID controller. The proposed controller here delivers a smoother output, and better maintain the rotor speed and the output power around the rated value.

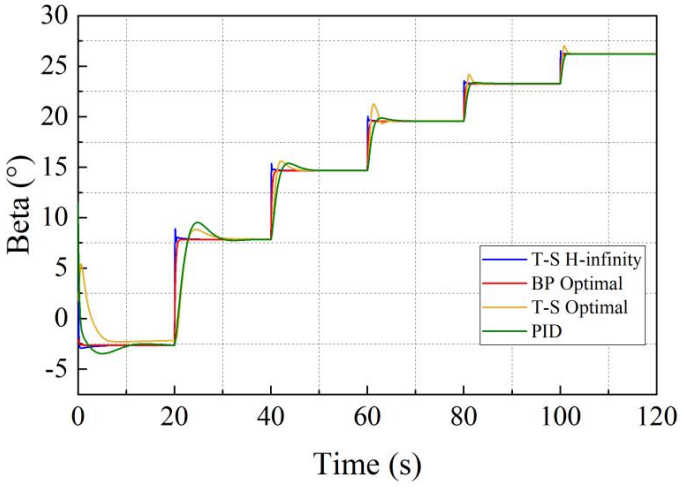
4.5.6 Conclusions

This section conducted simulation tests on WTGS containing a composite BP neural network optimal controller. The simulation results showed that the controller has good control effects under different wind speed components and natural wind, and can maintain the rotor speed and output power around the rated value. Compared to the control effect of T-S optimal controller, the controller proposed here provides better performance under all different scenatios and achieves highest robustness against field flux variation. The BP neural network optimal controller performs better than T-S optimal controller, mainly due to the differences in their ability to handle nonlinear systems and learning mechanisms. As a data-driven model, BP neural network can approximate complex nonlinear systems with arbitrary accuracy through multiple layers of neurons and nonlinear activation functions, and dynamically adjust weights through error backpropagation. It has strong self-learning ability and can adapt to time-varying or unknown dynamics of system

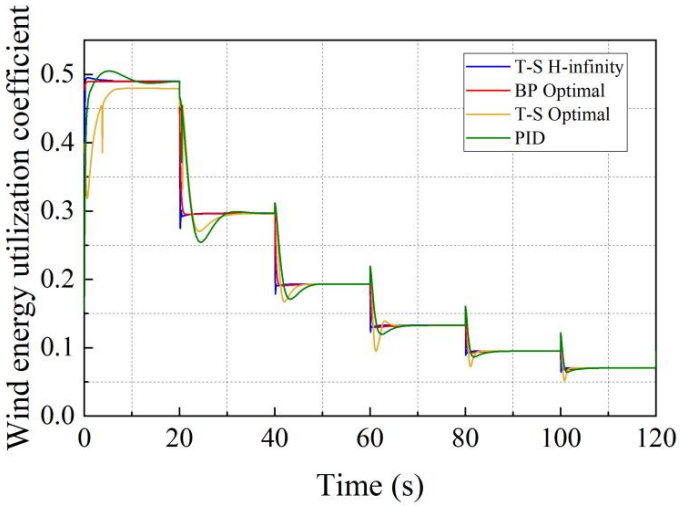
parameters. The T-S fuzzy controller relies on the "IF-THEN" rule library and needs to be constructed based on expert experience or mechanisms. The nonlinear expression is limited by the number of rules, and the characterization of complex dynamic systems is insufficient. Moreover, parameter optimization relies on prior knowledge, and the adaptive range is limited. Therefore, BP neural network has better control effect in complex scenes.

4.6 Conclusions

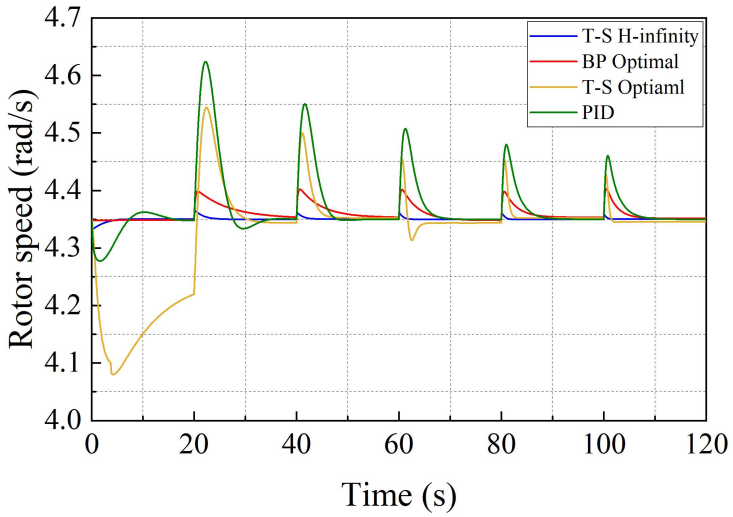
The response curves under various controllers are presented one by one in the above sections. From the above response curves, it can be seen that when the wind speed changes, after a period of controller's adjustment, both the rotor speed and output power can be stabilized at the rated values. Taking the example of step wind, compare the effects of the three different controllers.



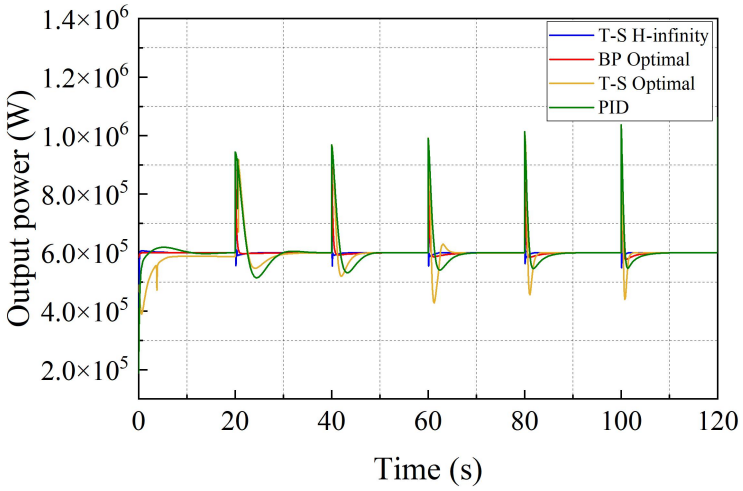
(a) Pitch angle



(b) Rotor power coefficient



(c) Rotor speed



(d) Output power

Figure 4.18: Response Curves at Step Wind Speed Under All Controllers

The above figure shows the response curves of four controllers under the step wind of 11 m/s - 21 m/s. Using the data from the 40th second for analysis and comparison, the data are summarized in the following two tables.

Table 4.1: Rotor speed parameters at the 40th second under different controllers

Controller	Response Time (s)	Peak Value (rad/s)	Overshoot (%)
T-S H-infinity controller	2	4.37	0.5
T-S Optimal controller	7	4.5	3.4
BP Optimal controller	12	4.4	1.1
PID controller	8	4.55	4.6

Table 4.2: Output power parameters at the 40th second under different controllers

Controller	Response Time (s)	Peak Value (rad/s)	Overshoot (%)
T-S H-infinity controller	2	7.5	25.0
T-S Optimal controller	5	9.5	58.3
BP Optimal controller	2	9.0	50.0
PID controller	9	9.7	61.7

At the 40th second, the wind speed jumps from 13 m/s to 15 m/s, and the response time and overshoot of the four different controllers are different. For rotor speed, the T-S H-infinity controller has the shortest response time of only 2 seconds, while the BP Optimal controller has the longest response time of 12 seconds. The T-S H-infinity controller has the smallest overshoot at only 0.5%, while the PID controller has the largest

overshoot at 4.6%. For output power, the T-S H-infinity controller and BP Optimal controller both have the shortest response time of only 2 seconds, while the PID controller has the longest response time of 9 seconds. The T-S H-infinity controller has the smallest overshoot at only 25%, while the PID controller has the largest overshoot at 61.7%. In summary, the response time under the T-S H-infinity controller is the shortest and the overshoot is the smallest, so T-S H-infinity controller is the best among the three.

CHAPTER 5

CONCLUSIONS AND RECOMMENDATIONS

5.1 Conclusions

In this research, three different novel hybrid variable pitch controllers are designed. They are T-S optimal hybrid controller, T-S H-infinity hybrid controller, and BP neural network hybrid optimal controller. The main contribution is to adopt T-S fuzzy theory or BP neural network theory, to optimize conventional optimal controller or H-infinity controller, to get hybrid high-performance controller. The main research results are as follows.

linearize the nonlinear wind turbine system into linear subsystems at six different wind speeds with Taylor expansion.

After obtaining the linear subsystem, select optimal control method, H-infinity control method to design sub-controllers for these subsystems. Then combine these sub-controllers with Takagi-Sugeno fuzzy theory or BP neural network control theory to obtain novel hybrid high-performance variable pitch controllers. The first is the T-S optimal hybrid controller, which uses optimal theory to design controllers for each subsystem, and then integrates all sub controllers into a global controller using T-S fuzzy theory. The second is the T-S H-infinity hybrid controller, which uses H-infinity theory to design controllers for each subsystem, and then integrates all sub controllers into a global controller using T-S fuzzy theory. The third is the BP neural network optimal hybrid controller, which uses optimal theory to design controllers for each subsystem, and then integrates all sub controllers into a global controller using BP neural network theory. Then,

the WTGS with different controllers are built in MATLAB/Simulink, the simulations are carried out under four different wind conditions with these controllers.

The simulation results show that regardless of the wind component, these three controllers can make the rotor speed and output power constant when the wind speed changes. But the control effects of various controllers are different.

From the simulation curves it can be seen that, T-S H-infinity hybrid controller has the shortest response time and the smallest overshoot, this indicates that it can output the most stable electrical energy and protect the wind turbine. The reason is that T-S H-infinity controller focuses on robustness, can suppress external disturbances and model perturbations, and ensure system stability under uncertainty. It optimizes worst-case performance, does not rely on precise models, minimizes constrained interference effects through H-infinity norm, and has strong adaptability to complex dynamics and unknown disturbances in practical engineering, making the control effect more reliable.

5.2 Recommendations

When designing the controller in this research, the disturbance of high-frequency wind speed changes on the system was not considered, so the control effect is not ideal when the wind speed randomly changes at high frequencies. In addition, this study did not consider the grid connected operation of the wind turbine, as well as the voltage and current phase issues that are of concern for grid connected operation. It only considered the wind turbine itself, which has certain limitations. Another limitation is that the normal operation stage of a wind turbine includes the start-up stage, low-power operation stage, and rated power operation stage. This thesis focuses on the constant power output stage of

the wind turbine above the rated wind speed. However, in the actual operation process of the wind turbine, there is a switching process in different operation stages.

In future research works, we can focus on studying control strategies for high-frequency wind speed fluctuations. Then, in addition to studying the section above the rated wind speed, the operation of the wind turbine at low wind speeds should also be studied, including the start-up stage, low-power operation stage, and rated power operation stage. Finally, wind turbines and the power grid can be studied as a whole. That is to say, taking into account the various working stages of the wind turbine and studying it in the power grid at the same time.

Furthermore, energy storage power stations have become the standard configuration for wind power plants at present and in the future, so energy storage equipment is a major hot-spot in future wind power research.

REFERENCES

Aghaeinezhad, SM., Taghizadeh, M., Mazare, M., & Kazemi, MG. (2021). Individual pitch angle control of a variable speed wind turbine using adaptive fractional order non-singular fast terminal sliding mode control. *International Journal of Precision Engineering and Manufacturing, 22*(4), 511-522.

Asghar, A. B., Naveed, K., Xiong, G., & Wang, Y. (2022). Adaptive Neuro-fuzzy Algorithm for Pitch Control of Variable-speed Wind Turbine. *International Journal of Control Automation and Systems, 21*(11), 3788-3798.

Bachmann, P., Ahmed, S., & Bajcinca, N. (2024). Lyapunov Characterization of Input-to-State Stability for a Class of Impulsive Systems. *IEEE Transactions on Automatic Control, 69*(10), 6996-7003.

Bortoff, S. A., Schwerdtner, P., Danielson, C., Di Cairano, S., & Burns, D. J. (2022). H-infinity Loop-Shaped Model Predictive Control with HVAC Application. *IEEE Transactions on Control Systems Technology, 30*(05), 2188-220.

Bustan, D., & Moodi,H. (2022). Adaptive interval type-2 fuzzy controller for variable-speed wind turbine. *Journal of Modern Power Systems and Clean Energy, 10*(02), 524-530.

Cao, Z. (2023). Research on Robust Control Method Based on T-S Fuzzy System Model Reconstruction. In *Doctoral Thesis, Harbin University of Science and Technology* (pp. 56-77).

Ceng, F. (2016). Variable pitch control of direct drive wind turbines based on fuzzy logic. In *Doctoral Thesis, Hunan University* (pp. 11-16).

Chao, Q., Zhang, Y., & Gao, X. (2016). Paris agreement-a new starting point for global climate governance. *Advances in Climate Change Research, 12*(01), 61-67.

Chen, H. (2017). Research on pitch control technology for doubly fed asynchronous wind power generation system. In *Doctoral Thesis, Xi'an University of Architecture and Technology* (pp. 18-23).

Chen, J., Yao, W., Lu, Q., Ren, Y., Duan, W., Kan, J., & Jiang, L. (2022). Adaptive active fault-tolerant MPPT control of variable-speed wind turbine considering generator actuator failure. *International Journal of Electrical Power and Energy Systems, 143*, 108443-108458

Chen, J., Yao, W., Ren, Y., Wang, R., Zhang, L., & Jiang, L. (2019). Nonlinear adaptive speed control of a permanent magnet synchronous motor: A perturbation estimation approach. *Control Engineering Practice, 85,* 163–175.

Chen, P., Han, D., Tan, F., & Wang, J. (2020). Reinforcement-based robust variable pitch control of wind turbines. *IEEE ACCESS, 8,* 20493-20502.

Chen, Y., Guo, W., Peter D. Lund, Na Du, Yang, K, & Wang J. (2024). Conffguration optimization of a wind-solar based net-zero emission tri-generation energy system considering renewable power and carbon trading mechanisms. *Renewable Energy*, *232*, 121086.

Chen, Y., Zhang, Y., & Cai, B. (2022). Suspension Strategy of Maglev Vertical Axis Wind Turbine Based on Sliding Mode Adaptive Neural Network Predictive Control. *IEEE ACCESS, 10*, 91712-91721.

Cheng, M. (2021). Research on aerodynamic load characteristics of wind turbines and design of pitch control system. In *Doctoral Thesis, Lanzhou University Of Technology* (pp. 22-27).

China Electricity Council. (2023). China Electricity Industry Annual Development Report 2022*, 2023*, 3-7.

Civelek, Z. (2020). Optimization of fuzzy logic (Takagi-Sugeno) blade pitch angle controller in wind turbines by genetic algorithm. *Engineering Science and Technology-an International Journal-Jestech, 23*(01), 1–9.

Colombo, L., Corradini, M., Ippoliti, G., & Orlando, G. (2020). Pitch angle control of a wind turbine operating above the rated wind speed: A sliding mode control approach," *ISA Transactions, 96,* 95-102.

Dai, R. (2018). Research on Joint Simulation and Control of Wind Turbine in Constant Power Stage. In *Doctoral Thesis, Beijing Jiaotong University* (pp. 17-20).

De Battista, H., Mantz, R.J., & Christiansen, C.F. (2000). Dynamical Sliding Mode Power Control of Wind Driven Induction Generators. *IEEE Transactions on Energy Conversion, 15*(4), 451-457.

Fan, Y., & Mu, A. (2020). Adaptive fuzzy Proportion Integration Differentiation control in hydraulic offshore wind turbine for optimal power extraction based on the estimated wind speed. *Energy Science and Engineering, 08*(05), 1604-1619.

Fan, Y., Xu, H., & He, Z. (2022). Smoothing the output power of a wind energy conversion system using a hybrid nonlinear pitch angle controller. *Energy Exploration & Exploitation, 40*(02), 539-553.

Führer, T., Fuica, F. (2024). A DPG method for linear quadratic optimal control problems. *Computers & Mathematics with Applications, 166*(15)*,* 106-117.

Gao, H., Yang, Y., Jiao, J., Qiu, M., Liu, Z., & Zhao, X. (2018). World renewable energy development trends. *Petroleum Science and Technology Forum, 37*(04), 62-67.

Goyal, S., Deolia, VK., & Agrawal, S. (2024). Performance Evaluation of GA-Optimized TSFL Pitch Controller for 2 Mass Drive Train HAWTs. *Journal of Electrical Engineering & Technology, 19*(05), 3515-3526.

Geng, H., Zhou, W., & Yang, G. (2010). An inverse system robust method for power control of variable pitch wind power systems. *Journal of Tsinghua University, 50*(5), 718-723.

Global Wind Energy Council (2022a). Global Wind Report 2022, *2023,* 1-5.

Global Wind Energy Council (2022b). Global Offshore Wind Report 2021, *2022,* 2-4.

Hamadou, M., & Belarbi, K. (2023). Actuator fault-tolerant control for discrete Takagi-Sugeno fuzzy systems using the matrices norms approach. *Proceedings of the Institution of Mechanical Engineers Part I-Journal of Systems and Control Engineering, 238*(3), 571-580.

Huang, H., Nong, Z., Li, G., & Li, J. (2023). Research and optimization of a built-in entity vertical axis wind turbine by variable pitch strategy. *Journal of Building Engineering, 68*, 105810-105826

Jiao, X., Meng, W., Yang, Q., Fu, L., & Chen, Q. (2019). Adaptive Continuous Neural Pitch Angle Control for Variable-Speed Wind Turbines. *Asian Journal of Control, 21*(04), 1966–1979.

Khezami, N., Guillaud, X., & Braiek, N. B. (2012). Multimodel LQ controller design for variable-speed and variable pitch wind turbines at high wind speeds. *International Journal of Modelling Identification and Control, 15*(2), 117-124.

Kong, Y., & Wang, Z. (2008). Design and Simulation of Fuzzy Sliding Mode Robust Controller for Large Wind Turbine Units. *Proceedings of the CSEE, 28*(14), 136-141

Lasheen, A., Elnaggar, M., & Yassin, H. (2020). Adaptive control design and implementation for collective pitch in wind energy conversion systems. *ISA Transactions, 102*, 251–263

Lei, F. (2019). Research on wind turbine pitch control system based on dual fuzzy PID control strategy. *Fuzzy Systems and Mathematics, 33*(03), 29-34.

Li P., & Chen L. (2013). Research on Variable Pitch Control of Wind Turbine Based on Variable Gain. *Electronic Design Engineering, 21* (16), 140-143.

Liu, J. (2021). *Intelligent Control*. 5th Ed., Beijing: Electronic Industry Press.

Liu, B., & Tang, W. (2022). *Modern Control Theory*. 3rd ed., Beijing: Machinery Industry Press

Liu, J., Cui, Y., Song, H., Zhang, X., & Qu, Y. (2021). Stability analysis of TS fuzzy-model-based coupled control systems with nonlinear T-S fuzzy control and its application. *Neural Computing and Applications, 33*(22)*,* 15481-15493.

Liu, J., & Gao, L. (2016). Variable pitch control and load optimization of variable speed wind turbines. *Electrical Automation, 38*(01), 44-47

Liu, J., Yin, T., Xie, X., Tian, E., & Fei, S. (2019). Event-triggered state estimation for T–S fuzzy neural networks with stochastic cyber-attacks. *International Journal of Fuzzy Systems, 21*(2), 532-544.

Liu, S., Li, D., & Bao, N. (2009). Nonlinear robust control of horizontal axis stall type wind turbines. *Acta Energiae Solaris Sinica, 30*(7), 966-971.

Liu, Y., Liu, S., Guo, H., & Wang, H. (2009). The Estimation of Wind Turbine Pitch Angle Based on ANN. In Proceeding of t*he Second International Conference on Intelligent Networks and Intelligent Systems*, (pp. 581–584).

Liu, Y., Liu, W., & Lu, H. (2016). Research on Maximum Wind Energy Tracking Control of Doubly Fed Asynchronous Wind Turbine Based on Fuzzy Neural Network. *Electric Engineering, (04),* 80-82+85

Liu, Y., Zhu, J., Yao, X., Ma, K., Wang, X., & Guo, Q. (2015). Research on Robust Control Technology of Variable Pitch for Large Wind Turbines Based on H_2/H-infinity Hybrid Optimization. *Acta Energiae Solaris Sinica,* 36(03), 714-719.

Ma, L. (2020). Research on intelligent sliding mode fault-tolerant control for variable pitch wind turbines. In *Doctoral Thesis, Nanjing University of Aeronautics and Astronautics* (pp. 83-95).

Ma, X., Wong, P. K., Zhao, J., & Xie, Z. (2019). Cornering stability control for vehicles with active front steering system using TS fuzzy based sliding mode control strategy. *Mechanical Systems and Signal Processing, 125*, 347-364.

Mendi, B., Pattnaik, M., & Srungavarapu, G. (2023). Design, analysis, and adaptive maximum power point tracking control of small-scale wind turbine system. *International Journal of Circuit Theory and Applications, 51*(7), 3316-3330.

Menezes, E. J. N., & Araujo, A. M. (2023). Wind turbine structural control using H-infinity methods. *Engineering Structures, 286*, 116095

Mlayeh, H., & Khedher, A. (2024). Actuator Fault Accommodation of an Aerial Vehicle Described by Takagi-Sugeno Models. *Studies in Informatics and Control, 33*(2), 73-81.

Munehiro Yoshitake, Yasumasa Fujii, Ryouichi Komiyama. (2022). Analysis of the Strategy for Carbon Neutrality with Global Energy Model considering Power Output Variability of Offshore Wind Power Generation. *Journal of Japan Society of Energy and Resources, 45*(6)

National Development and Reform Commission, National Energy Administration. (2021). “14th Five-Year” Renewable Energy Development Plan (2021-2025)*,2021*,13-25

Olfa Berrich, Fereshteh Mafakheri, & Halim Dabbou (2024). Renewable Energy Transition and the Paris Agreement: How Governance Quality Makes a Difference? *Energies, 17*, 4238

Prats M, Carrasco J, Galvan E, etc. Improving transition between power optimization and power limitation of variable speed, variable pitch wind turbines using fuzzy control techniques[C]. The 26th Annual Confjerence of the IEEE, 2000: 1497-1502.

Qin, S. (2010). Research on Variable Pitch Control Strategy for Wind Power Generation Systems. In *Master's Thesis, Nanjing University of Science and Technology* (pp. 13-23).

Qin, S., Hu, G., & Gu, C. (2012). Constant power H_∞ robust control of wind power generation system. *Control Theory & Applications, 29*(05), 617-622.

Rajesh, R., & Kaimal, M. R. (2007). T-S fuzzy model with nonlinear consequence and PDC controller for a class pf nonlinear control system. *Applied Soft Computing, 7*(3), 772-782.

Razavi-Pana, J., & Majd, V. J. (2008). A robust multi-objective DPDC for uncertain T-S fuzzy systems. *Fuzzy Sets and Systems, 159*(20), 2749-2762.

Ren, H., Hou, B., Zhou, G., Shen, L., Wei, C., & Li, Q. (2020). Variable Pitch Active Disturbance Rejection Control of Wind Turbines Based on BP Neural Network PID. *IEEE ACCESS, 8,* 71782-71797.

Ren, Y., Li, L., Brindley, J., & Jiang, L. (2016). Nonlinear PI control for variable pitch wind turbine. *Control Engineering Practice, 50*(05), 84-94

Saini, P., & Thakur, P. (2022). H-infinity Based Robust Temperature Controller Design for a Non-linear Systems. *Wireless Personal Communications, 126*(01), 305-333.

Senjyu, T., Sakamoto, R., Urasaki, N., Funabashi, T., Fujita, H., & Sekine, H. (2006). Output power leveling of wind turbine generator for all operating regions by pitch angle control. *IEEE Transactions on Energy Conversion, 21*(2)*,* 467-475.

Shalbafian, A., & Ganjefar, S. (2023). Variable Speed Wind Turbine Control Using the Homotopy Perturbation Method. *International Journal of Precision Engineering and Manufacturing-Green Technology, 10*(01), 141–150.

Shi, J., & Zhang, Q. (2019). Dynamic sliding-mode control for *T-S* fuzzy singular time-delay systems with H_∞ Performance. *IEEE Access, 7*, 115388-115399.

Shi, X., & Hao, Z. (2018). *Fuzzy Control and its MATLAB Simulation*. 2nd ed., Beijing:Beijing Jiaotong University Press.

Song, Y., Jeon, T., Paek, I., & Dugarjav, B. (2022). Design and Validation of Pitch H-infinity Controller for a Large Wind Turbine. *Energies, 15*(12), 8763

Taghavipour, A., Foumani, M. S., & Boroushaki, M. (2012). Implementation of an optimal control strategy for a hydraulic hybrid vehicle using CMAC and RBF networks. *Scientia Iranica B, 19*(2), 327–334.

Takagi, T., & Sugeno, M. (1985). Fuzzy identification of systems and its applications to modeling and control. *IEEE Transactions on Systems Man and Cybernetics, 15*(01), 116-132.

Tan Z., Wen X., Yang T. (2023). Research on grid connected control strategy of doubly fed wind turbines for new power systems. *Power System Protection and Control, 51*(3), 181-187.

Tian, H., Xie, Y., Shi, L., & Liu, H. (2021) Application of fuzzy cuckoo search algorithm in active disturbance rejection control of variable pitch of wind turbines. *Acta Energiae Solaris Sinica, 42*(01), 222-229.

Tong, S., Wang, T., & Wang, Y. (2004). Design and Stability Analysis of Fuzzy Control System. 2nd ed., Beijing: Science Press

Ulazia, A., Ezpeleta, H., Ibarra-Berastegi, G., Saenz, J., Martinez, I.N., Ringwood, J.V. (2024). Historical trends of floating wind turbine fatigue loads (Ireland 1920-2010). *Ocean Engineering, 299* (2024), 117424

Valle, M.E., Vital, W.L., Vieira, G. (2024). Universal approximation theorem for vector- and hypercomplex-valued neural networks. *Neural Networks, 180* (2024), 106632

Wang, B., Yuan, Y., Yuan, X., Chen, Y., & Huo, Z. (2021). *Wind Turbine and Offshore Wind Turbine Control Technology*. 3rd ed., Nanjing: Nanjing University Press.

Wang, P., & Li, N. (2019). Stable controller design for T–S fuzzy control systems with piecewise multi-linear interpolations into membership functions. *International Journal of Fuzzy Systems, 21*(05), 1585-1596.

Wind Energy Professional Committee of China Renewable Energy Society (2022). 2021 China Wind Power Hoisting Capacity Statistical Briefing. *Wind Energy, 05,* 38-52

Wu, H., Liu, W., & Ran, W. (2018). *Research on Stability of Several Types of Power Systems.* 1st ed., Xi'an: Xi'an Jiaotong University Press.

Wu, Z. (2005). *Robust Control and Application of Nonlinear Systems*. 1st ed., Beijing: Machinery Industry Press

Xing, Z., Zheng, Q., Yao, X., & Wang, F. (2006). Neural network-based control of variable pitch wind turbines. *Journal of Shenyang University of Technology, 28*(06), 681-686.

Xu, L. (2008). Research on Intelligent Control of Variable Pitch Wind Turbine. In *Doctoral Thesis, North China Electric Power University* (pp. 10–14).

Xu Y., Jia L., & Fu X. (2022). Variable pitch control of wind power generation system based on Wiener model. *Journal of System Simulation, 34* (8), 1741-1749.

Yang, Q., Jiao, X., Luo, Q., Chen, Q., & Sun, Y. (2020). L1 adaptive pitch angle controller of wind energy conversion systems. *ISA Transactions, 103*, 28–36.

Yang, Q., & Zhang, R. (2013). Research on fuzzy genetic control algorithm for variable pitch of wind turbine. *Computer Engineering and Applications, 49*(07), 217-220.

Yao, X., Liu, S., Shan, G., Xing, Z., Guo, C., & Yi, C. (2009). LQG Controller for a Variable Speed Pitch Regulated Wind Turbine. In *Proceeding of the 2009 International Conference on Intelligent Human-Machine Systems and Cybernetics,* (pp. 210–213).

Yarmohammadi, M. J., Sadeghzadeh, A., & Taghizadeh, M. (2020). Gain-scheduled control of wind turbine exploiting inexact wind speed measurement for full operating range. *Renewable Energy, 149*, 890-901.

Ye, H. (2015). *Wind Turbine Control Technology*. 3rd ed., Beijing: Mechanical Industry Press.

Yuan, C., Li, J., Chen, J., & Xu, Q. (2019). Research on variable pitch ABC-PID control of large wind turbines. *Acta Energiae Solaris Sinica, 40*(10), 3002-3008.

Zhang, J., Ji, R., Ma, Y., Yang, M., & Wang, K. Fuzzy adaptive PID control for variable pitch wind power generation. *Technology Innovation and Application, 12*(33), 16-19

Zhang, K. (2021). *Fuzzy Mathematics*. 3rd ed., Beijing: Peking University Press.

Zhang, L., Jin, S., & Nie, S. (2006). Simulation research on large wind turbine control based on PID method. *China Science and Technology Information, 22*(01), 34-36.

Zhang Q., He S., & Huang S. (2023). Research on Variable Pitch Control of Wind Turbine Based on DDPG Algorithm. *Science Technology and Engineering, 23* (18), 7764-7771.

Zhang, X. (2004). Adaptive Fuzzy Control for Large Variable Speed Wind Turbine Generators. *Journal of System Simulation,16*(03), 574-877

Zhao W., Zhang L., & Jing Y. (2014). Optimization design of variable pitch wind turbine controller. *Grid Technology, 38* (12), 3436-3440.

Zheng, Y. (2012). Independent pitch control of wind turbine based on neuron PID. *Water Resources and Power, 30*(01), 151-154.

Zhu, P., Zhang, Q., Zhao, Z., & Yang, B. (2023). BP fuzzy neural network PID based constant tension control of traction winch. *Measurement & Control, 56*(3-4), 857-873.

Zou, C., Zhao, Q., Zhang, G., & Xiong, B. (2016). Energy revolution: from fossil energy to new energy. *Natural Gas Industry, 36*(01), 1-10.

APPENDICES

Appendix A: Journal Publications

1. **Shengsheng Qin**, Sze Song Ngu, Tingting Zeng. (2022) Optimal constant power control of wind turbine generators based on Takagi-Sugeno fuzzy model. *Alexandria Engineering Journal, 61*(8).
2. **Shengsheng Qin**, Sze Song Ngu, Chaoqun Zhang, Yujian Chen, Ruiqi Chen, Tingxuan Liu. (2023) H-infinity Variable-pitch Control for Wind Turbines Based on Takagi-Sugeno Fuzzy Theory. *Tehnicki Vjesnik-Technical Gazette, 30*(5).
3. **Shengsheng Qin**, Zhipeng Cao, Feng Wang, Sze Song Ngu, Lee Chin Kho, Hui Cai. (2024) Design of Optimal Controller for Wind Turbine with Constant Power Based on BP Neural Network. *Energies, 17*(16).
4. **Shengsheng Qin,** Feng Wang, Zhipeng Cao, Sze Song Ngu, Lee Chin Kho, Hui Cai. Overview of Variable Pitch Control Technology for Wind Turbine Generator System. Being written.